

1 Deep Underground Neutrino Experiment (DUNE)

2 Technical Design Report

3 **Volume IV:**

4 for DP CISC TDR development

5 October 17, 2019

6 The DUNE Collaboration



# 1 Contents

2	<b>Contents</b>	<b>i</b>
3	<b>List of Figures</b>	<b>iii</b>
4	<b>List of Tables</b>	<b>iv</b>
5	<b>1 Cryogenics Instrumentation and Slow Controls</b>	<b>1</b>
6	1.1 Introduction . . . . .	1
7	1.1.1 Scope . . . . .	4
8	1.1.2 Design Considerations . . . . .	6
9	1.1.3 Fluid Dynamics Simulation . . . . .	8
10	1.2 Cryogenic Instrumentation . . . . .	15
11	1.2.1 Thermometers . . . . .	15
12	1.2.2 Purity Monitors . . . . .	28
13	1.2.3 Liquid Level Meters . . . . .	34
14	1.2.4 Pressure Meters . . . . .	35
15	1.2.5 Gas Analyzers . . . . .	36
16	1.2.6 Cameras . . . . .	39
17	1.2.7 Cryogenic Instrumentation Test Facility . . . . .	43
18	1.2.8 Validation in ProtoDUNE . . . . .	43
19	1.3 Slow Controls . . . . .	44
20	1.3.1 Slow Controls Hardware . . . . .	44
21	1.3.2 Slow Controls Infrastructure . . . . .	46
22	1.3.3 Slow Controls Software . . . . .	47
23	1.3.4 Slow Controls Quantities . . . . .	48
24	1.3.5 Local Integration . . . . .	48
25	1.3.6 Validation in ProtoDUNE . . . . .	50
26	1.4 Organization and Management . . . . .	50
27	1.4.1 Institutional Responsibilities . . . . .	52
28	1.4.2 Schedule . . . . .	54
29	1.4.3 Risks . . . . .	56
30	1.4.4 Interfaces . . . . .	59
31	1.4.5 Installation, Integration, and Commissioning . . . . .	59
32	1.4.6 Quality Control . . . . .	65
33	1.4.7 Safety . . . . .	69
34	1.5 Blank section for avoiding missing label errors . . . . .	69

1	<b>Glossary</b>	<b>70</b>
2	<b>References</b>	<b>76</b>
3		

# 1 List of Figures

2	1.1	CISC subsystem chart . . . . .	2
3	1.2	CFD example . . . . .	12
4	1.3	Distribution of temperature sensors inside the cryostat . . . . .	12
5	1.4	Streamlines for LAr flow inside ProtoDUNE-SP . . . . .	15
6	1.5	Cryostat bolts and temperature sensor support . . . . .	17
7	1.6	Principle of cross-calibration with dynamic T-gradient monitor . . . . .	18
8	1.7	Temperature profile for dynamic T-Gradient with pumps-off . . . . .	19
9	1.8	Dynamic T-gradient monitor overview . . . . .	19
10	1.9	Sensor-cable assembly for dynamic T-gradient monitor . . . . .	20
11	1.10	ProtoDUNE-SP Static T-gradient results . . . . .	20
12	1.11	Temperature sensor resolution and reproducibility . . . . .	21
13	1.12	Conceptual design of the static T-gradient monitor . . . . .	22
14	1.13	Arrays in gas phase . . . . .	24
15	1.14	ProtoDUNE-SP instrumentation map . . . . .	25
16	1.15	ProtoDUNE-SP T-gradient results . . . . .	25
17	1.16	ProtoDUNE-SP bottom sensor results . . . . .	26
18	1.17	The ProtoDUNE-SP purity monitoring system . . . . .	29
19	1.18	Measured electron lifetimes in the three purity monitors at ProtoDUNE-SP . . . . .	30
20	1.19	Schematic diagram of the baseline purity monitor design . . . . .	31
21	1.20	Block diagram of the purity monitor system. . . . .	32
22	1.21	LAr level measurements . . . . .	35
23	1.22	Photo of the pressure sensors installed on a flange in ProtoDUNE-SP . . . . .	36
24	1.23	Photo of a gas analyzer switchyard valve assembly . . . . .	37
25	1.24	Impurity levels during the pre-fill stages for the 35 t phase 1 . . . . .	38
26	1.25	O <sub>2</sub> just after the 35 ton prototype was filled with LAr . . . . .	39
27	1.26	A camera enclosure . . . . .	40
28	1.27	Inspection camera design . . . . .	42
29	1.28	Example schematic for LED chain . . . . .	43
30	1.29	Slow controls connections and data . . . . .	45
31	1.30	Rack monitoring box prototype for the SBND; based on MicroBooNE design . . . . .	46
32	1.31	Diagram of the ProtoDUNE-SP control system topology . . . . .	51
33	1.32	CISC consortium organization . . . . .	52

# 1 List of Tables

2	1.1	Specifications for DP-CISC <code>ref tab:spec:DP-CISC</code> . . . . .	7
3	1.2	Specifications for CISC subsystems . . . . .	9
4	1.3	Specifications for CISC subsystems. . . . .	10
5	1.4	Specifications for CISC subsystems. . . . .	11
6	1.5	CFD parameters for ProtoDUNE . . . . .	13
7	1.6	Slow controls quantities . . . . .	49
8	1.7	CISC consortium institutions. . . . .	53
9	1.8	Institutional responsibilities in the CISC consortium . . . . .	54
10	1.9	DP CISC schedule . . . . .	55
11	1.10	Risks for DP-FD-CISC . . . . .	57
12	1.11	CISC system interface links . . . . .	60

13

# **1 Todo list**

2 refer to table 1.5 here or move table down to after reference . . . . . 13

# Chapter 1

## Cryogenics Instrumentation and Slow Controls

### 1.1 Introduction

The cryogenic instrumentation and slow controls (CISC) consortium provides comprehensive monitoring for all detector components and for liquid and gaseous argon quality and behavior as well as a control system for many detector components. The dual-phase (DP) and single-phase (SP) modules both use the same control system and have nearly identical cryogenic instrumentation except for differences in location due to the different time projection chamber (TPC) geometries and the presence of dedicated instrumentation for monitoring temperature and pressure in the gas phase for the DP module which is unnecessary in the SP module. Volume III, The DUNE Far Detector Single-Phase Technology, Chapter 8 of this technical design report (TDR) is virtually the same as this chapter apart from those few differences.

The consortium responsibilities are split into two main branches: cryogenics instrumentation and slow controls (see Figure 1.1).

Each element of CISC contributes to the DUNE physics program primarily by maintaining high detector live time. As described in Volume II, DUNE Physics, of this TDR, neutrino charge-parity symmetry violation (CPV) and resolution of the neutrino mass hierarchy over the full range of possible neutrino oscillation parameters will require at least a decade of running the far detector (FD). Similar requirements apply to searches for nucleon decay and supernova neutrino burst (SNB) events from within our galaxy. Throughout this long run time, the interior of any DUNE cryostat remains completely inaccessible. Repairs cannot be made to any damaged components within the TPC structure; hence, environmental conditions that present risks must be detected and reported quickly and reliably.

Detector damage risks peak during the initial fill of a module with LAr because temperature gradients take on their highest values during this phase. For example, thermal contractions outside



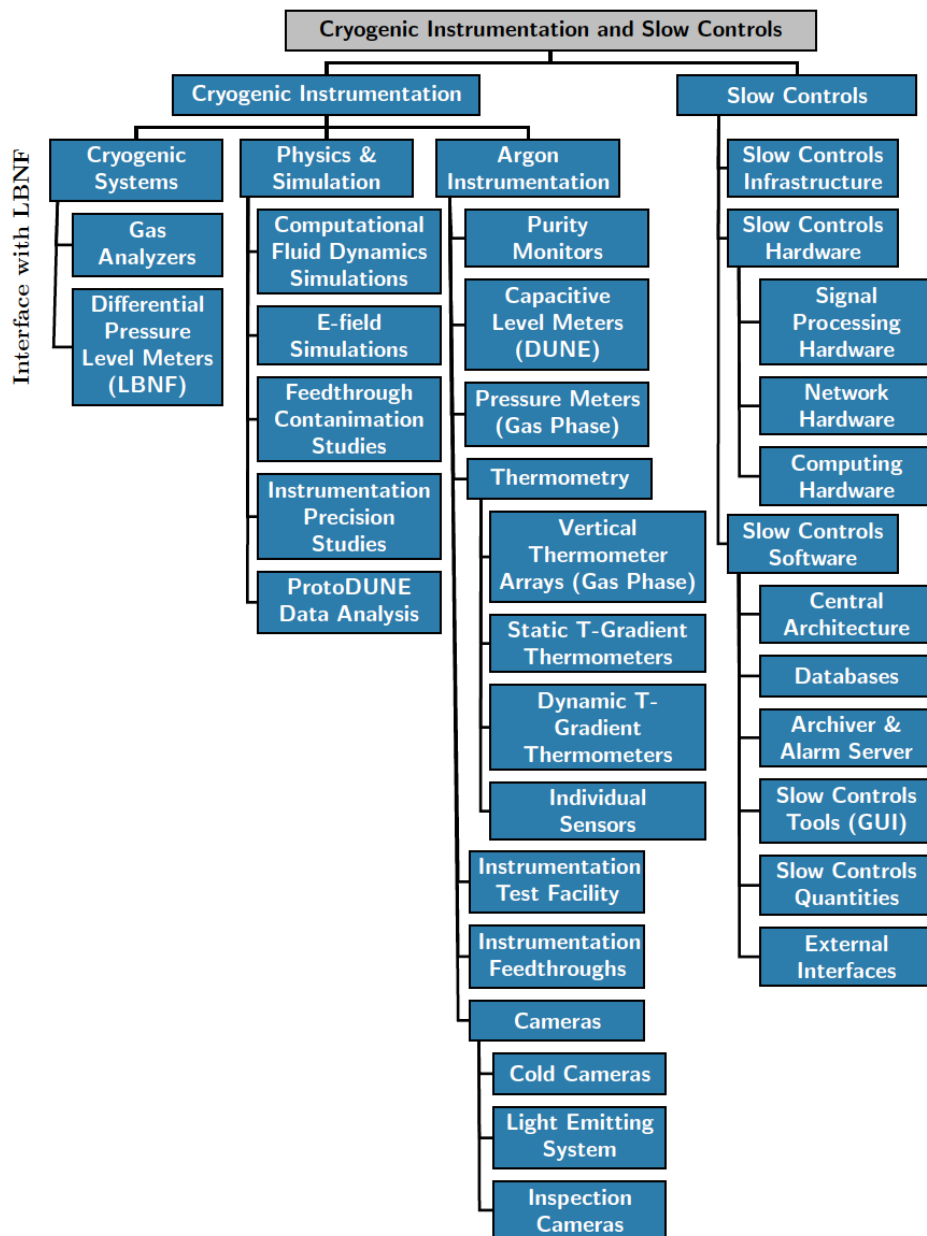


Figure 1.1: CISC subsystem chart.

1 of the range of design expectations could result in broken extraction grid wires or poor connections  
2 at the cathode high voltage (HV) feedthrough point that could lead to unstable E fields. Additional  
3 care is needed to monitor the gas phase above the liquid level. The temperature and the pressure  
4 of the gas phase affect gas density, and consequently, the large electron multiplier (LEM) gain  
5 calibration. These considerations require a robust temperature monitoring system for the detector  
6 both in liquid and gas phase and a pressure monitoring system in the gas phase, supplemented with  
7 liquid level monitors and a high-performance camera system for visual inspection of the interior  
8 of the cryostat during the filling process. These systems are fully described in Section 1.2 of this  
9 chapter.

10 Argon purity must be established as early as possible in the filling process, a period during which  
11 gas analyzers are most useful, and must maintain an acceptable value, corresponding to a mini-  
12 mum electron drift lifetime of 3 ms throughout the data-taking period. Dedicated purity monitors  
13 (Section 1.2.2) provide precise lifetime measurements up to values of 10 ms (current capability  
14 based on ProtoDUNE-SP). Purity requirements are more stringent in a dual phase detector due  
15 to longer drift paths, so CISC plans to build longer purity monitors to increase this capability  
16 to approximately 20 ms for the DP FD. The purity monitors and gas analyzers remain important  
17 even after high lifetime has been achieved because periodic detector top-off fills occur; the new  
18 LAr must be very high quality to be introduced into the cryostat.

19 The CISC system must prevent fault conditions that could develop in the detector module over long  
20 periods of operation. A drop in liquid level could affect the behavior of the extraction grid, which  
21 lies 5 mm below the liquid surface; the liquid level monitors must head off this possibility. Very  
22 slow-developing outgassing phenomena could conceivably occur, with associated bubble generation  
23 creating another source of HV breakdown events. The cold camera system allows bubbling sites  
24 to be detected and identified, and mitigation strategies to be developed such as reducing HV  
25 operation for some time. A more subtle fault is the formation of quasi-stable eddies in argon fluid  
26 flow that could prevent positive argon ions from being cleared from TPC volume, resulting in  
27 space charge build up that would not otherwise be expected at the depth of the FD. The space  
28 charge could in turn cause distortions in the TPC drift field that degrade tracking and calorimetry  
29 performance. The high-performance thermometry of the DUNE CISC system creates input for  
30 well developed complex fluid flow models described in Section 1.1.3 that should enable detecting  
31 conditions associated with these eddies.

32 Finally, a high detector live-time fraction for operation over several years cannot be achieved  
33 without an extensive system for monitoring all aspects of detector performance, reporting this  
34 information intelligently to detector operators, and archiving the data for deeper offline studies.  
35 Section 1.1.1.2 details the Deep Underground Neutrino Experiment (DUNE) slow controls system  
36 designed for this task.

37 Some of the baseline designs for the CISC systems (e.g., pressure meters in gas, capacitive level  
38 meters, slow controls system) have been used in ProtoDUNE-DP, and corresponding design pa-  
39 rameters are extrapolated from these designs. For systems that are currently not deployed in  
40 ProtoDUNE-DP, the goal is deploy them in ProtoDUNE-DP-Run-II phase. The ProtoDUNE-DP  
41 data from Run-I and Run-II will be used to validate the instrumentation designs and to under-  
42 stand their performance. For some of the CISC systems (e.g., static and dynamic T-gradient  
43 thermometers, purity monitors), validation and performance in ProtoDUNE-SP will provide im-

1 portant inputs to DP FD. More details are provided in sections 1.1.3.1, 1.2.8, and 1.3.6.

## 2 **1.1.1 Scope**

### 3 **1.1.1.1 Cryogenics Instrumentation**

4 Cryogenics instrumentation includes purity monitors, various types of temperature monitors (gas  
5 and liquid phase), capacitive level meters, pressure meters (gas phase), and cameras with their  
6 associated light emitting systems. Also included are gas analyzers and differential pressure level  
7 monitors that are directly related to the external cryogenics system, which have substantial inter-  
8 faces with the Long-Baseline Neutrino Facility (LBNF). LBNF provides the needed expertise for  
9 these systems and is responsible for the design, installation, and commissioning, while the CISC  
10 consortium provides the resources and supplements labor as needed.

11 A cryogenic instrumentation test facility (CITF) for the instrumentation devices is also part of  
12 the cryogenics instrumentation. CISC is responsible for design through commissioning in the  
13 DP module of liquid and gaseous argon instrumentation devices: purity monitors, thermometers,  
14 capacitive level meters, pressure meters, cameras, and light-emitting system, and their associated  
15 feedthroughs.

16 Cryogenics instrumentation requires significant physics and simulation work, such as E field simu-  
17 lations and cryogenics modeling studies using computational fluid dynamics (CFD). E field simu-  
18 lations identify desirable locations for instrumentation devices in the cryostat, away from regions  
19 of high E field, so their presence does not induce large field distortions. CFD simulations help  
20 identify expected temperature, impurity, and velocity flow distributions and guide the placement  
21 and distribution of instrumentation devices inside the cryostat.

### 22 **1.1.1.2 Slow Controls**

23 The slow controls portion of CISC comprises three main components: hardware, infrastructure,  
24 and software. The slow controls hardware and infrastructure comprises networking hardware,  
25 signal processing hardware, computing hardware, and associated rack infrastructure. The slow  
26 controls software provides, for every slow control quantity, the central slow controls processing  
27 architecture, databases, alarms, archiving, and control room displays.

28 CISC provides software and infrastructure for controlling and monitoring all detector elements  
29 that provide data on the health of the detector module or conditions important to the experiment,  
30 as well as certain hardware. Slow controls includes the systems detailed below.

31 Slow controls base software and databases are the central tools needed to develop control and  
32 monitoring for various detector systems and interfaces. These include

- 1 • base input/output software;
- 2 • alarms, archiving, display panels, and similar operator interface tools; and
- 3 • slow controls system documentation and operations guidelines.

4 Slow controls for external systems collect data from systems external to the detector module and  
5 provide status monitoring to operators and for archiving. They collect data on beam status,  
6 cryogenics status, data acquisition (DAQ) status, facilities systems status, interlock status bit  
7 monitoring (but not the actual interlock mechanism), ground impedance monitoring, and possibly  
8 building and detector hall monitoring, as needed.

9 The DUNE detector safety system (DDSS) can provide inputs to CISC on safety interlock status,  
10 and CISC will monitor and make that information available to the experiment operators and  
11 experts as needed. However, DDSS and CISC are separate monitors, and the slow controls portion  
12 of CISC does not provide any inputs to DDSS. A related question is whether CISC can provide  
13 software intervention before a hardware safety interlock. In principle such intervention can be  
14 implemented in CISC, presumably by (or as specified by) the hardware experts. For example, at  
15 ProtoDUNE-SP, the automatic lowering of HV to clear streamers was implemented in the software  
16 for the HV control using CISC-level software.

17 Slow controls covers software interfaces for detector hardware devices:

- 18 • monitoring and control of all power supplies,
- 19 • full rack monitoring (rack fans, thermometers and rack protection system),
- 20 • CISC instrumentation device monitoring (and control to the extent needed),
- 21 • calibration device monitoring (and control to the extent needed),
- 22 • charge-readout plane (CRP) instrumentation device monitoring (and control to the extent  
23 needed),
- 24 • power distribution unit and computer hardware monitoring,
- 25 • HV system monitoring through cold cameras, and
- 26 • inspection of detector components using warm cameras.

27 CISC will develop, install, and commission any hardware related to rack monitoring and control  
28 for the detector racks. Most power supplies may only require a cable from the device to an  
29 Ethernet switch, but some power supplies might require special cables (e.g., GPIB or RS232) for  
30 communication. The CISC consortium will provide these control cables.

31 CISC participates in additional activities outside the scope of the consortium that require coordi-  
32 nation with other groups. This is discussed in Section 1.4.4.

## 1.1.2 Design Considerations

Important design considerations for instrumentation devices include stability, reliability, and longevity, so that devices can survive for at least 20 years. Such longevity is uncommon for any device, so the overall design allows replacement of devices where possible. Some devices are critical for filling and commissioning but less critical for later operations; for these devices we specify a minimum lifetime of 18 months and 20 years as a desirable goal. DUNE requires the E field on any instrumentation devices inside the cryostat to be less than 30 kV/cm to minimize the risk of dielectric breakdown in LAr.

An important consideration for event reconstruction is the maximum noise level, induced by instrumentation devices, that the readout electronics can tolerate. ProtoDUNE-DP is evaluating this. Table 1.1 shows the selected top-level specifications for CISC subsystems. Tables 1.2, 1.3, and 1.4 show the full set of specifications for the CISC subsystems. In all those tables two values are quoted for most of the design parameters: i) *specification*, which is the minimal requirement to guarantee the detector performance, and ii) *goal*, an improved version enabling more detailed studies which could lead to an improved design of the cryogenics system for subsequent detectors.

Data from purity monitors and different types of thermometers will be used to validate the LAr fluid flow model. A number of requirements drive the design parameters for the precision and granularity of monitor distribution across the cryostat. For example, the electron lifetime measurement precision must be 2.3 % to keep the bias on the charge readout in the TPC below 0.5 % at 5 ms lifetime. For thermometers, the parameters are driven by ProtoDUNE-SP and ProtoDUNE-DP designs as well as the comparison of ProtoDUNE-SP data to CFD simulations. The temperature measurement resolution in liquid phase must be less than 2 mK, and the relative precision of those measurements must be less than 5 mK. The resolution is defined as the temperature root mean square (RMS) for individual measurements and is driven by the electronics. The relative precision also includes the effect of reproducibility for successive immersions in liquid argon (LAr). The relative precision is particularly important in characterizing gradients less than 20 mK. As described below, the laboratory calibration data and the recent analysis of thermometer instrumentation data from ProtoDUNE-SP shows that a 2.5 mK relative precision is achievable.

It is also important to monitor the temperature and pressure in the gas phase over the liquid phase because they affect the large electron multiplier (LEM) gain calibration. The gas pressure must be monitored to 1 mbar precision and accuracy. Near the surface of the liquid, the temperature gradient of the gas must be measured with an array of temperature probes with a vertical pitch that increases with height (from 1 to 5 cm). The LAr differential pressure level meters must be precise to 14 mm to measure accurately during filling. Moreover, multiple capacitive level meters with better than 5 mm precision will be needed to more precisely measure the LAr level and for LAr-level based interlocks for other systems (e.g., HV).

As shown in Table 1.3, several requirements drive the design of cold and warm cameras and the associated light emitting system. The components of the camera systems must not contaminate the LAr or produce bubbles to avoid increasing the risk of HV discharge. Both cold and warm cameras must provide coverage of at least 80 % of the TPC volume with a resolution of 1 cm for cold cameras and 2 mm for warm cameras on the TPC.

- 1 For the CITF, a cryostat with a capacity of only 0.5 to approximately 3 m<sup>3</sup> will suffice and will  
 2 keep turn around times and filling costs low. For gas analyzers, the operating range must allow us  
 3 to establish useful electron lifetimes; details are in Table 1.2.
- 4 For slow controls, the system must be sufficiently robust to monitor a minimum of 150,000 variables  
 5 per detector module, and support a broad range of monitoring and archiving rates; the estimated  
 6 variable count, data rate, and archive storage needs are discussed in section 1.3.4. The system  
 7 must also interface with a large number of detector subsystems and establish two-way communi-  
 8 cation with them for control and monitoring. For the alarm rate, 150 alarms/day is used as the  
 9 specification as it is the maximum to which humans can be expected to respond. The goal for the  
 10 alarm rate is less than 50 alarms/day. The alarm logic system will need to include features for  
 11 managing “alarm storms” using alarm group acknowledgment, summaries, delays, and other aids.

Table 1.1: Specifications for DP-CISC [ref tab:spec:DP-CISC](#)

Label	Description	Specification (Goal)	Rationale	Validation
DP-FD-5	Liquid argon purity	> 5 ms	Directly impacts the number of electrons received at the CRP collection strips and hence the S/N.	Purity monitors and cosmic ray tracks
DP-FD-15	LAr nitrogen contamination	< 25 ppm	Maintain 0.5 PE/MeV PDS sensitivity required for triggering proton decay near cathode.	In situ measurement
DP-FD-18	Cryogenic monitoring devices		Constrain uncertainties on detection efficiency, fiducial volume.	ProtoDUNE
DP-FD-25	Non-FE noise contributions	$\ll 1000 e^-$	High S/N for high reconstruction efficiency.	Engineering calculation and ProtoDUNE
DP-CISC-1	Noise from Instrumentation devices	$\ll 1000 e^-$	Max noise for 5:1 S/N for a MIP passing near cathode; per SBND and DUNE CE	ProtoDUNE
DP-CISC-2	Max. E field near instrumentation devices	< 30 kV/cm (< 15 kV/cm)	Significantly lower than max field of 30 kV/cm per DUNE HV	3D electrostatic simulation
DP-CISC-3	Precision in electron lifetime	< 1.4% (< 1%)	Required to accurately reconstruct charge per DUNE-FD Task Force report.	ProtoDUNE and CITF
DP-CISC-4	Range in electron lifetime	0.04 ms to 10 ms in cryostat, 0.04 ms to 30 ms inline	Slightly more than best values so far observed in other detectors.	ProtoDUNE and CITF
DP-CISC-11	Precision: temperature reproducibility	< 5 mK (2 mK)	Allows validating CFD models that predict gradients less than 15 mK.	ProtoDUNE and CITF
DP-CISC-14	Temperature stability	< 2 mK at all places and times (Match precision requirement at all places, at all times)	Measures temperature map with sufficient precision for the duration of thermometer operations.	ProtoDUNE

DP-CISC-27	Cold camera coverage	> 80% of HV surfaces (100%)	Enables detailed inspection of issues near HV surfaces.	Calculated from location, validated in prototypes.
DP-CISC-51	Slow control alarm rate	< 150/day (< 50/day)	Keeps rate low enough to allow response to every alarm.	Detector module; depends on experimental conditions
DP-CISC-52	Total No. of variables	> 150,000 (150,000 to 200,000)	Scaled from ProtoDUNE	ProtoDUNE and CITF
DP-CISC-54	Archiving rate	0.02 Hz (Broad range 1 Hz to 1 per few min.)	Archiving rate differs by variable, optimized to store important information	ProtoDUNE

### 1.1.3 Fluid Dynamics Simulation

Proper placement of purity monitors, thermometers, and liquid level monitors within the detector module requires knowing how LAr flows within the cryostat, given its fluid dynamics, heat and mass transfer, and distribution of impurity concentrations. Fluid flow is also important in understanding how the positive and negative ion excess created by various sources (e.g., ionization from cosmic rays and  $^{36}\text{Ar}$ ; ion feedback at the liquid-gas interface in a DP detector) is distributed across the detector as it affects E field uniformity. Finally, CFD simulations are crucial to predict the purity of the argon in regions where experimental data is unavailable. The overall goal of the CFD simulations is to better understand and predict the fluid (in either liquid or vapor state) motions and the implications for detector performance.

Fluid motion within the cryostat is driven primarily by small changes in density caused by thermal gradients within the fluid although pump flow rates and inlet and outlet locations also contribute. Heat sources include exterior heat from the surroundings, interior heat from electronics, and heat flow through the pump inlet. In principle, purity monitors can be placed throughout the cryostat to determine if the argon is pure enough for experimentation. However, some areas inside the cryostat are off limits for such monitors.

The fluid flow behavior can be determined by simulating LAr flow within a detector module using Siemens Star-CCM+<sup>1</sup>, a commercially available CFD code. Such a model must properly define the fluid characteristics, solid bodies, and fluid-solid interfaces, as well as provide a way to measure contamination, while still maintaining reasonable computation times. In addition, these fluid dynamics simulations can be compared to available experimental data to assess simulation accuracy and credibility.

Although simulation of the detector module presents challenges, acceptable simplifications can accurately represent the fluid, the interfacing solid bodies, and variations of contaminant concentrations. Because of the magnitude of thermal variation within the cryostat, modeling the LAr is simplified by using constant thermophysical properties, calculating buoyant force with the Boussi-

<sup>1</sup><https://mdx.plm.automation.siemens.com/star-ccm-plus>

Table 1.2: List of specifications for the different CISC subsystems.

Quantity/Parameter	Specification	Goal
Noise from instrumentation devices	$\ll 1000 e^-$	
Max. E field near instrumentation devices	$< 30 \text{ kV/cm}$	$< 15 \text{ kV/cm}$
<b>Thermometers (LAr)</b>		
Vertical density of sensors for T-gradient monitors	$> 2 \text{ sensor/m}$	$> 4 \text{ sensors/m}$
2D horizontal density for bottom individual sensors	$1 \text{ sensor}/5(10) \text{ m}$	$1 \text{ sensor}/3(5) \text{ m}$
Resolution of temperature measurements	$< 2 \text{ mK}$	$< 0.5 \text{ mK}$
Precision: temperature reproducibility	$< 5 \text{ mK}$	$2 \text{ mK}$
Stability	$< 2 \text{ mK}$ at all places and times	Match precision requirement at all places/times
Discrepancy between laboratory and <i>in situ</i> calibrations for temperature sensors	$< 5 \text{ mK}$	$< 3 \text{ mK}$
Discrepancy between measured temperature map and CFD simulations in ProtoDUNE-SP	$< 5 \text{ mK}$	
<b>Thermometers (GAr)</b>		
Thermometer density (decreases with height)	$1 \text{ sensor}/2-10 \text{ cm}$	$1 \text{ sensor}/1-5 \text{ cm}$
Thermometer coverage	$40 \text{ cm}$	$60 \text{ cm}$
Resolution of temperature measurements	$5 \text{ mK}$	$0.5 \text{ mK}$
Precision: temperature reproducibility	$100 \text{ mK}$	$100 \text{ mK}$
<b>Thermometers (All)</b>		
Reliability	$80\%$ (in 18 months)	$50\%$ (during 20 years)
Longevity	$> 18 \text{ months}$	$> 20 \text{ years}$
<b>Level Meters</b>		
Precision (LBNF side)	$0.1\%$ over $14 \text{ m}$ ( $14 \text{ mm}$ )	
Precision (capacitive level meters, DUNE side)	$1 \text{ cm}$	$< 5 \text{ mm}$
Longevity	$20 \text{ years}$	$> 20 \text{ years}$
<b>Gas Analyzers</b>		
Operating Range O2	$0.2 \text{ (air) to } 0.1 \text{ ppt}$	
Operating Range H2O	Nom. air to sub ppb; contaminant-dependent	
Operating Range N2	Nominally Air Nom. air to sub ppb; contaminant-dependent	
Precision: 1 sigma at zero	per gas analyzer range	
Detection limit: 3 sigma	Different analyzer modules needed to cover entire range	
Stability	$< \%$ of full scale range.	
Longevity	$> 10 \text{ years}$	



Table 1.3: List of specifications for the different CISC subsystems.

Quantity/Parameter	Specification	Goal
<b>Purity Monitors</b>		
Precision in electron lifetime	<2.3% at 5 ms (<4% at 9 ms)	< 1%
Range in electron lifetime	0.04 - 10 ms	(0.04 - 30 ms inline)
Longevity	20 years	> 20 years
Stability	Match precision requirement at all places/times	
Reliability	Daily measurements	Measurements as needed
<b>Pressure Meters (GAR)</b>		
Relative precision (DUNE side)	0.1 mbar	
Absolute precision (DUNE side)	<5 mbar	
<b>Cold cameras</b>		
Coverage	80% of the exterior of HV surfaces	100%
Frames per second	yet to be defined	
Resolution	1 cm on the TPC	yet to be defined
Duty cycle	yet to be defined	
Longevity	> 18 months	> 20 years
<b>Inspection cameras</b>		
Coverage	80% of the TPC	yet to be defined
Frames per second	yet to be defined	
Resolution	2 mm on the TPC	yet to be defined
Heat transfer	no generation of bubbles	
Longevity	> 18 months	> 20 years
<b>Light emitting system</b>		
Radiant flux	> 10 mW/sr	100 mW/sr
Power	< 125 mW/LED	
Wavelength	red/green	IR/white
Longevity	> 18 months (for cold cameras)	> 20 years
<b>cryogenic instrumentation test facility (CITF)</b>		
Dimensions	0.5 to 3 cubic meters	
Temperature stability	$\pm 1$ K	
Turn-Around time	$\sim 9$ days	9 days
LAr purity	O <sub>2</sub> , H <sub>2</sub> O: low enough to measure drifting electrons of devices under test, $\sim 0.5$ ms. N <sub>2</sub> : ppm for scintillation light tests.	>1.0 ms

Table 1.4: List of specifications for the different CISC subsystems.

Quantity/Parameter	Specification	Goal
<b>Slow Controls</b>		
Alarm rate	<150/day	< 50/day
Total No. of variables	150,000	150,000 - 200,000
Server rack space	2 racks	3 racks
Archiving rate	0.02 Hz	Broad range 1 Hz to 1 per few min.
Near detector status	Beam conditions and detector status	Full beam and detector status

1 nesq Model (using a constant density for the fluid with application of a temperature-dependent  
 2 buoyant force), and a standard shear stress transport turbulence model. Solid bodies that touch  
 3 the LAr include the cryostat wall, photon detectors, and light reflector foils. The field cage (FC)  
 4 planes, cathode planes, and grounding grid can be represented by porous bodies. Because impu-  
 5 rity concentration and electron lifetime do not affect fluid flow, these variables can be simulated  
 6 as passive scalars, as is commonly done for smoke released [2] in air or dyes released in liquids.

7 Discrepancies between real data and simulations may affect detector performance. Simulation  
 8 results contribute to decisions about where to place sensors and monitors and to the definitions  
 9 of various calibration quantities. Methods of mitigating such risks include well established con-  
 10 vergence criteria, sensitivity studies, and comparison to results of previous CFD simulation work.  
 11 Moreover, the simulation will be improved with input from LAr temperature and purity measure-  
 12 ments and validation tests from ProtoDUNE-SP<sup>2</sup>.

13 Taking into account that the CFD model can predict both temperature and impurity levels, the  
 14 procedure for validating and tuning the CFD model will be the following: i) temperature predic-  
 15 tions will be constrained with temperature measurements in numerous locations in the cryostat to  
 16 improve the CFD model, ii) the improved model is then used to predict the LAr impurity level at  
 17 the location of purity monitors, iii) this prediction is compared with the actual measurement from  
 18 purity monitors to further constraint the CFD model.

19 Figure 1.2 shows an example of the temperature distribution on a plane intersecting an LAr inlet  
 20 and at a plane halfway between an inlet and an outlet in the SP module. Note the plume of higher  
 21 temperature LAr between the walls and the outer anode plane assembly (APA) on the inlet plane.  
 22 The current placement of instrumentation in the cryostat as shown in Figure 1.3 was determined  
 23 using temperature and impurity distributions from CFD simulations.

24 The strategy for future CFD simulations begins with validating a CFD model for ProtoDUNE-  
 25 DP using ProtoDUNE-DP LAr instrumentation data, followed by modeling the FD DP module  
 26 to derive specifications for instrumentation. We are pursuing a prioritized set of studies to help

<sup>2</sup>Because ProtoDUNE-DP was not instrumented with high-precision thermometers in the liquid phase and because the cryogenics design is the same for SP and DP modules of the DUNE FD, ProtoDUNE-SP data will be used to validate the liquid CFD model.

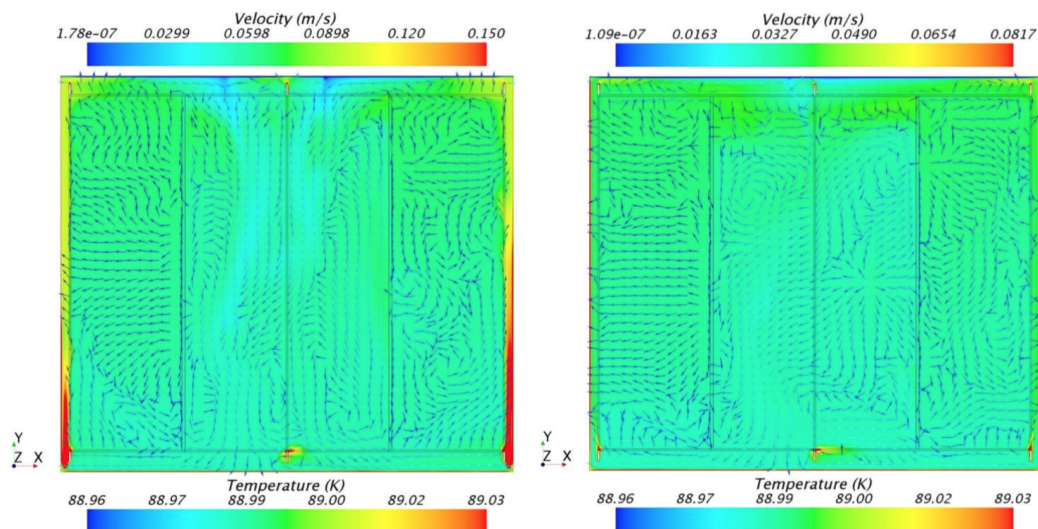


Figure 1.2: Distribution of temperature on a plane intersecting an inlet (left) and halfway between an inlet and an outlet (right), as predicted by previous CFD simulations for the SP module (from [3]).

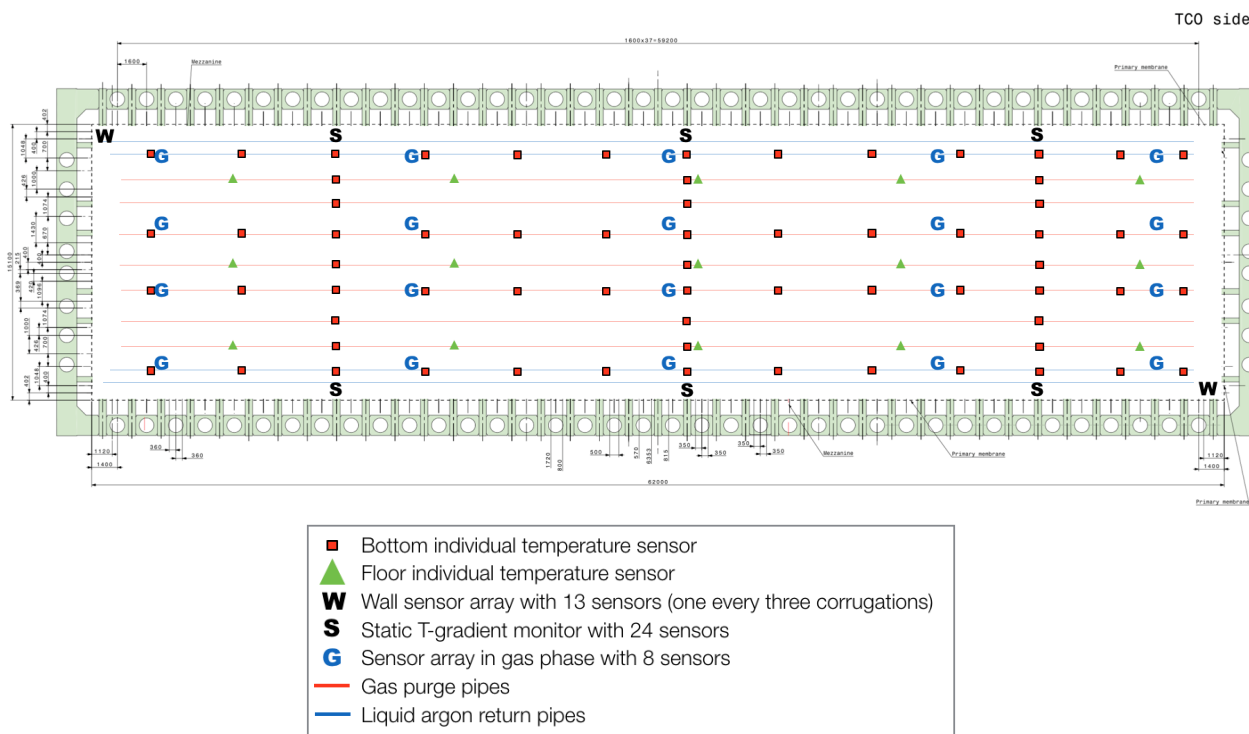


Figure 1.3: Distribution of temperature sensors inside the cryostat.

- 1 determine requirements for other systems. We plan to
- 2 • review the DUNE DP FD cryogenics system design and verify the current implementation
  - 3 in simulation to ensure that the simulation represents the actual design;
  - 4 • validate the liquid CFD model using thermometer data from ProtoDUNE-SP because we
  - 5 have no high precision T-gradient thermometers in ProtoDUNE-DP to validate the liquid
  - 6 model;
  - 7 • model the ProtoDUNE-DP gas regions with the same precision as the FD. The gas model
  - 8 should how to place thermometers in the argon gas and verify the design of the gaseous argon
  - 9 purge system;
  - 10 • perform a CFD study to determine the feasibility of a weir for DP; this should determine if
  - 11 it can be used to clean the LAr surface before the extraction grid is submerged in the DP
  - 12 module.

13 refer to table 1.5 here or move table down to after reference

Table 1.5: CFD input parameters for ProtoDUNE.

Parameter	Value	Comments
Cryostat height	7.878 m	Measured with laser (1 cm error approx.)
LAr surface height	7.406 m	Measured by capacitive level meter (< 1 cm error)
Ullage pressure	1.045 bar	Measured by pressure gauges
LAr surface temperature	87.596 K	Computed using ullage pressure and [4]
LAr inlet temperature	outlet + 0.2 K	Estimated
LAr flow rate per pipe	0.4170025 kg/s	
Heat flux	5.76 W/m <sup>2</sup>	This is the heat flux from all four walls as well as the ground
Vapor drawn from the chimneys	5-7 gr/sec	Among all chimneys

### 14 1.1.3.1 Validation in ProtoDUNE

15 Given the HV configuration in ProtoDUNE-DP is more complex than ProtoDUNE-SP (much  
 16 higher electric potential and no zero field regions on the TPC sides), ProtoDUNE-DP was not in-  
 17 strumented with vertical arrays of high precision temperature sensors in the liquid as in ProtoDUNE-  
 18 SP. These temperature sensors are important elements for validating CFD simulations, but because  
 19 the cryostat and cryogenics system designs are identical in both the SP and DP far detector mod-  
 20 ules, temperature data from ProtoDUNE-SP can be used to validate the liquid model for the DP  
 21 FD. For validating the gas model, data from the vertical array of thermometers installed in the  
 22 ProtoDUNE-DP will be used.

23 ProtoDUNE-SP has collected data to validate the CFD using

- 1 • static and dynamic T-gradient thermometers,
- 2 • individual temperature sensors placed in the return LAr inlets,
- 3 • two 2D grids of individual temperature sensors installed below the bottom ground planes
- 4 and above the top ground planes,
- 5 • a string of three purity monitors vertically spaced from near the bottom of the cryostat to
- 6 just below the LAr surface,
- 7 • two pressure sensors (relative and absolute) in the argon gas,
- 8 • H<sub>2</sub>O, N<sub>2</sub>, and O<sub>2</sub> gas analyzers,
- 9 • LAr level monitors, and
- 10 • standard cryogenic sensors, individual temperature sensors placed around the cryostat on
- 11 the membrane walls, and recirculation flow rates transducers.

12 On the other hand, ProtoDUNE-DP has installed the following instrumentation devices to validate  
13 CFD:

- 14 • two purity monitors, one at the bottom of the cryostat and another 2 m from the bottom;
- 15 • two pressure sensors (relative and absolute) in the argon gas;
- 16 • vertical array of thermometers in argon gas;
- 17 • H<sub>2</sub>O, N<sub>2</sub>, and O<sub>2</sub> gas analyzers;
- 18 • LAr level monitors; and
- 19 • standard cryogenic sensors and individual temperature sensors placed around the cryostat
- 20 on the membrane walls and recirculation flow rates transducers.

21 The data, which has been logged through the ProtoDUNE-SP slow control system [5], is available  
22 for offline analysis.

23 In parallel, CISC has produced a ProtoDUNE-SP CFD model with input from ProtoDUNE-SP  
24 measurements (see Table 1.5). Streamlines<sup>3</sup> from the current simulation (Figure 1.4) show the flow  
25 paths from the four cryostat inlets to the outlet. Validating this model requires an iterative process  
26 in which several versions of the CFD simulation, using different input parameters, eventually  
27 converge to a reasonable agreement with data from instrumentation devices.

28 The agreement is already quite good.

29 Once the ProtoDUNE-SP CFD model predicts the fluid temperature in the entire cryostat to a  
30 reasonable level under different conditions, this model will be extrapolated to ProtoDUNE-DP  
31 to produce maps of impurity levels in the detector module. These can be converted easily into  
32 electron lifetime maps, which we will compare to the ProtoDUNE-DP purity monitor data.

---

<sup>3</sup>In fluid mechanics, a streamline is a line that is everywhere tangent to the local velocity vector. For steady flows, a streamline also represents the path that a single particle of the fluid will take from inlet to exit.

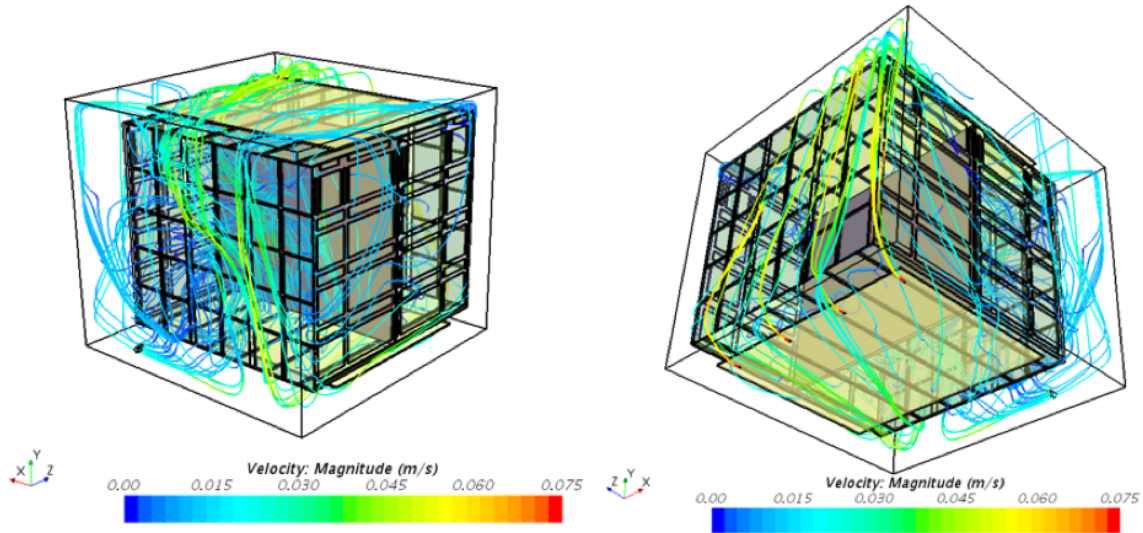


Figure 1.4: Streamlines for LAr flow inside ProtoDUNE-SP.

## 1.2 Cryogenic Instrumentation

Instrumentation inside the cryostat must accurately report the condition of the LAr, so we can ensure that it is adequate for operating the TPC. This instrumentation includes purity monitors to check the level of impurity in the argon and provide high-precision electron lifetime measurements, as well as gas analyzers to verify that levels of atmospheric contamination do not drop below certain limits during cryostat purging, cooling, and filling. Temperature sensors deployed in vertical arrays and at the top and bottom of the detector module monitor the cryogenics system operation, providing a detailed 3D temperature map that helps predict LAr purity across the entire cryostat. The cryogenics instrumentation also includes LAr level monitors and a system of internal cameras to help find sparks in the cryostat and to monitor the overall cryostat interior.

The proper placement of purity monitors, thermometers, and liquid-level monitors in the detector module requires understanding LAr fluid dynamics, heat and mass transfer, and distribution of impurity concentrations within the cryostat. Both this and coherent analysis of the instrumentation data require CFD simulation results.

ProtoDUNE-SP and ProtoDUNE-DP are testing the performance of all cryogenic instrumentation for the DP module, validating the baseline design. See Section 1.2.8 for more detail.

### 1.2.1 Thermometers

As discussed in Section 1.1.3, a detailed 3D temperature map is important in monitoring the cryogenic system for correct functioning and the LAr for uniformity. Given the complexity and size of purity monitors, they can only be installed where there is sufficient space to provide a local measurement of LAr purity. A direct measurement of the LAr purity across the entire cryostat is

1 not feasible, but a sufficiently detailed 3D temperature map based on CFD simulations can predict  
2 the purity. The vertical coordinate is especially important because it will relate closely to the LAr  
3 recirculation and uniformity. Monitoring the gas phase in the DP technology is also important  
4 because the LEM gain calibration depends on gas temperature.

5 The baseline sensor distribution is shown in Figure 1.3. This baseline distribution will evolve as  
6 more information becomes available (precise CFD simulations, better understanding of cryostat  
7 ports, installation interfaces with other groups), but the baseline suffices to establish the overall  
8 strategy.

9 High-precision temperature sensors will be distributed near the TPC FC walls in two ways: (1)  
10 in high density ( $> 1$  sensors/m) vertical arrays (called T-gradient monitors) and (2) in coarser  
11 ( $\sim 1$  sensor/5 m) 2D arrays (called individual sensors) at the bottom of the detector module.  
12 The temperature map in the gas phase will be measured using several vertical arrays of standard  
13 Resistance temperature detector (RTD)s distributed above the CRPs.

14 Temperature variations inside the cryostat should be very small (0.02 K for the liquid phase (see  
15 Figure 1.2), so sensors must be cross-calibrated to more than 0.005 K. Most sensors will be cal-  
16 ibrated in the laboratory before installation. (Installation is described in Section 1.4.5.2.) Cali-  
17 brating sensors before installation is the only option for sensors installed in places where space is  
18 limited. Given the precision required and the unknown longevity of the sensors, possibly requiring  
19 another calibration after some time, an additional method will be used for one of the T-gradient  
20 monitors based on a movable system that can be used to cross calibrate the temperature sensors  
21 *in situ*, as described in Section 1.2.1.1.

22 The baseline designs for all thermometer systems have three elements in common: sensors, cables,  
23 and readout system. We plan to use Lake Shore PT100-series<sup>4</sup> platinum sensors with 100  $\Omega$  resis-  
24 tance because, in the temperature range 83 K to 92 K, they show high reproducibility of  $\sim 5$  mK  
25 and absolute temperature accuracy of 100 mK. Using a four-wire readout greatly reduces issues  
26 with lead resistance, any parasitic resistances, connections through the flange, and general electro-  
27 magnetic noise pick up. Lakeshore PT102 sensors (see Figure 1.5, right) were used in the 35 ton  
28 prototype prototype and ProtoDUNE-SP, giving excellent results. For the inner readout cables,  
29 a custom cable made by Axon<sup>5</sup> is the baseline. It consists of four teflon-jacketed copper wires  
30 (AWG28), forming two twisted pairs, with a metallic external shield and an outer teflon jacket.  
31 The readout system is described in Section 1.2.1.6.

32 Another set of lower-precision sensors epoxied into the bottom membrane of the cryostat will  
33 monitor cryostat filling in the initial stage. Finally, the inner walls and roof of the cryostat will  
34 have the same types of sensors to monitor the temperature during cooldown and filling (W sensors  
35 in Figure 1.3).

---

<sup>4</sup>Lake Shore Cryotronics™ platinum RTD series, <https://www.lakeshore.com/>.

<sup>5</sup>Axon™ Cable, <http://www.axon-cable.com>.

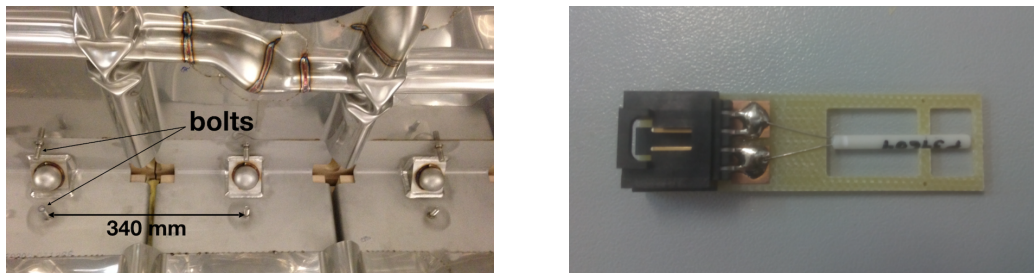


Figure 1.5: Left: bolts at the bottom corner of the cryostat. Right: Lakeshore PT102 sensor mounted on a PCB with an IDC-4 connector.

### 1 1.2.1.1 Dynamic T-gradient monitors

2 Potential differences in sensor readings before and after sensors are installed in a detector module  
3 and potential drifts over the lifetime of the module may affect accuracy of the vertical temperature  
4 gradient measurement. Thus, to address these concerns, a dynamic temperature monitor can cross-  
5 calibrate sensor readings *in situ*. This T-gradient monitor is motorized, allowing vertical movement  
6 of the temperature sensor array in the detector module, enabling precise cross-calibration between  
7 the sensors *in situ*, as illustrated in Figure 1.6.

8 Cross-calibrations requires several steps. In step 1, the temperature reading of all sensors is taken  
9 at the home (lowest) position of the carrier rod. In step 2, the stepper motor moves the carrier  
10 rod up 25 cm. The sensors along the entire carrier rod are positioned 25 cm apart, so when the  
11 system moves up 25 cm, each sensor is positioned at the height occupied by another sensor in step  
12 1. Then a second temperature reading is taken. Other than the lowest position, this means two  
13 temperature measurements are taken at each location with different sensors. Assuming that the  
14 temperature at each location is stable over the few minutes required to make the measurements,  
15 any differences in the temperature readings between the two different sensors would be due to their  
16 relative measurement offset. This difference is then calculated for all locations. In step 3, readout  
17 differences between pairs of sensors at each location are linked to one another, so each sensor  
18 measures the temperature at all heights. In this way, temperature readings from all sensors are  
19 cross-calibrated *in situ*, canceling all possible offsets due to electromagnetic noise or any parasitic  
20 resistances that may occur despite the four-point connection to the sensors that should cancel  
21 most offsets. These measurements are taken with a very stable current source, which ensures high  
22 precision of repeated temperature measurements over time. The dynamic T-monitor operates with  
23 a stepper-motor, so measurements are delivered with high spatial resolution.

24 A total of 72 sensors will be installed and spaced 25 cm apart, although at the top and bottom  
25 1 m of the carrier rod, sensor spacing is decreased to 10 cm. With the vertical displacement of  
26 the system, every sensor can be moved to the nominal position of at least five other sensors,  
27 minimizing any risks associated with sensor failure and providing several points of comparison.  
28 The total expected motion range of the carrier rod is 1.35 m.

29 This procedure was tested in ProtoDUNE-SP, where the system was successfully moved up by a  
30 maximum of 51 cm, allowing cross-calibration of all sensors (22 sensors with 10.2 cm spacing at  
31 top and bottom and 51 cm in the middle).



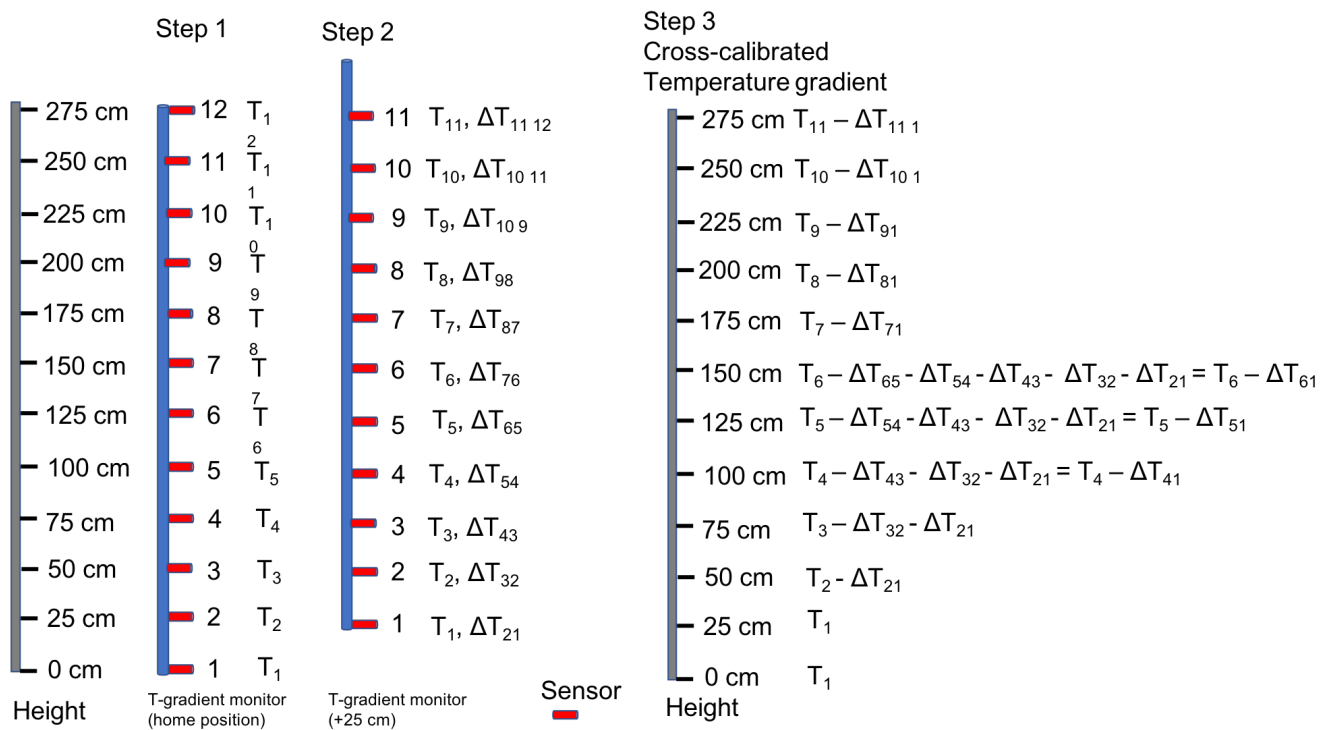


Figure 1.6: In step 1, sensor temperature measurements are taken with the T-gradient monitor in the home position. In step 2, the entire system is moved up 25 cm, and another set of temperature readings is taken by all sensors. Then, the offsets between pairs of sensors are calculated for each position. In step 3, offsets are linked together, providing cross-calibration of all sensors, to obtain the entire vertical temperature gradient measurement for a single sensor (number 1 in this case).

- 1 Figure 1.7 shows the temperature profile after calibration when the recirculation pumps are off.
- 2 Under these conditions the temperature should be very homogeneous except near the surface. This
- 3 is indeed what is observed in that figure, demonstrating the reliability of the method.

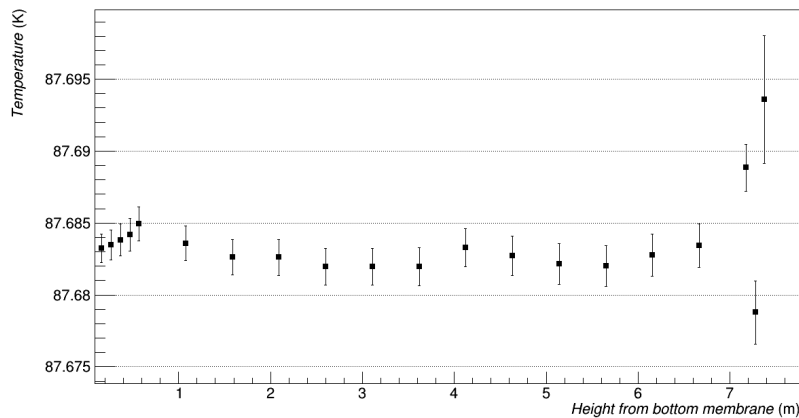


Figure 1.7: Temperature profile as measured by the dynamic T-gradient monitor after cross-calibration when the recirculation pumps are off. Temperature variation is approximately 3 mK except close to the top and the gas phase interface, as expected.

- 4 A dynamic T-gradient monitor has three parts: a carrier rod on which sensors are mounted; an
- 5 enclosure above the cryostat housing space that allows the carrier rod to move vertically 1.5 m
- 6 over its lowest location; and the motion mechanism. The motion mechanism is a stepper motor
- 7 connected through a ferrofluidic dynamic seal to a gear and pinion motion mechanism. The sensors
- 8 have two pins soldered to a PCB. Two wires are individually soldered to the common soldering
- 9 pad for each pin. A cutout in the PCB around the sensor allows free flow of argon for more
- 10 accurate temperature readings. Stepper motors typically have very fine steps that allow highly
- 11 precise positioning of the sensors. Figure 1.8 shows the overall design of the dynamic T-gradient
- 12 monitor. The enclosure has two parts connected by a six-cross flange. One side of this flange will
- 13 be used for signal wires, another will be used as a viewing window, and the two other ports will
- 14 be spares. Figure 1.9, left, shows the PCB mounted on the carrier rod and the sensor mounted
- 15 on the PCB along with the four point connection to the signal readout wires. Figure 1.9, right,
- 16 shows the stepper motor mounted on the side of the rod enclosure. The motor remains outside
- 17 the enclosure, at room temperature, as do its power and control cables.



Figure 1.8: A schematic of the dynamic T-gradient monitor.

### 18 1.2.1.2 Static T-gradient monitors

- 19 Several vertical arrays of high-precision temperature sensors cross-calibrated in the laboratory will
- 20 be installed behind the lateral FCs.

- 21 The baseline design assumes six arrays with 24 sensors each. Spacing between sensors is 40 cm at
- 22 the top and bottom and 80 cm in the middle area.

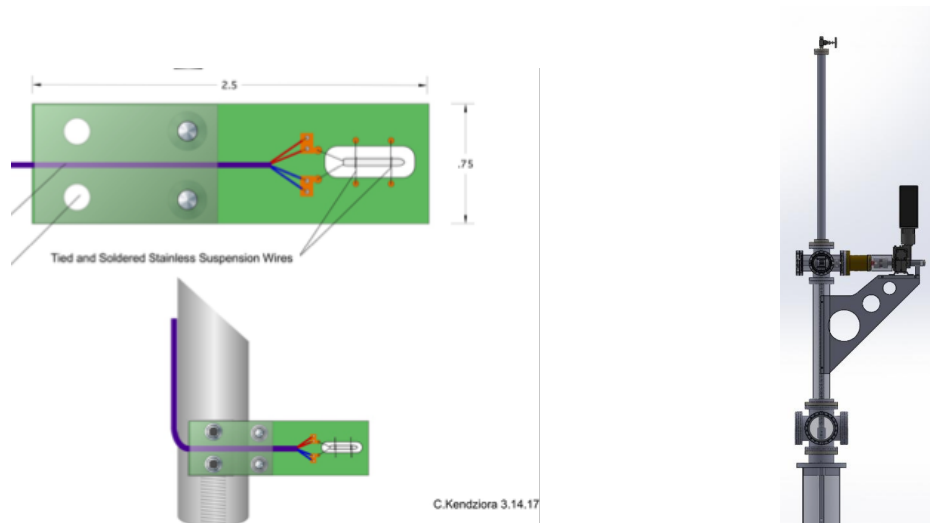


Figure 1.9: Left: Sensor mounted on a PCB board, and PCB board mounted on the rod. Right: The driving mechanism of the dynamic T-gradient monitor consisting of a stepper motor driving the pinion and gear linear motion mechanism.

- 1 As shown in Figure 1.10 a configuration with 48 sensors was appropriate in ProtoDUNE-SP, as it
- 2 should be in the DP module where the expected total gradient is no larger than in ProtoDUNE-SP
- 3 (see Figure 1.2).

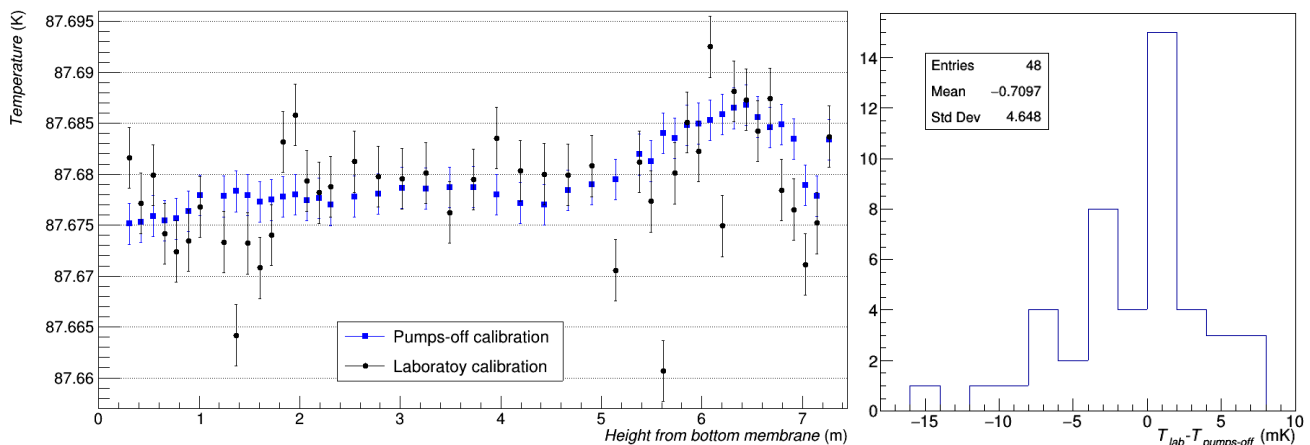


Figure 1.10: Left: Temperature profile as measured by the static T-gradient monitor for two different calibration methods. Right: Distribution of the difference between both methods.

- 4 Sensors will be cross-calibrated in the laboratory using a controlled environment and a high-
- 5 precision readout system, described in Section 1.2.1.6.
- 6 The accuracy of the calibration for ProtoDUNE-SP was estimated to be 2.6 mK (see Figure 1.11).
- 7 Figure 1.10 shows the preliminary results of the analysis of ProtoDUNE-SP static T-gradient
- 8 monitor data. The temperature profile was computed using both the laboratory calibration and
- 9 the so-called *in-situ pump-off calibration*, which consists of estimating the offsets between sensors
- 10 assuming the temperature of LAr in the cryostat is homogeneous when the re-circulation pumps
- 11 are off. (The validity of this method is demonstrated in Section 1.2.1.1.) The RMS of the difference

- 1 between both methods is 4.6 mK, slightly more than the value quoted above for the accuracy of  
 2 laboratory calibration, due to the presence of a few outliers (under investigation) and the imperfect  
 3 assumption of homogeneous temperature when pumps are off (see Figure 1.7).

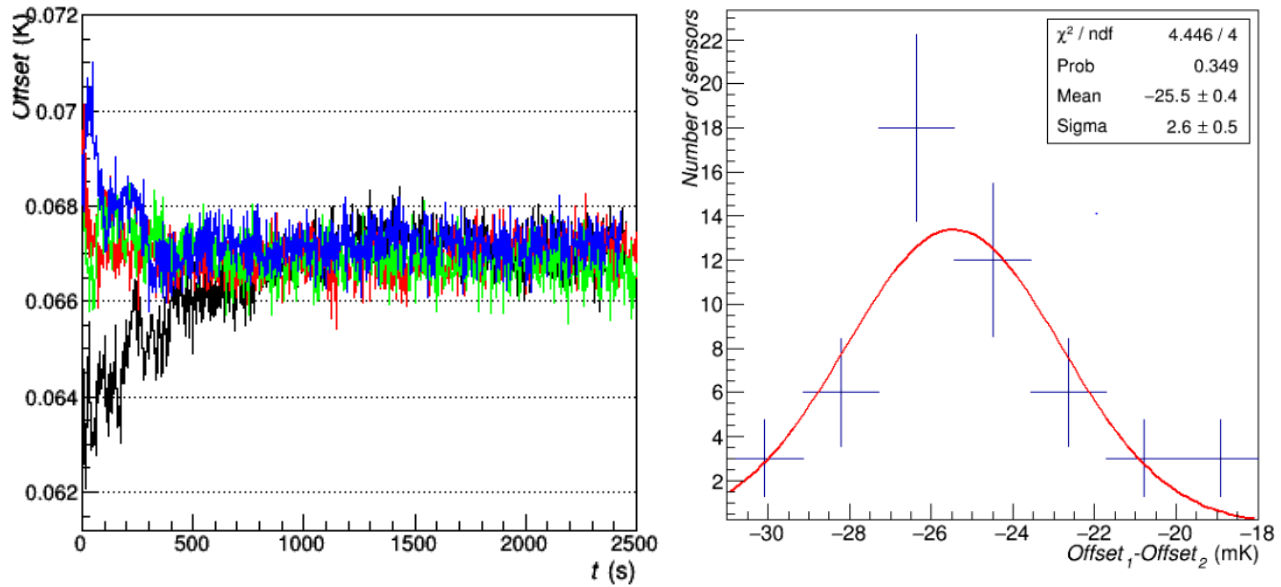


Figure 1.11: Left: Temperature offset between two sensors as a function of time for four independent immersions in LAr. The reproducibility of those sensors, defined as the RMS of the mean offset in the flat region, is  $\sim 1$  mK. The resolution for individual measurements, defined as the RMS of one offset in the flat region, is more than 0.5 mK. Right: Difference between the mean offset obtained with two independent calibration methods for the 51 calibrated sensors. The standard deviation of this distribution is interpreted as precision of the calibration.

- 4 Figure 1.12 shows the baseline mechanical design of the static T-gradient monitor. Two vertical  
 5 strings are anchored at the top and bottom corners of the cryostat using the available M10 bolts  
 6 (see Figure 1.5, left). One string routes the cables while the other, separated from the first by  
 7 150 mm, supports the temperature sensors and the individual Faraday cages. Given the height  
 8 of the cryostat, an intermediate anchoring point might be needed to reduce swinging. To reduce  
 9 the effect of shrinkage in the strings under cryogenic conditions and to guarantee that the same  
 10 tension is always applied, springs will be made of materials with low coefficients of linear thermal  
 11 expansion like carbon fiber or invar. A special spring could be also used. A prototype is being  
 12 built at IFIC, where the full system will be mounted using two dummy cryostat corners.

- 13 Figure 1.5, right shows the baseline design of the  $(52 \times 15 \text{ mm}^2)$  PCB support for temperature  
 14 sensors with an IDC-4 male connector.

- 15 A narrower connector (with two rows of two pins each) is being studied. This alternative design  
 16 would reduce the width of the PCB assembly and allow more sensors to be calibrated simultane-  
 17 ously. Each four-wire cable from the sensor to the flange will have an IDC-4 female connector on  
 18 the sensor end; the flange end of the cable will be soldered or crimped to the appropriate connector,  
 19 whose type and number of pins depend on the final design of the detector support system (DSS)  
 20 ports that will be used to extract the cables. SUBD-25 connectors were used in ProtoDUNE-SP.

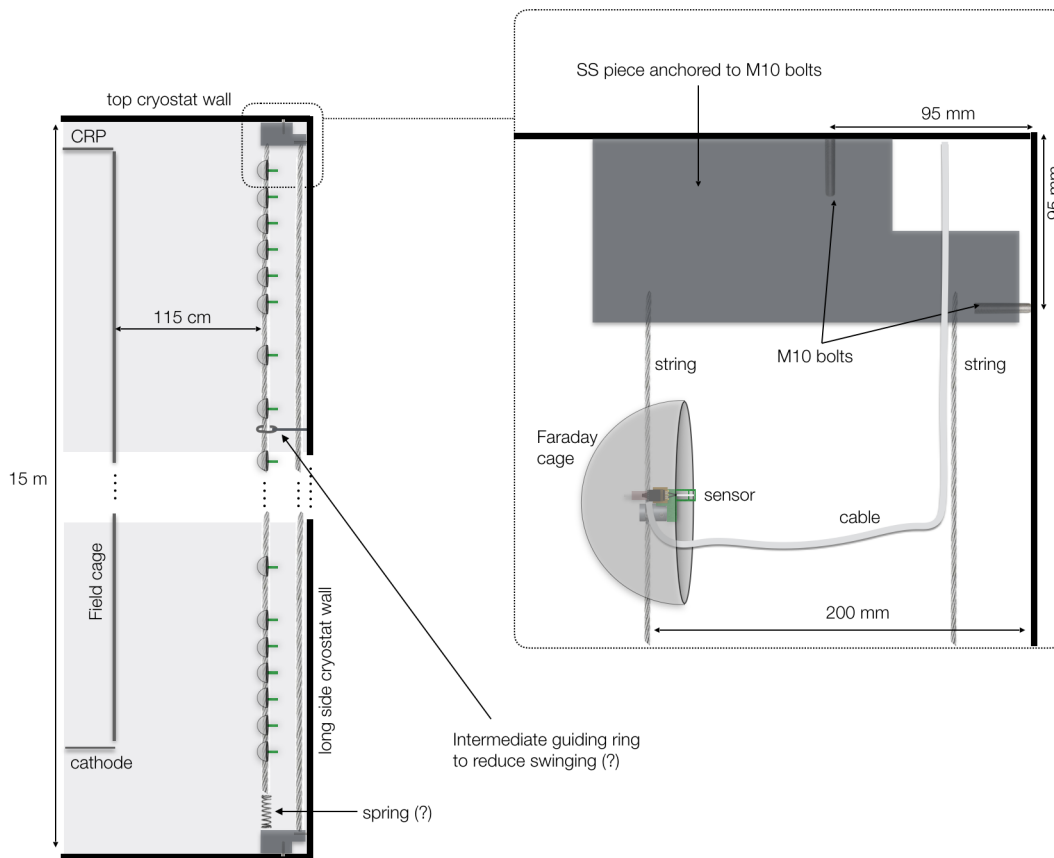


Figure 1.12: Conceptual design of the static T-gradient monitor.

### 1.2.1.3 Individual Temperature Sensors

T-gradient monitors will be complemented by a coarser 2D array (every 5 m) of precision sensors at the bottom of the detector module, as shown in Figure 1.3. These sensors could use the cryogenic pipes as a support structure following the ProtoDUNE-SP design. An alternative design using the support structure for photon detector (PD)s is also under consideration.

As in ProtoDUNE-SP, another set of standard sensors will be evenly distributed and epoxied to the bottom membrane. They will detect the presence of LAr when cryostat filling starts. Finally, two vertical arrays of standard sensors will be epoxied to the lateral walls in two opposite vertical corners, spaced 102 cm apart (every three corrugations), to monitor the cryostat membrane temperature during cooldown and filling.

Whereas in ProtoDUNE-SP, cables were routed individually (without touching neighboring cables or any metallic elements) to prevent grounding loops in case the outer Teflon jacket broke, such a failure is very unlikely. Thus, in the detector modules, cables will be routed in bundles, simplifying the design enormously. Cable bundles of several sizes will be configured using custom made Teflon pieces that will be anchored to different cryostat and detector elements to route cables from sensors to the assigned cryostat ports. For sensors at the bottom (on pipes/PDs and floor), cables will be routed towards the bottom horizontal corner of the cryostat using stainless steel split clamps anchored to pipes (successfully prototyped in ProtoDUNE-SP) and from there, to the top of the cryostat using vertical strings (as with static T-gradient monitors).

Sensors on the walls will use bolts in the vertical corners for cable routing.

For all individual sensors, PCB sensor support, cables, and connection to the flanges will be the same as for the T-gradient monitors.

### 1.2.1.4 Vertical arrays in gas phase

The temperature map in the gas is specially important for the dual phase technology. As in ProtoDUNE-DP, the region immediately above (about 40 cm) the CRPs will be instrumented with vertical arrays of temperature sensors. The baseline design foresees for each of these arrays 8 standard RTDs with increasing pitch with height above the CRP, as shown in Figure 1.13 for the device installed in ProtoDUNE-DP. Twenty (20) of these arrays would be distributed throughout the top of the cryostat. Unlike the liquid, where the temperature gradient is not larger than 10 mK, the temperature in the gas changes very rapidly with height, and a relative precision of 0.1 K is sufficient for those sensors. Thus, standard RTDs with calibration can be used.

### 1.2.1.5 Analysis of temperature data in ProtoDUNE-SP

Temperature data from ProtoDUNE-SP has been recorded since LAr filling in August 2018. The analysis of this data and the comparison with CFD simulations is actively underway, but interesting



Figure 1.13: Vertical array of temperature sensors in ProtoDUNE-DP.

1 preliminary results are available and will be described below. Figure 1.14 shows the distribution  
 2 of temperature sensors in the ProtoDUNE-SP cryostat.

3 All precision temperature sensors (for the static and dynamic T-gradient monitors, and the 2D ar-  
 4 rays at top and bottom) were calibrated in the laboratory prior to installation. However, since the  
 5 calibration method was still under development when those sensors were installed, this calibration  
 6 was only satisfactory (2.6 mK precision) for the static T-gradient monitor, whose sensors were cali-  
 7 brated the last and plugged in just few days prior to installation in the cryostat. In section 1.2.1.2,  
 8 an additional calibration method, the so called *pumps-off calibration*, has been described and the  
 9 agreement with the laboratory calibration was proved (see Figure 1.10). Since this is the only  
 10 reliable calibration for individual sensors, this method will be used for the data analysis presented  
 11 in this section, for all sensors except for the dynamic T-gradient monitor, whose calibration based  
 12 on the movable system is more precise (see Sec. 1.2.1.1).

13 Figure 1.15 shows the vertical temperature profiles as measured by the dynamic and static T-  
 14 gradient monitors at a given moment in time (10 minutes in May 2019). The stability of those  
 15 profiles has been carefully studied: the relative variation between any two sensors on the same  
 16 profiler is below 3 mK along the entire data taking, probing that the shape of the profiles is nearly  
 17 constant in time. In Figure 1.15 one immediately observes that the shapes of the two profiles are  
 18 similar, with a bump at 6.2 m, but the magnitude of variation of the static profile almost doubles  
 19 compared to the dynamic profile. This effect is attributed to the fact that the dynamic T-gradient  
 20 monitor is on the path of the LAr flow, which makes the temperature more uniform, while the  
 21 static profiler is on the side.

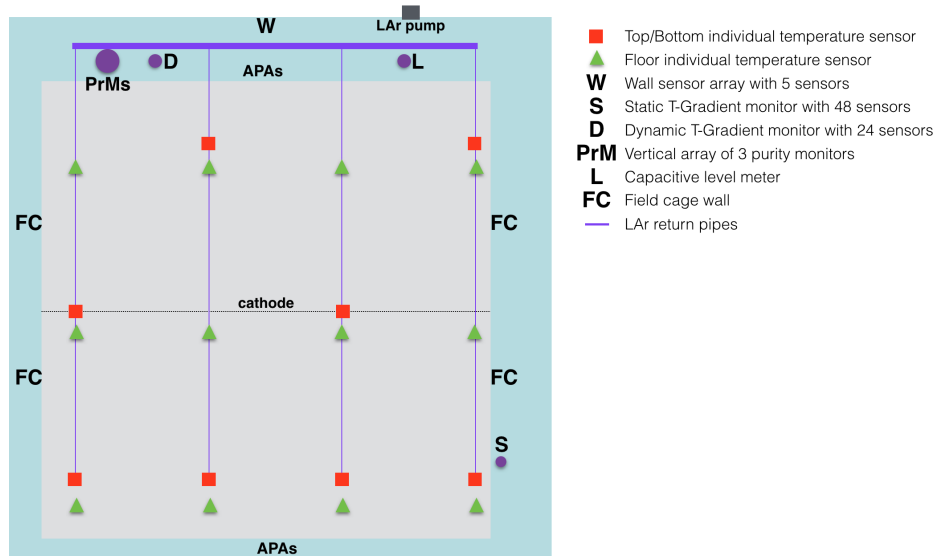


Figure 1.14: Distribution of temperature sensors in the ProtoDUNE-SP cryostat. Notice that four of the bottom sensors are located right above the LAr inlets. Purity monitors and level meters are also indicated.

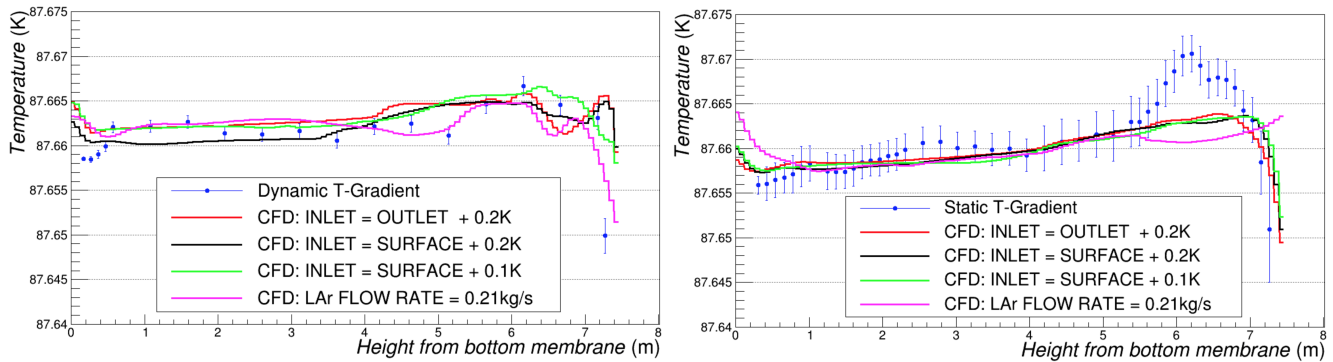


Figure 1.15: Temperature profiles measured by the T-gradient monitors and comparison to the CFD model with different boundary conditions. Left: dynamic T-gradient monitor; Right: Static T-gradient monitor.



1 In order to connect the two different regions covered by the T-gradient monitors, temperature  
 2 measurements by the bottom sensor grid can be used. Figure 1.16 shows the temperature difference  
 3 between bottom sensors and the second sensor of the static T-gradient monitor (the one at 40 cm  
 4 from the floor), which is used as reference. Also shown in the figure is the third sensor of the  
 5 dynamic T-gradient monitor, located at a similar height. Three different periods are shown in the  
 6 figure: two periods with pumps-on and one period with pumps-off. It is observed that when the  
 7 pumps are working the temperature decreases towards the LAr pump, being higher in the sensors  
 8 below the cathode. The horizontal gradient observed in this situation is of the order of 20 mK  
 9 – larger than the vertical gradient. When the pumps are off the horizontal gradient decreases,  
 10 although a residual gradient of 5 mK is observed. This gradient is attributed to the inertia of  
 11 the liquid once the pumps are switched off: it takes more than one day to recover the horizontal  
 12 homogeneity.

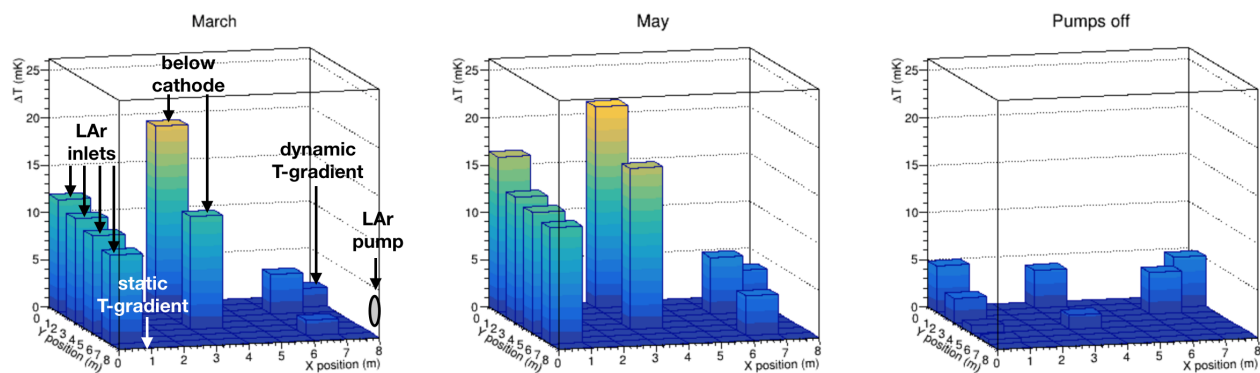


Figure 1.16: Temperature difference between bottom sensors at 40 cm from the floor and static T-gradient sensor at same height. The third dynamic T-gradient sensor, which is at the same height, is also shown. Two pumps-on periods (left and middle panels) and one pump-off period (right panel) are shown.

13 CFD simulations have been produced with different inputs. Two parameters have been identified  
 14 as potential drivers of the convection regime: i) the incoming LAr flow rate and ii) the incoming  
 15 LAr temperature. The result of varying those parameters was shown in Figure 1.15. The CFD  
 16 model reasonably predicts the main features of the data but the details still need to be understood:  
 17 the bump at 6.2 m or the lower measured temperature at the bottom. It is worth noting that  
 18 the simulation depends minimally on the LAr temperature while the flow rate has more impact,  
 19 specially in the regions where discrepancies are larger. All simulations use the nominal LAr flow  
 20 rate, 0.42 kg/s, except the one explicitly indicated in the plots, which uses half of the rate. More  
 21 simulations with other LAr flow rates are needed to conclude.

22 The CFD reassuringly predicts a reasonable response for more than one set of initial conditions.  
 23 It is still important to instrumentation response to help establish the validity of the CFD model.  
 24 We did not run tests with differing initial conditions during the beam run because even controlled  
 25 changes of the cryostat environment could have undesirable effects. However, dedicated tests to  
 26 validate the CFD under various deliberate changes of the cryostat were performed recently. Those  
 27 additional tests include pump and recirculation manipulations such as pump on-off, change of  
 28 pumping speed, and bypassing of filtration, and changing the cryostat pressure set point to a

1 higher (or lower) value<sup>6</sup> to induce changes in the pressure for a specified time while monitoring  
2 the instrumentation. Any change in pressure could change the temperatures everywhere in the  
3 cryostat. Studying the rate of this change, as detected at various heights in the cryostat, might  
4 provide interesting constraints on the CFD model.

#### 5 **1.2.1.5.1 Comparison of calibration methods**

6 Three different calibration methods have been described above, each of them having a different  
7 purpose. The underlying assumption is that reliable temperature monitoring at the few mK level is  
8 desirable during the entire lifetime of the experiment, both to guarantee the correct functioning of  
9 the cryogenics system and to compute offline corrections based on temperature measurements and  
10 CFD simulations. This is only possible if an insitu calibration method is available since relative  
11 calibration between sensors is expected to diverge with time with respect to the one performed in  
12 the laboratory. Two insitu methods have been used. The pumps-off calibration method is very  
13 powerful since it is the only way of cross-calibrating all sensors in the cryostat at any point in  
14 time. However it relies on the assumption that the temperature is uniform when the recirculation  
15 pumps are off. The validity of this assumption has to be bench-marked with real data and this  
16 is done in ProtoDUNE-SP using the calibration based on the movable system (see Fig 1.7). The  
17 last is the most precise calibration method and the one that sustains all other methods, providing  
18 a reliable reference during the entire lifetime of the experiment. This method is even more crucial  
19 for the far detector. Indeed, recirculation pumps will be located on one side of the cryostat, very  
20 far (almost 60 m) from some regions of the LAr volume, where the inertia will be more pronounced  
21 and the homogeneous temperature assumption becomes less valid.

#### 22 **1.2.1.6 Readout system for thermometers**

23 A high-precision and very stable system is required to achieve a readout level of  $< 5$  mK. The  
24 proposed readout system was used in ProtoDUNE-SP and relies on a variant of an existing mass  
25 PT100 temperature readout system developed at European Organization for Nuclear Research  
26 (CERN) for an LHC experiment; it has already been tested and validated by the collaboration  
27 experts. The system has an electronic circuit that includes

- 28 • a precise and accurate current source for exciting the temperature sensors measured using  
29 the four-wires method;
- 30 • a multiplexing circuit connecting the temperature sensor signals and forwarding the selected  
31 signal to a single line; and
- 32 • a readout system with a high-accuracy voltage signal readout module<sup>7</sup> with 24 bit resolution  
33 over a 1 V range.

34 This readout system also drives the multiplexing circuit and calculates temperature values. The

---

<sup>6</sup>The HV was ramped down for this exercise because dropping the pressure too fast might provoke boiling of the LAr near the surface.

<sup>7</sup>National Instrument CompactRIO™ device with a signal readout NI9238™ module

1 CompactRIO device is connected to the detector Ethernet network, sending temperature values  
2 to the DCS software through a standard OPC-UA driver.

3 The current mode of operation averages more than 2000 samples taken every second for each  
4 sensor. Figure 1.11 shows the system has a resolution higher than 1 mK, the RMS of one of the  
5 offsets in the stable region.

## 6 1.2.2 Purity Monitors

7 A fundamental requirement of a LAr TPC is that ionization electrons drift over long distances  
8 in LAr. Part of the charge is inevitably lost because of electronegative impurities in the liquid.  
9 To keep this loss to a minimum, monitoring impurities and purifying the LAr during operation is  
10 essential.

11 A purity monitor is a small ionization chamber used to infer independently the effective free electron  
12 lifetime in the LArTPC. It illuminates a cathode with UV light to generate a known electron  
13 current, then collects the drifted current at an anode a known distance away. Attenuation of the  
14 current is related to the electron lifetime. Electron loss can be parameterized as  $N(t) = N(0)e^{-t/\tau}$ ,  
15 where  $N(0)$  is the number of electrons generated by ionization,  $N(t)$  is the number of electrons  
16 after drift time  $t$ , and  $\tau$  is the electron lifetime.

17 For the DP module, the drift distance is 12 m, and the E field is  $500 \text{ V} \cdot \text{cm}^{-1}$ . Given the drift  
18 velocity of approximately  $1.5 \text{ mm} \cdot \mu\text{s}^{-1}$  in this field, the time to go from cathode to anode is  
19 roughly  $\sim 8 \text{ ms}$  [6]. For an LAr TPC signal attenuation,  $[N(0) - N(t)]/N(0)$ , of 50% over the  
20 entire drift distance, the corresponding electron lifetime is  $8 \text{ ms}/[-\ln(0.5)] \simeq 11 \text{ ms}$ .

21 Residual gas analyzers can monitor the gas in the ullage of the tank and would be an obvious choice  
22 for analyzing argon gas. Unfortunately, suitable and commercially available mass spectrometers  
23 have a detection limit of  $\sim 10$  parts per billion (ppb), whereas DUNE requires a sensitivity of parts  
24 per trillion (ppt). Therefore, specially constructed and distributed purity monitors will measure  
25 LAr purity in all phases of operation. These measurements, along with an accurate CFD model,  
26 enable determining LAr purity at all positions throughout the detector module.

27 Purity monitors also mitigate the risk of LAr contamination. The large scale of the detector  
28 modules increases the risk of failing to notice a sudden, unexpected infusion of contaminated LAr  
29 back into the cryostat. If this condition were to persist, it could cause irreversible contamination  
30 to the LAr and terminate useful data taking. Strategically placed purity monitors mitigate this  
31 risk as demonstrated in ProtoDUNE-SP.

32 Purity monitors are placed inside the cryostat but outside the TPC. They are also placed within  
33 the recirculation system outside the cryostat, both in front of and behind the filtration system.  
34 Continuous monitoring of the LAr supply lines to the detector module provides a strong line  
35 of defense against contamination from sources both in the LAr volume and from components  
36 in the recirculation system. Similarly, gas analyzers (described in Section 1.2.5) protect against  
37 contaminated gas.

1 Furthermore, using several purity monitors to measure lifetime with high precision at carefully  
 2 chosen points provides key input, e.g., vertical gradients in impurity concentrations, for CFD  
 3 models of the detector module.

4 Purity monitors were deployed in previous liquid argon time-projection chamber (LArTPC) exper-  
 5 iments, i.e., ICARUS, MicroBooNE, and the 35 ton prototype. During the first run of the 35 ton  
 6 prototype, two of the four purity monitors stopped working during cooldown, and a third operated  
 7 intermittently. We later found this was due to poor electrical contacts between the resistor chain  
 8 and the purity monitor. A new design was implemented and successfully tested in the second run.

9 ProtoDUNE-SP and ProtoDUNE-DP implement purity monitors to measure electron lifetime at  
 10 different heights. Both use a similar design. The baseline design for the DP FD will be the one used  
 11 in ProtoDUNE-SP. Figure 1.17 shows the assembly of the ProtoDUNE-SP purity monitors. The  
 12 design reflects improvements to ensure electric connectivity and improve signals. ProtoDUNE-  
 13 SP uses a string of purity monitors connected with stainless steel tubes to protect the optic  
 14 fibers. The purity monitor system at ProtoDUNE-SP measured electron lifetime every hour during  
 15 commissioning and daily during the beam test. During this time, it alerted us to serious problems  
 16 twice, first for filter saturation and then because the recirculation pump had stopped. This enabled  
 17 us to prevent situations that otherwise could have had serious consequences.

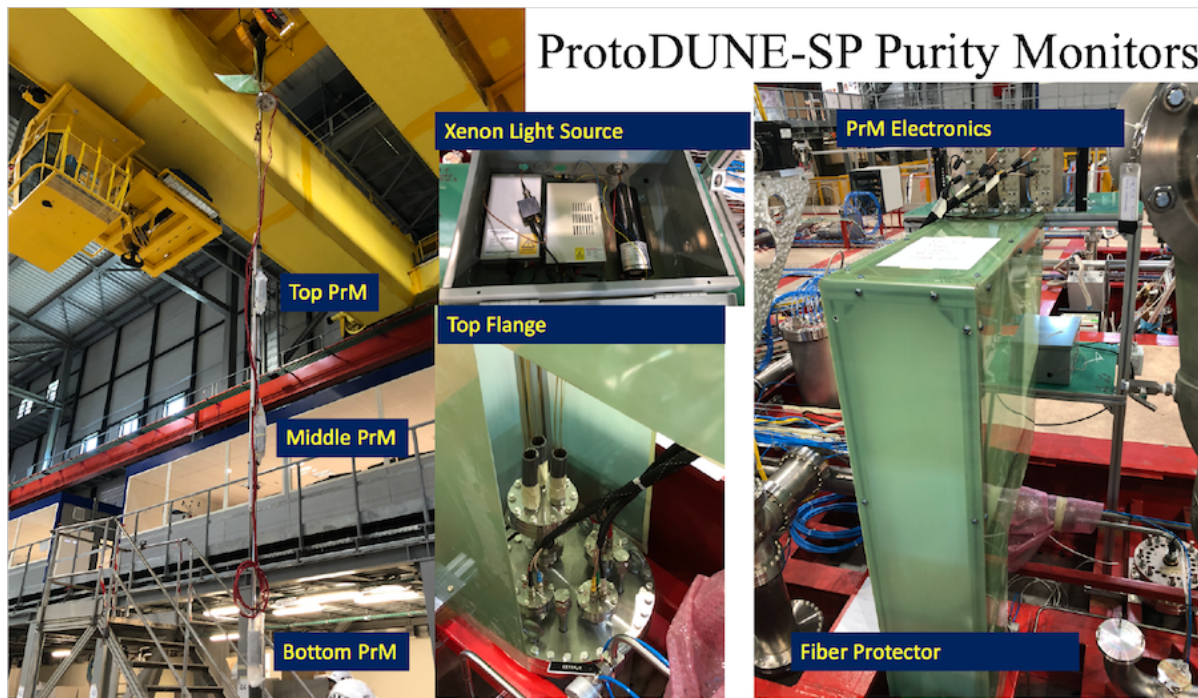


Figure 1.17: The ProtoDUNE-SP purity monitoring system.

18 During the commissioning and beam test of ProtoDUNE-SP, the purity monitors operated with  
 19 different high voltages to change electron drift time, ranging from  $150\ \mu\text{s}$  to 3 ms. This allowed  
 20 the ProtoDUNE-SP purity monitors to measure electron lifetime from  $35\ \mu\text{s}$  to about 10 ms with  
 21 high precision, a dynamic range greater than 300. This measurement was also valuable for the  
 22 ProtoDUNE-SP lifetime calibration. Because purity monitors have much smaller drift volumes  
 23 than the TPC, they are less affected by the space charge caused by cosmic rays.

- 1 A similar operation plan is foreseen for the DP module, with modifications to accommodate the  
 2 relative positions of the instrumentation port and the purity monitor system and the different  
 3 geometric relationships between the TPC and cryostat.
- 4 ProtoDUNE-SP implements three purity monitors instead of the two deployed in ProtoDUNE-DP.  
 5 Figure 1.18 shows the ProtoDUNE-SP data taken using its three purity monitors from commis-  
 6 sioning of ProtoDUNE-SP starting in September 2018, through the entire beam running, to July  
 7 2019.

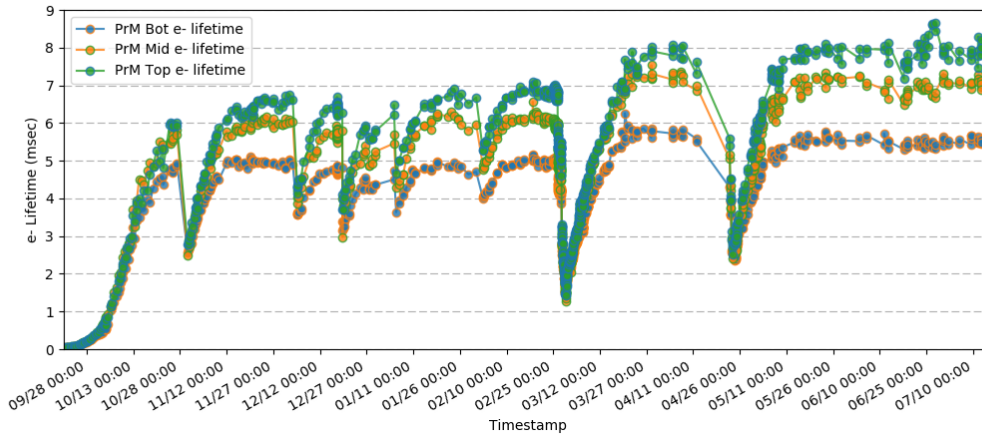


Figure 1.18: The electron lifetimes measured by three purity monitors in ProtoDUNE-SP as a function of time, September 2018 through July 2019. The purity is low prior to start of circulation in October. Reasons for later dips include recirculation studies and recirculation pump stoppages.

### 8 1.2.2.1 Purity Monitor Design

9 The DP module baseline purity monitor design follows that of the ICARUS experiment (Fig-  
 10 ure 1.19)[7]. It consists of a double-gridded ion chamber immersed in the LAr volume with four  
 11 parallel, circular electrodes, a disk holding a photocathode, two grid rings (anode and cathode),  
 12 and an anode disk. The cathode grid is held at ground potential. The cathode, anode grid, and  
 13 anode each hold separate bias voltages and are electrically accessible via modified vacuum-grade  
 14 HV feedthroughs. The anode grid and the field shaping rings are connected to the cathode grid  
 15 by an internal chain of 50 M $\Omega$  resistors to ensure the uniformity of the E fields in the drift regions.  
 16 A stainless mesh cylinder is used as a Faraday cage to isolate the purity monitor from external  
 17 electrostatic background.

18 The purity monitor measures the electron drift lifetime between its anode and cathode. The purity  
 19 monitor’s UV-illuminated photocathode generates electrons via the photoelectric effect. Because  
 20 electron lifetime in LAr is inversely proportional to the electronegative impurity concentration, the  
 21 fraction of electrons generated at the cathode that arrives at the anode ( $Q_A/Q_C$ ) after the electron  
 22 drift time  $t$  gives a measure of the electron lifetime  $\tau$ :  $Q_A/Q_C \sim e^{-t/\tau}$ .

23 Once the electron lifetime becomes much larger than the drift time  $t$ , the purity monitor reaches

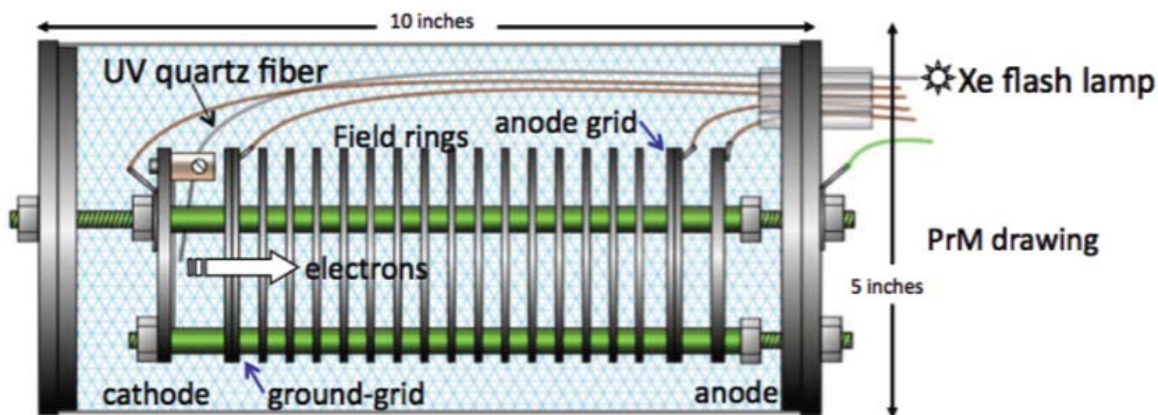


Figure 1.19: Schematic diagram of the basic purity monitor design [7].

1 its sensitivity limit. For  $\tau \gg t$ , the anode-to-cathode charge ratio becomes  $\sim 1$ . Because the  
 2 drift time is inversely proportional to the E field, in principle, reducing the field should make it  
 3 possible to measure lifetimes of any length regardless of the length of the purity monitor. On the  
 4 other hand, increasing the voltage will shorten the drift time, allowing measurement of a short  
 5 lifetime when purity is low.

6 Varying the operational HV on the anode from 250 V to 4000 V in the ProtoDUNE-SP's 24 cm (9.5  
 7 inch) long purity monitor allowed us to make the 35  $\mu$ s to 10 ms electron lifetime measurements.

8 The electron lifetime of the purest commercial LAr, after the first filtering and during the filling  
 9 process, is typically longer than 40  $\mu$ s. However, when the filter starts to saturate, the lifetime  
 10 decreases to less than 30  $\mu$ s. To reduce the energy loss due to impurities, the DP module requires  
 11 at least 3 ms electron lifetime, with a goal of 10 ms. Therefore, purity monitors with different  
 12 lengths (drift distances) are needed to extend the measurable range to less than 35  $\mu$ s and more  
 13 than 10 ms.

14 The photocathode that produces the photoelectrons is an aluminum plate coated first with 50 Å  
 15 of titanium followed by 1000 Å of gold; it is attached to the cathode disk. Three photocathodes  
 16 per purity monitor are implemented in ProtoDUNE-DP, two of silver and one of gold, with each  
 17 cathode lit by one fiber. The gold cathode is the standard used in ProtoDUNE-SP, but R&D has  
 18 shown silver emits more photoelectrons. A xenon flash lamp is the light source in the baseline  
 19 design, although a more reliable and possibly submersible light source, perhaps LED-driven, could  
 20 replace this in the future. The UV output of the lamp is quite good, approximately  $\lambda = 225$  nm,  
 21 which corresponds closely to the work function of gold (4.9 eV to 5.1 eV). Three UV quartz  
 22 fibers carry the xenon UV light into the cryostat to illuminate the photocathode. Another quartz  
 23 fiber delivers the light into a properly biased photodiode outside the cryostat to provide the trigger  
 24 signal when the lamp flashes.

### 1.2.2.2 Electronics, DAQ, and Slow Controls Interfacing

The purity monitor electronics and DAQ system consist of front-end (FE) electronics, waveform digitizers, and a DAQ PC. Figure 1.20 illustrates the system.

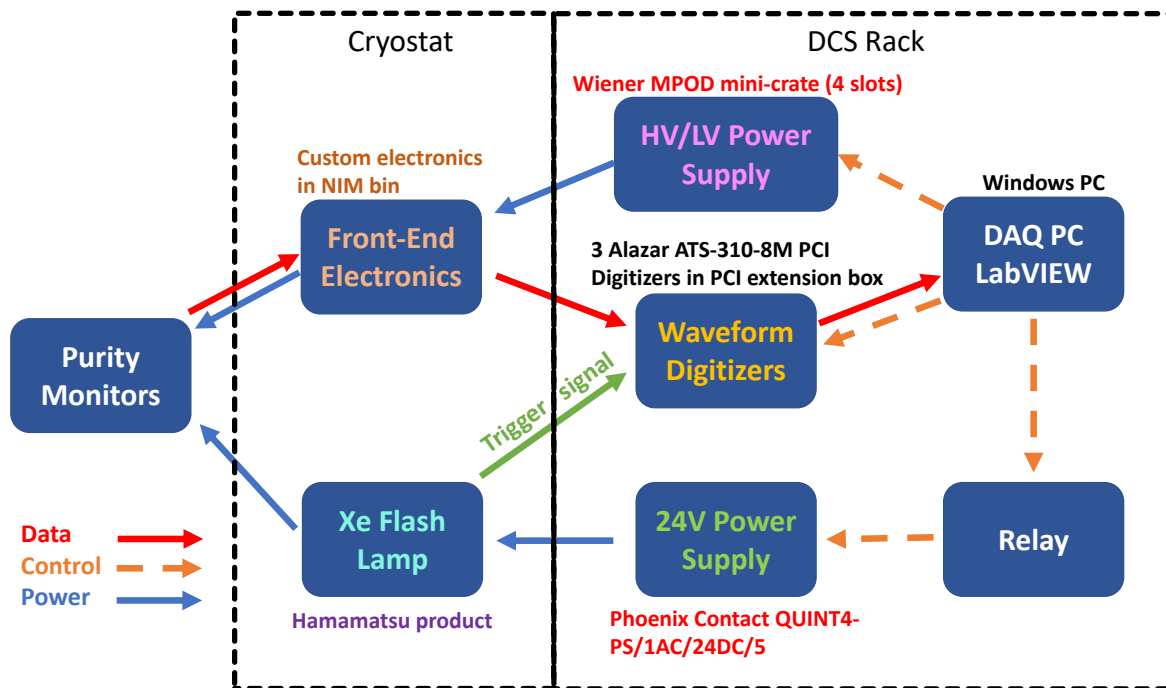


Figure 1.20: Block diagram of the purity monitor system.

The baseline design of the FE electronics follows the one used in the 35 ton prototype, Liquid Argon Puri./wty Demonstrator (LAPD), and MicroBooNE. The cathode and anode signals are fed into two charge amplifiers within the purity monitor electronics module. This electronics module includes a HV filter circuit and an amplifier circuit, both shielded by copper plates, to allow the signal and HV to be carried on the same cable and decoupled inside the purity monitor electronics module. A waveform digitizer that interfaces with a DAQ PC records the amplified anode and cathode outputs. The signal and HV cable shields connect to the grounding points of the cryostat and are separated from the electronic ground with a resistor and a capacitor connected in parallel and mitigating ground loops between the cryostat and the electronics racks. Amplified output is transmitted to an AlazarTech ATS310 waveform digitizer<sup>8</sup> containing two input channels, each with 12 bit resolution. Each channel can sample a signal at a rate of  $20 \text{ MS} \cdot \text{s}^{-1}$  to  $1 \text{ kS} \cdot \text{s}^{-1}$  and store up to 8 MS in memory. One digitizer is used for each purity monitor, and each digitizer interfaces with the DAQ PC across the PCI bus.

A custom LabVIEW<sup>9</sup> application running on the DAQ PC has two functions: it controls the waveform digitizers and the power supplies, and it monitors the signals and key parameters. The application configures the digitizers to set the sampling rate, the number of waveforms to be stored in memory, the pre-trigger data, and a trigger mode. A signal from a photodiode triggered

<sup>8</sup>AlazarTech ATS310™ - 12 bit, 20 MS/s, <https://www.alazartech.com/Product/ATS310>.

<sup>9</sup>National Instruments, LabVIEW™, <http://www.ni.com/en-us.html>

1 by the xenon flash lamp is fed directly into the digitizer as an external trigger to initiate data  
2 acquisition. LabVIEW automatically turns on the xenon flash lamp by powering a relay when  
3 data taking begins and then turning it off when finished. The waveforms stored in the digitizers  
4 are transferred to the DAQ PC and used to obtain averaged waveforms to reduce any electronic  
5 noise in them.

6 The baseline is estimated by averaging the waveform samples prior to the trigger. This baseline is  
7 subtracted from the waveforms prior to calculating peak voltages of the cathode and anode signals.  
8 The application performs these processes in real time. The application continuously displays the  
9 waveforms and important parameters like measured electron lifetime, peak voltages, and drift time  
10 in the purity monitors and shows the variation in these parameters over time, thus pointing out  
11 effects that might otherwise be missed. Instead of storing the measured parameters, the waveforms  
12 and the digitizer configurations are recorded in binary form for offline analysis. HV modules<sup>10</sup> in  
13 a WIENER MPOD mini crate<sup>11</sup> supply negative voltages to the cathode and positive voltages to  
14 the anode. The LabVIEW application controls and monitors the HV systems through an Ethernet  
15 interface.

16 The xenon flash lamp and the FE electronics are installed close to the purity monitor flange to  
17 reduce light loss through the optical fiber and prevent signal loss. Other pieces of equipment  
18 that distribute power to these items and collect data from the electronics are mounted in a rack  
19 separate from the cryostat. The slow control system communicates with the purity monitor DAQ  
20 software and controls the HV and LV power supplies of the purity monitor system. The optical  
21 fiber must be placed within 0.5 mm of the photocathode for efficient photoelectron extraction, so  
22 little interference with the photon detection system (PD system) is expected. The purity monitors  
23 could induce noise in the TPC electronics, in particular via the current surge through a xenon  
24 lamp when it is flashed. This source of noise can be controlled by placing the lamp inside its own  
25 Faraday cage with proper grounding and shielding. At ProtoDUNE-SP, after careful checks of the  
26 grounding, this noise has remained well below the noise generated by other sources.

27 In the DP module we can make use of triggering to prevent any potential noise from the purity  
28 monitor's flash lamp from affecting TPC and PD system signals. The LArTPC trigger rate is a  
29 few hertz, and each trigger window is one or a few milliseconds. The pulse from a flash lamp is  
30 very short (a microsecond or so, much shorter than the gaps between LArTPC trigger windows).  
31 Thus, an LArTPC trigger signal may be sent to a programmable pulse generator, which generates  
32 a trigger pulse that does not overlap with LArTPC trigger windows. This trigger pulse is then sent  
33 to the external trigger port on the flash lamp HV controller, so the lamp flashes between LArTPC  
34 trigger windows. In this way, the electronic and light noises from the flash lamp do not affect data  
35 taking at all.

### 36 1.2.2.3 Production and Assembly

37 The CISC consortium will produce the individual purity monitors, test them in a test stand, and  
38 confirm that each monitor operates at the required level before assembling them into strings of

---

<sup>10</sup>iseg Spezialelektronik GmbH™ high voltage supply systems, <https://iseg-hv.com/en>.

<sup>11</sup>W-IE-NE-R MPOD™ Universal Low and High Voltage Power Supply System, <http://www.wiener-d.com/>.



1 three monitors that will be mounted in the detector module cryostat using support tubes. The  
2 assembly process will follow the methodology developed for ProtoDUNE.

3 A short version of the string with all purity monitors will be tested at the CITF. The full string  
4 will be assembled and shipped to SURF. A vacuum test in a long vacuum tube will be performed  
5 on site before inserting the full assembly into the SP module cryostat.

### 6 **1.2.3 Liquid Level Meters**

7 The LAr level monitoring system has two goals: basic level sensing when filling and precise level  
8 sensing during stable operations. The system also provides signals for DDSS interlocks that protect  
9 the detector (e.g. HV). DUNE will use both differential pressure level meters (LBNF scope) and  
10 capacitive level meters (DUNE scope). Liquid level meters provide useful information for both  
11 cryostat filling and stable operation. Dedicated level meters will be complemented by vertical  
12 arrays of temperature sensors (see Section 1.2.1), located at known heights and used to determine  
13 the LAr level (they will change temperature dramatically when the cold liquid reaches each of  
14 them), and by cameras, which will focus on the LAr surface at all times.

15 Filling the cryostat with LAr will take several months. During this operation, several systems  
16 will monitor the LAr level. The first 5.5 m of LAr will be monitored by cameras and by the  
17 vertical arrays of RTDs. Once the liquid reaches the level of the cryogenic pipes going out of  
18 the cryostat, the differential pressure between that point and the bottom of the cryostat can be  
19 converted to depth using the known density of LAr. Fine tuning the final LAr level require several  
20 capacitive level meters at the top of the cryostat; this system comprises several 4 m long capacitive  
21 level sensors (with a precision of less than 5 mm) which will be checked against each other. One  
22 capacitive level sensor at each of the four corners of the cryostat will provide sufficient redundancy  
23 to ensure that no single point of failure compromises the measurement.

24 During operations, liquid level monitoring has two purposes: monitoring to tune the LAr flow, and  
25 monitoring for safety interlocking purposes and for cross checks.

26 The LAr flow is tuned using two differential pressure level meters, installed as part of the cryo-  
27 genics system, one on each side of the detector module. They have a precision of 0.1%, which  
28 corresponds to 14 mm at the nominal LAr surface. Cryogenic pressure sensors will be purchased  
29 from commercial sources. Installation methods and positions will be determined as part of the  
30 cryogenics internal piping plan. The dual phase technology must control the LAr surface at the  
31 sub-millimeter level, so fine tuning the LAr level will require two high precision capacitive level  
32 meters attached to the inner cryostat membrane at the appropriate height.

33 For safety interlocking and to cross check measurements with differential pressure level meters the  
34 long capacitive level meters will be used.

35 In addition to these level meters, CRP will use high precision (less than 1 mm) capacitive level  
36 meters attached to the CRP frame to monitor constant CRP alignment to the liquid phase. These  
37 fall under the scope of the CRP consortium and are described in Chapter 1.5 of this TDR volume.

- 1 Figure 1.21 shows the evolution of the ProtoDUNE-SP LAr level over two months as measured by  
 2 the differential pressure and capacitive level meters.

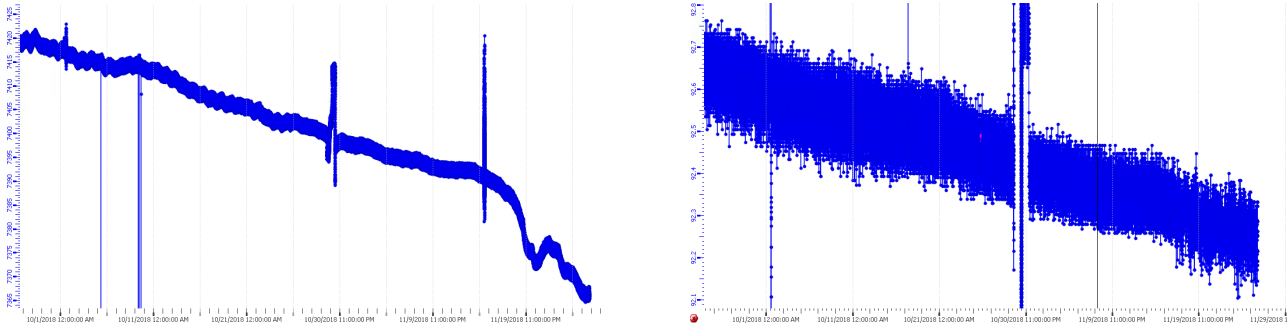


Figure 1.21: Evolution of the ProtoDUNE-SP LAr level over two months. Left: Measured by the capacitive level meter. Right: Measured by the differential pressure level meter. The units in the vertical axis are percentages of the cryostat height (7878 mm).

- 3 ProtoDUNE-SP and ProtoDUNE-DP use the same design for differential pressure level meters  
 4 and will also be used in the far detector SP and DP modules. For the capacitive level meters,  
 5 ProtoDUNE-SP is using commercial 1.5 m long level meters while ProtoDUNE-DP is using 4 m  
 6 long level meters custom-built by CERN. For the DUNE FD, we plan to use the longer capacitive  
 7 level meters custom-built by CERN for both SP and DP modules.

## 8 1.2.4 Pressure Meters

- 9 Measuring the pressure of argon gas in the DUNE FD is important because it can affect gas  
 10 density, and consequently, the LEM gain calibration. The accuracy of the pressure sensors should  
 11 be within at least 0.1% or more of the real value. Moreover, the absolute temperature in the liquid  
 12 varies with the pressure in the argon gas, so precise measurements of pressure inside the cryostat  
 13 provides a better picture of temperature gradients and CFD simulations. In ProtoDUNE, pressure  
 14 values were also used to understand the strain gauge signals installed in the cryostat frame.

- 15 Standard industrial pressure sensors can be used for this. For the DUNE FD, the plan is to follow  
 16 the same design and configuration used in ProtoDUNE-SP and ProtoDUNE-DP. ProtoDUNE uses  
 17 two types of pressure sensors and a pressure switch as described below:

- 18 • A relative pressure sensor (range: 0-400 mbar, precision: 0.01 mbar),
- 19 • An absolute pressure sensor (range: 0-1600 mbar, precision: 0.05 mbar),
- 20 • A mechanical relative pressure switch adjustable from 50 to 250 mbar.

- 21 Both sensors and the pressure switch are installed in a dedicated flange as shown in Figure 1.22  
 22 and are connected directly to a slow controls system PLC circuit. Dedicated analogue inputs are  
 23 used to read the current values (4 to 20 mA), which are then converted to pressure according to  
 24 sensor range. Given the much larger size of DUNE FD, this system will be doubled for redundancy:  
 25 two flanges in opposite cryostat sides will be instrumented with three sensors each.

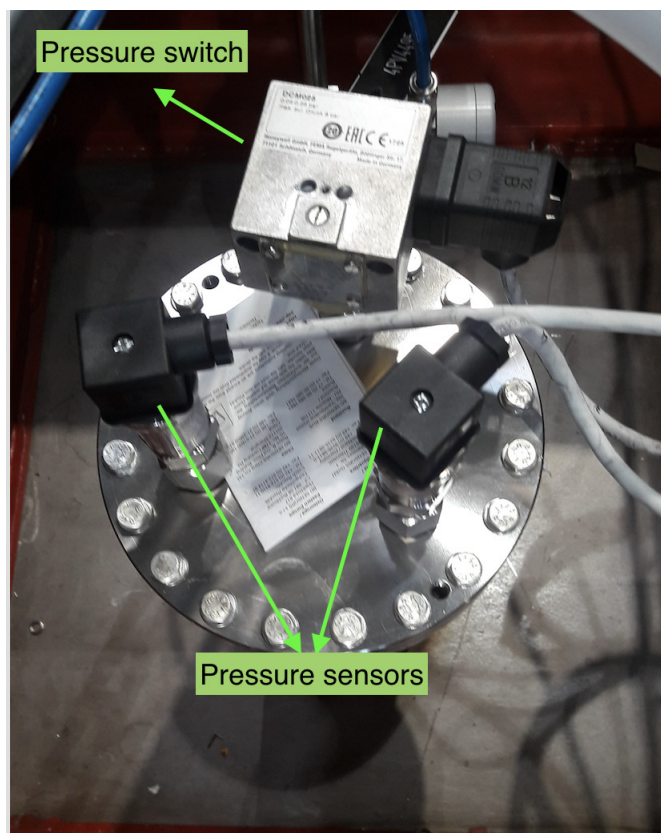


Figure 1.22: Photograph of the pressure sensors installed on a flange in ProtoDUNE-SP.

- 1 Further, relative and absolute pressure sensors (with comparatively lower precision) are installed
- 2 by LBNF that are also recorded by the slow controls system. The availability of two types of
- 3 sensors from LBNF and CISC provides redundancy, independent measurements, and cross checks.

#### 4 1.2.5 Gas Analyzers

- 5 Gas analyzers are commercially produced modules that measure trace quantities of specific gases
- 6 contained within a stream of carrier gas. The carrier gas for DUNE is argon, and the trace gases of
- 7 interest are oxygen ( $O_2$ ), water ( $H_2O$ ), and nitrogen ( $N_2$ ).  $O_2$  and  $H_2O$  affect the electron lifetime
- 8 in LAr and must be kept below 0.1 ppb ( $O_2$  equivalent) while  $N_2$  affects the efficiency of scintillation
- 9 light production at levels higher than 1 ppm. The argon is sampled from either the argon vapor
- 10 in the ullage or from the LAr by using small diameter tubing run from the sampling point to the
- 11 gas analyzer. Typically, the tubing from the sampling points are connected to a switchyard valve
- 12 assembly used to route the sample points to the desired gas analyzers (see Figure 1.23).

- 13 The gas analyzer would be predominantly used during three periods:

- 14 1. Once the detector is installed and after the air atmosphere is eliminated from the cryostat
- 15 to levels low enough to begin cooldown. This purge and gas recirculation process is detailed
- 16 in Section 1.4.5.3. Figure 1.24 shows the evolution of the  $N_2$ ,  $O_2$ , and  $H_2O$  levels from gas

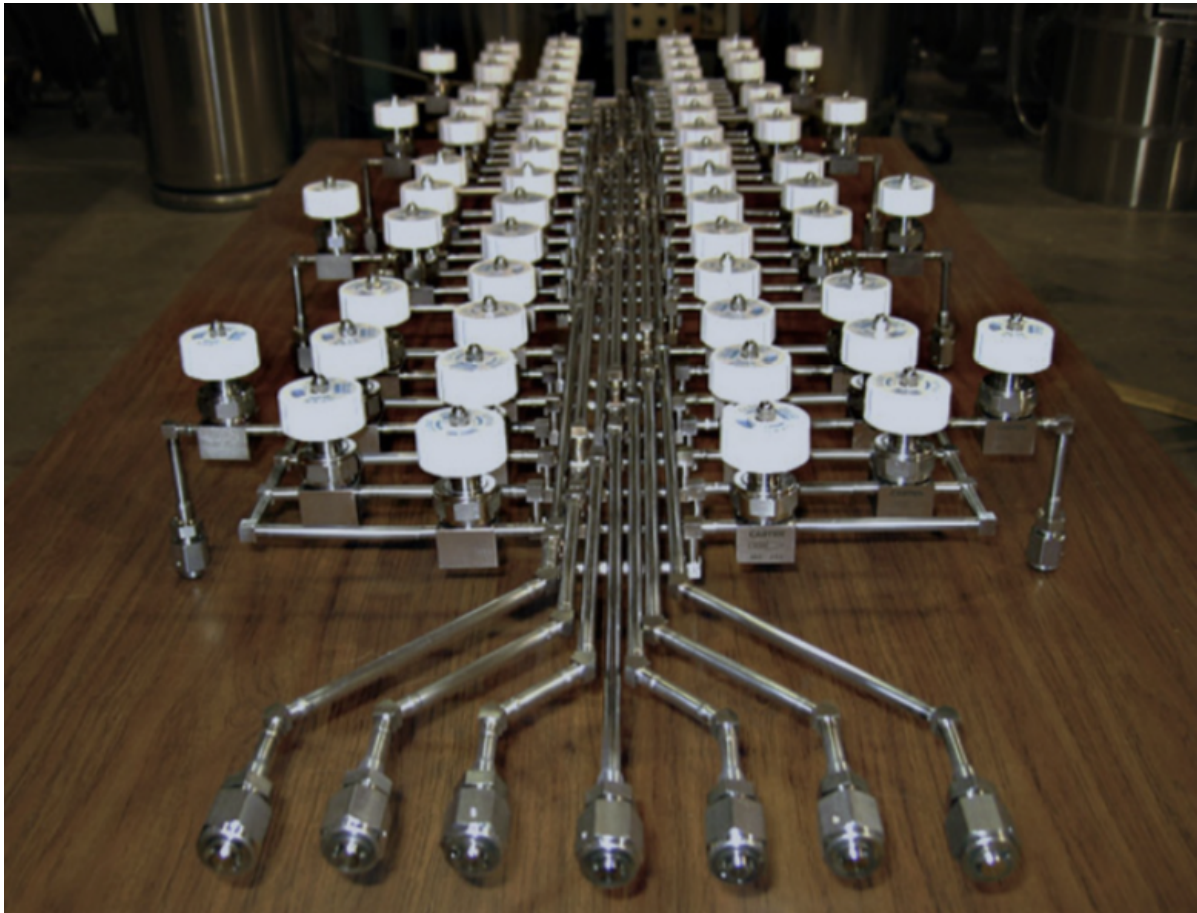


Figure 1.23: A gas analyzer switchyard that routes sample points to the different gas analyzers.

- 1 analyzer data taken during the purge and recirculation stages of the DUNE 35 ton prototype  
 2 phase 1 run.
- 3 2. Before other means of monitoring impurity levels (e.g., purity monitors or TPC tracks) are  
 4 sensitive, to track trace  $O_2$  and  $H_2O$  contaminants from tens of ppb to hundreds of ppt.  
 5 Figure 1.25 shows an example plot of  $O_2$  levels at the beginning of LAr purification from one  
 6 of the later 35 ton prototype HV runs.
- 7 3. During cryostat filling to monitor the tanker LAr delivery purity. This tracks the impurity  
 8 load on the filtration system and rejects any deliveries that do not meet specifications. Likely  
 9 specifications for delivered LAr are in the 10 ppm range per contaminant.

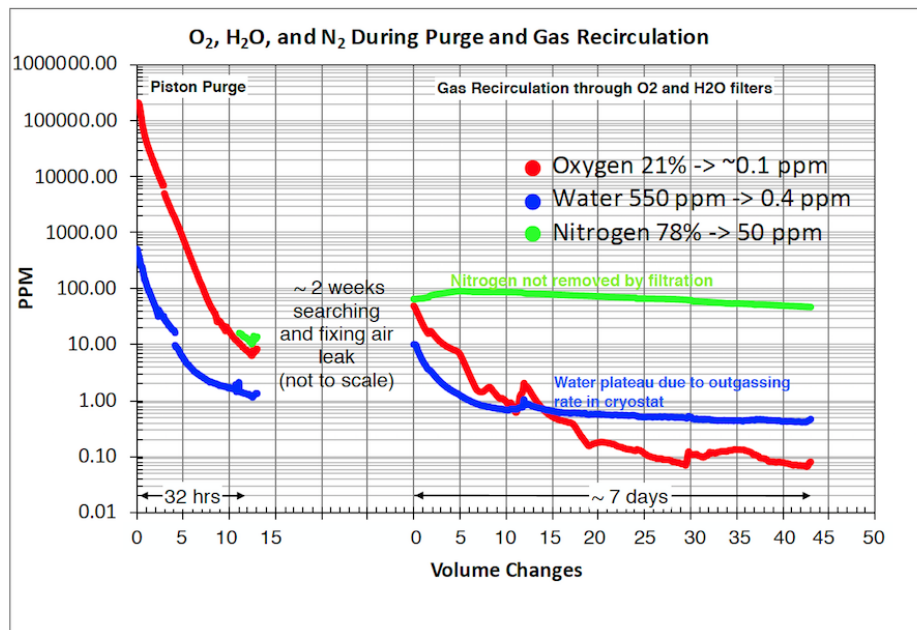


Figure 1.24: Plot of the  $O_2$ ,  $H_2O$ , and  $N_2$  levels during the piston purge and gas recirculation stages of the 35 ton prototype Phase 1 run.

10 Because the filling and commissioning of different cryostats will occur at different times, sharing  
 11 the same gas analyzer installation between them should be possible with minimal effect on the  
 12 operation on other cryostats. The gas analyzer switchyard can easily switch between cryostat  
 13 source lines. Since any one gas analyzer covers only one contaminant species and a range of 3 to  
 14 4 orders of magnitude, several units are needed both for the three contaminant gases and to cover  
 15 the ranges seen between cryostat closure and the beginning of TPC operations: 20% to  $\lesssim$  100 ppt  
 16 for  $O_2$ , 80% to  $\lesssim$  1 ppm for  $N_2$ , and  $\sim$  1% to  $\lesssim$  1 ppb for  $H_2O$ . Because the total cost of these  
 17 analyzers exceeds \$100k, we want to be able to sample more than a single location or cryostat  
 18 with the same gas analyzer. At the same time, the tubing run lengths from the sample point  
 19 should be as short as possible to maintain a timely response for the gas analyzer. This puts some  
 20 constraints on sharing devices because, for example, argon is delivered at the surface, so a separate  
 21 gas analyzer may be required there.

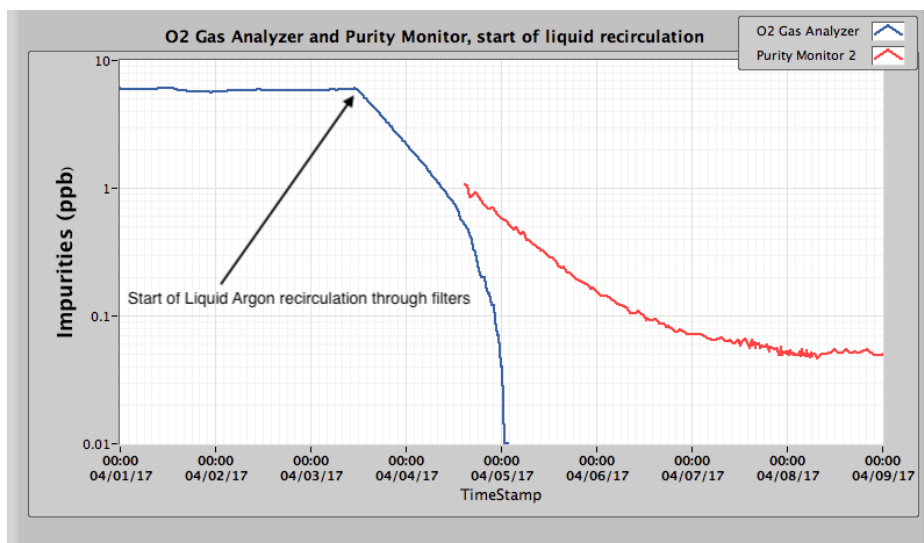


Figure 1.25:  $O_2$  as measured by a precision  $O_2$  analyzer just after the 35 ton prototype cryostat is filled with LAr, continuing with the LAr pump start and beginning of LAr recirculation through the filtration system. As the gas analyzer loses sensitivity, the purity monitor can pick up the impurity measurement. Note that the purity monitor is sensitive to both  $O_2$  and  $H_2O$  impurities giving rise to its higher levels of impurity.

## 1 1.2.6 Cameras

2 Cameras provide direct visual information about the state of the detector module during critical  
 3 operations and when damage or unusual conditions are suspected. Cameras in the WA105 DP  
 4 demonstrator showed spray from cooldown nozzles and the level and state of the LAr as it covered  
 5 the CRP [8]. A camera was used in the Liquid Argon Purity Demonstrator cryostat[7] to study  
 6 HV discharges in LAr and in EXO-100 while a TPC was operating [9]. Warm cameras viewing LAr  
 7 from a distance have been used to observe HV discharges in LAr in fine detail [10]. Cameras are  
 8 commonly used during calibration source deployment in many experiments (e.g., the KamLAND  
 9 ultra-clean system [11]).

10 In DUNE, cameras will verify the stability, straightness, and alignment of the hanging TPC struc-  
 11 tures during cooldown and filling; ensure that no bubbling occurs near the ground planes (GPs)  
 12 (SP) or CRPs (DP); inspect the state of movable parts in the detector module (calibration de-  
 13 vices, dynamic thermometers); and closely inspect parts of the TPC after any seismic activity  
 14 or other unanticipated event. For these functions, a set of fixed cold cameras are used; they are  
 15 permanently mounted at fixed points in the cryostat for use during filling and commissioning. A  
 16 movable, replaceable warm inspection camera can be deployed through any free instrumentation  
 17 flange at any time during the life of the experiment.

18 As this is written, the ProtoDUNE-DP installation is nearing completion, and no validation of  
 19 camera operation in ProtoDUNE-DP is yet available. However, eleven cameras were deployed in  
 20 ProtoDUNE-SP. They successfully provided views of the detector during filling and throughout its  
 21 operation. The camera designs used in ProtoDUNE will be the basis for the final camera designs  
 22 used in the DP module.

1 The following sections describe the design considerations for both cold and warm cameras and  
 2 the associated lighting system. ProtoDUNE-SP camera system designs and performance are also  
 3 discussed. The same basic designs can be used for both the SP and DP detector modules.

#### 4 1.2.6.1 Cryogenic Cameras (Cold)

5 The fixed cameras monitor the following items during filling:

- 6 • positions of corners of CRPs, cathode, FCs, GPs (1 mm resolution),
- 7 • relative straightness and alignment of CRPs, cathode, and FCs ( $\lesssim 1$  mm),
- 8 • relative positions of FC profiles and resistive sheaths between super-modules (0.5 mm reso-  
 9 lution), and
- 10 • the LAr surface, specifically, the presence of bubbling or debris.

11 One design for the DUNE fixed cameras uses an enclosure similar to the successful EXO-100 design  
 12 [9], which was also used successfully in the Liquid Argon Purity Demonstrator and ProtoDUNE-SP  
 13 (see Figure 1.26). A thermocouple in the enclosure allows temperature monitoring and a heating  
 14 element provides temperature control. SUB-D connectors are used at the cryostat flanges and the  
 15 camera enclosure for signal, power, and control connections.

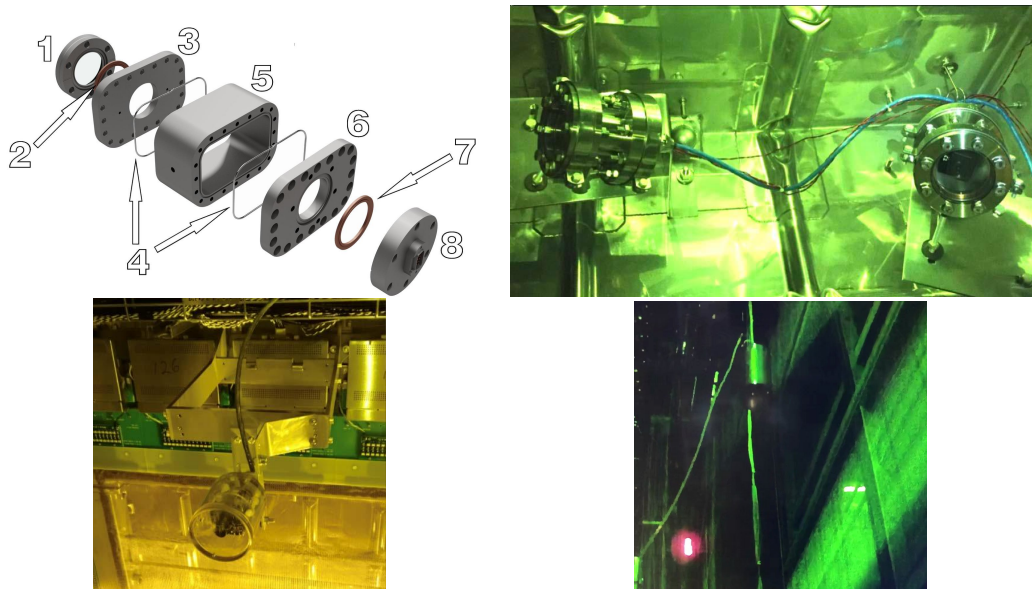


Figure 1.26: Top left: a CAD exploded view of a vacuum-tight camera enclosure suitable for cryogenic applications [9]. (1) quartz window, (2 and 7) copper gasket, (3 and 6) flanges, (4) indium wires, (5) body piece, (8) signal feedthrough. Top right: two of the ProtoDUNE-SP cameras using a stainless steel enclosure. Bottom left: one of the ProtoDUNE-SP cameras using acrylic enclosure. Bottom right: a portion of an image taken with ProtoDUNE-SP camera 105 showing a purity monitor mounted outside the APA on the beam left side. This photo was taken with ProtoDUNE-SP completely filled.

16 An alternative design uses an acrylic enclosure. This design was used successfully in ProtoDUNE-  
 17 SP (see Figure 1.26, bottom left).

- 1 All operate successfully, including those at the bottom of the cryostat. Please note that the DUNE
- 2 FD will be twice as deep as ProtoDUNE, and therefore cameras observing the lowest surfaces of
- 3 the FC must withstand twice the pressure.
- 4 Improved designs for the cold cameras will be tested in ProtoDUNE-DP and CITF for improved
- 5 imaging including focus adjustment, and in CITF for pressure resistance, during 2020.

### 6 **1.2.6.2 Inspection Cameras (Warm)**

7 The inspection cameras are intended to be as versatile as possible. However, the following inspec-  
8 tions have been identified as likely uses:

- 9 • status of HV feedthrough and cup,
- 10 • status and relative position of FC profiles, resistive sheaths between FC super-modules  
11 (0.5 mm resolution),
- 12 • vertical deployment of calibration sources,
- 13 • status of thermometers, especially dynamic thermometers,
- 14 • HV discharge, corona, or streamers on HV feedthrough, cup, or FC,
- 15 • relative straightness and alignment of CRPs, cathode, and FC (1 mm resolution), and
- 16 • gaps between CRP frames (1 mm resolution).

17 Unlike the fixed cameras, the inspection cameras operate only as long as any inspection; the  
18 cameras can be replaced in case of failure. It is also more practical to keep the cameras continuously  
19 warmer than  $-150^{\circ}\text{C}$  during deployment; this permits using commercial cameras. For example,  
20 cameras of the same model were used successfully to observe discharges in LAr from 120 cm away  
21 [10].

22 The inspection cameras use the same basic enclosure design as cold cameras, but the cameras are  
23 mounted on a movable fork, so each camera can be inserted and removed from the cryostat using  
24 a design similar to the dynamic temperature probes (see Figures 1.27 (left) and 1.9). To avoid  
25 contaminating the LAr with air, the entire system is sealed, and the camera can only be deployed  
26 through a feedthrough equipped with a gate valve and a purging system, similar to the one used  
27 in the vertical axis calibration system at KamLAND [11]. The entire system is purged with pure  
28 argon gas before the gate valve is opened.

29 Motors above the flange allow the fork to be rotated and moved vertically to position the camera.  
30 A chain drive system with a motor mounted on the end of the fork allows the camera assembly to  
31 tilt, creating a point-tilt mount that can be moved vertically. With the space above the cryostat  
32 flanges and the thickness of the cryostat insulation, cameras can be moved vertically up to 1 m  
33 inside the cryostat. The motors for rotation and vertical motion are outside the sealed volume,  
34 coupled mechanically using ferrofluidic seals, thus reducing any risk of contamination and allowing  
35 manual rotation of the vertical drive if the motor fails.



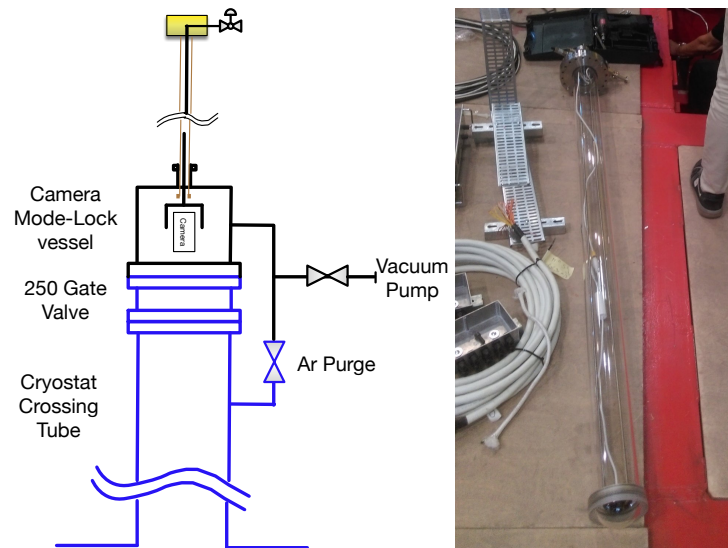


Figure 1.27: Left: An overview of the inspection camera design using a sealed deployment system opening directly into the cryostat. Right: A photograph of the ProtoDUNE-SP warm inspection camera acrylic tube immediately before installation; the acrylic tube is sealed with an acrylic dome at the bottom and can be opened at the top.

- 1 An alternative design was demonstrated in ProtoDUNE-SP. In this design, the warm camera is
- 2 contained inside a gas-tight acrylic tube inserted into the feedthrough, so a gate valve or a gas-tight
- 3 rotatable stage is not needed; the warm cameras can thus be removed for servicing or upgrade
- 4 at any time. Figure 1.27 (right) shows an acrylic tube enclosure and camera immediately before
- 5 deployment. Three such tubes were installed in ProtoDUNE-SP, and cameras with fisheye lenses
- 6 were operated successfully. One camera was removed without any evidence of contamination of
- 7 the LAr.
- 8 Improved designs for the inspection cameras will be tested in the CITF and ProtoDUNE-SP during
- 9 2020 and 2021, focusing particularly on longevity, camera replaceability, and protection of the LAr.

### 10 1.2.6.3 Light-emitting system

11 The light-emitting system uses LEDs to illuminate the parts of the detector module in the camera's  
 12 field of view with selected wavelengths (IR and visible) that cameras can detect. Performance  
 13 criteria for the light-emission system include the efficiency with which the cameras can detect the  
 14 light and the need to avoid adding heat to the cryostat. Very high-efficiency LEDs help reduce  
 15 heat generation; one 750 nm LED [12] has a specification equivalent to 33% conversion of electrical  
 16 input power to light.

17 While data on how well LEDs perform at cryogenic temperatures is sparse, some studies of NASA  
 18 projects [13] indicate that LED are more efficient at low temperatures and that emitted wave-  
 19 lengths may change, particularly for blue LEDs. In ProtoDUNE-SP, amber LEDs were observed  
 20 to emit green light at LAr temperature (see bottom right photo in 1.26). To avoid degradation of  
 21 wavelength-shifting materials in the PD system, short wavelength LEDs are not used in the FD;

- 1 LEDs will be tested in LN to ensure their wavelength is long enough.
- 2 LEDs are placed in a ring around the outside of each camera, pointing in the same direction
- 3 as the lens, to illuminate nearby parts of the detector module within the camera's field of view.
- 4 Commercially available LEDs exist with a range of angular spreads that can match the needs of
- 5 the cameras without additional optics.
- 6 Additionally, chains of LEDs connected in series and driven with a constant-current circuit are
- 7 used for broad illumination, with each LED paired in parallel with an opposite polarity LED and
- 8 a resistor (see Figure 1.28). This gives two different wavelengths of illumination using a single
- 9 chain simply by changing the direction of the drive current and allows continued use of an LED
- 10 chain even if individual LEDs fail.

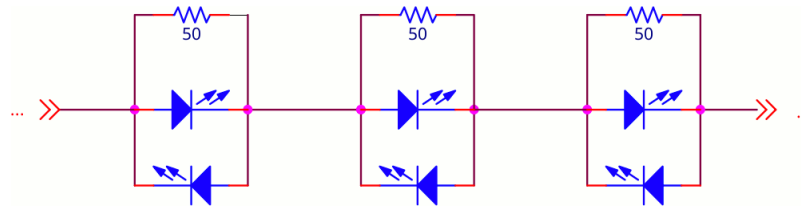


Figure 1.28: Example schematic for LED chain, allowing failure tolerance and two LED illumination spectra.

## 11 1.2.7 Cryogenic Instrumentation Test Facility

12 The CISC consortium plans to build a cryogenic instrumentation test facility (CITF) at Fermilab  
 13 to facilitate testing of various cryogenic instrumentation devices and small-scale assemblies of CISC  
 14 systems. In the past and recent times, various test facilities at Fermilab have provided access to  
 15 small ( $< 1$  ton) to intermediate ( $\sim 1$  ton) volumes of purified TPC-grade LAr, required for any  
 16 device intended for drifting electrons for millisecond periods.

17 The Proton Assembly Building (PAB) facility at Fermilab houses the ICEBERG R&D cryostat  
 18 and electronics (ICEBERG) 3000 liter cryostat that allows fast turnaround for testing of the DUNE  
 19 cold electronics (CE).

20 The PAB facility also includes TallBo (450 liter), Blanche (500 liter), and Luke (250 liter) cryostats.  
 21 In the recent past, Blanche has been used for HV studies, TallBo for PD studies, and Luke for the  
 22 material test stand work. These studies have contributed to the design and testing of ProtoDUNE-  
 23 SP components.

## 24 1.2.8 Validation in ProtoDUNE

25 Design validation and testing of many planned CISC systems for the DUNE DP FD will be done  
 26 using data from both ProtoDUNE-SP and ProtoDUNE-DP detectors as discussed below.

- 1 • **Level Meters:** The same differential pressure level meters that are already validated in  
2 ProtoDUNE-SP will be used in DP FD. The same capacitive level meters currently used  
3 in ProtoDUNE-DP will be used in the DP FD. These will be validated in the upcoming  
4 ProtoDUNE-DP run.
- 5 • **Pressure Meters (GAR):** The same high precision pressure sensors which are already vali-  
6 dated in ProtoDUNE-SP will be used in DP FD.
- 7 • **Gas Analyzers:** The same gas analyzers currently used in ProtoDUNE-SP will be used in  
8 DP FD. They have already been validated.
- 9 • **Vertical array of thermometers in GAR:** The same design of vertical array of thermometers  
10 currently used in ProtoDUNE-DP will be used in DP FD but with different distribution  
11 density. This design will be validated with ProtoDUNE-DP data.
- 12 • **High precision thermometer arrays in LAR:** The static and dynamic T-gradient thermome-  
13 ters discussed in previous sections are not yet installed in ProtoDUNE-DP, but the plan is  
14 to deploy them in the DP FD. Therefore, the validation of these devices will be performed  
15 using ProtoDUNE-SP data and can also be tested in future running of ProtoDUNE-DP.
- 16 • **Purity monitors:** The purity monitors are being validated at both ProtoDUNE-SP and  
17 ProtoDUNE-DP. Currently, ProtoDUNE-SP and ProtoDUNE-DP are using slightly different  
18 designs. For the DP FD, the plan is to use the same design as ProtoDUNE-SP along with  
19 some improvements such as longer drift purity monitors to increase the range of measured  
20 lifetime values. The ProtoDUNE-SP and ProtoDUNE-DP run 2 phase provides opportunities  
21 to test improved designs.
- 22 • **Cameras:** The various cameras are actively developed in both ProtoDUNE-SP and ProtoDUNE-  
23 DP, so the designs will be validated at both the ProtoDUNE-SP and ProtoDUNE-DP. Future  
24 improvements can be tested in ProtoDUNE-SP and ProtoDUNE-DP run 2 phase at CERN.

## 25 1.3 Slow Controls

26 The slow controls system collects, archives, and displays data from a broad variety of sources and  
27 provides real-time status, alarms, and warnings for detector operators. The slow control system  
28 also provides control for items such as HV systems, TPC electronics, and PD systems. Data are  
29 acquired via network interfaces. Figure 1.29 shows connections between major parts of the slow  
30 controls system and other systems. Hardware, infrastructure, and software are the three main  
31 components of the slow controls system.

32 The ProtoDUNE-SP detector control system[5] met its operational requirements fully. Section 1.3.6  
33 provides a short description of the ProtoDUNE-SP slow controls and its performance.

### 34 1.3.1 Slow Controls Hardware

35 Slow controls requires a modest amount of dedicated hardware, mostly for rack monitoring, and a  
36 small amount of dedicated network and computing hardware. Slow controls also relies on common

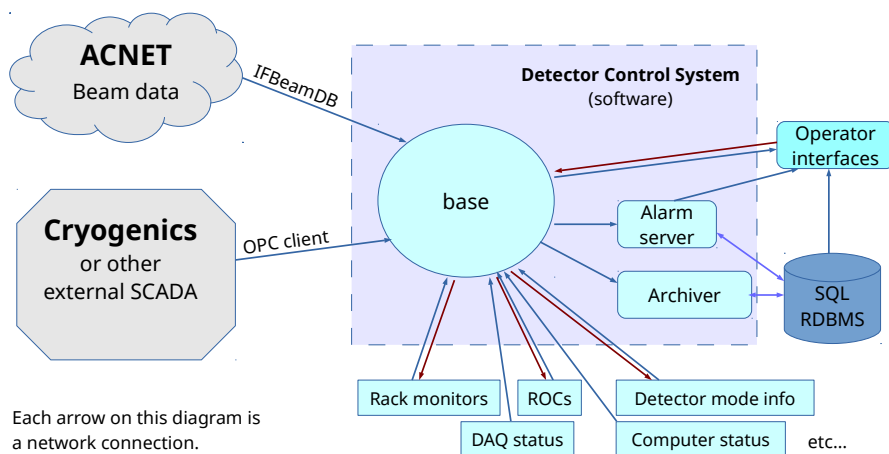


Figure 1.29: Typical slow controls system connections and data flow.

1 infrastructure as described in Section 1.3.2.

### 2 1.3.1.1 Dedicated Monitoring Hardware

3 Every rack (including those in the central utility cavern (CUC)) should have dedicated hardware  
 4 to monitor rack parameters like rack protection system, rack fans, rack air temperatures, thermal  
 5 interlocks with power supplies, and any interlock bit status monitoring needed for the racks. For the  
 6 racks in the CUC server room, this functionality is built into the proposed water cooled racks, much  
 7 like what is already in place at ProtoDUNE. For the racks on the detector itself, the current plan is  
 8 to design and install a custom-built 1U rack-mount enclosure containing a single-board computer  
 9 to control and monitor various rack parameters. Such a system has been successfully used in  
 10 MicroBooNE. The design is being improved for the SBND experiment (see Figure 1.30). Other  
 11 slow controls hardware includes interfacing cables like adapters for communication and debugging  
 12 and other specialized cables like GPIB or National Instruments cables. The cable requirements  
 13 must be determined in consultation with other groups once hardware choices for various systems  
 14 are chosen.

### 15 1.3.1.2 Slow Controls Network Hardware

16 The slow controls data originates from the cryogenic instrumentation and from other systems as  
 17 listed in Table 1.6. This data is collected by software running on servers (see Section 1.3.1.3)  
 18 housed in the underground data room in the CUC, where data is archived in a central CISC  
 19 database. The instrumentation data is transported over conventional network hardware from any  
 20 sensors located in the cryogenic plant. However, we must remain aware of grounding and noise  
 21 in readouts in the racks on top of the cryostats. Therefore, each rack on the cryostat has a small  
 22 network switch that sends any network traffic from that rack to the CUC via a fiber transponder.  
 23 This is the only network hardware specific to slow controls and will be provided by SURF's general

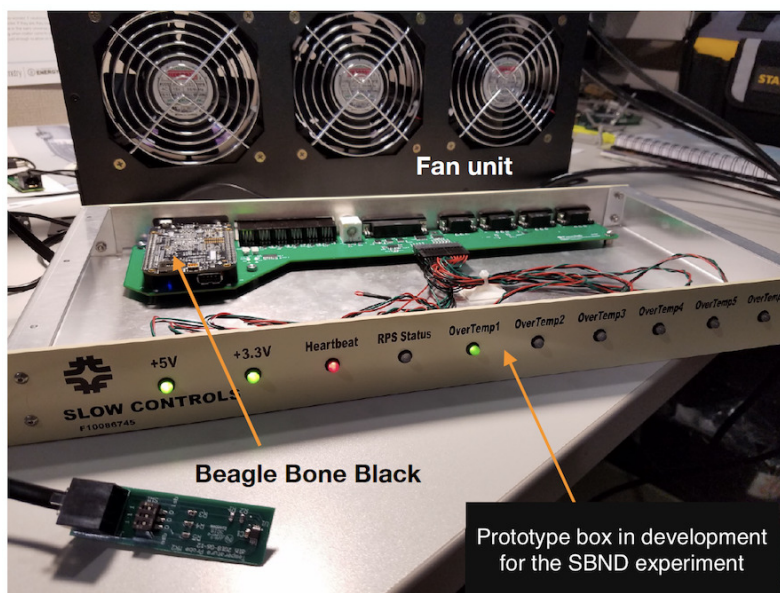


Figure 1.30: Rack monitoring box prototype in development for the short-baseline near detector (SBND) experiment based on the original design from MicroBooNE.

1 computing infrastructure. The network infrastructure requirements are described in Section 1.3.2.

### 2 1.3.1.3 Slow Controls Computing Hardware

3 Two servers (a primary server and a replicated backup) suitable for the relational database dis-  
 4 cussed in Section 1.3.3 are located in the CUC data room along with an additional two servers  
 5 for the FE monitoring interface. These additional servers would cover assembling dynamic CISC  
 6 monitoring web pages from adjacent databases. Yet another server will be needed to run back-end  
 7 I/O. Any special purpose software, such as iFix used by the cryogenics experts, would also run  
 8 here. One or two additional servers should accommodate these programs. Replicating this setup  
 9 for each module would make commissioning and independent operation easier, accommodate dif-  
 10 ferent module designs (with resulting differences in database tables), and ensure sufficient capacity.  
 11 These four sets of networking hardware would fit tightly into one rack or very comfortably into  
 12 two. Using the requirements from CISC, the DAQ consortium will provide the cost estimates for  
 13 servers and racks.

## 14 1.3.2 Slow Controls Infrastructure

15 The data rate will be in the range of tens of kilobytes per second, given the total number of  
 16 slow controls quantities and the update rate (see Section 1.3.4), placing minimal demands on local  
 17 network infrastructure. Network traffic out of SURF to Fermilab will primarily be database calls to  
 18 the central CISC database, either from monitoring applications or from database replication to the  
 19 offline version of the CISC database. This traffic requires little bandwidth, so the proposed general

1 purpose links both out of the underground area at SURF and back to Fermilab can accommodate  
2 the traffic.

3 Up to two racks of space and appropriate power and cooling are available in the CUC's DAQ server  
4 room for CISC use. This is ample space (see Section 1.3.1.3).

### 5 **1.3.3 Slow Controls Software**

6 To provide complete monitoring and control of detector subsystems, the slow controls software  
7 includes

- 8 • the control systems base for input and output operations and defining processing logic, scan  
9 conditions, and alarm conditions;
- 10 • an alarm server to monitor all channels and send alarm messages to operators;
- 11 • a data archiver for automatic sampling and storing values for history tracking; and
- 12 • an integrated operator interface providing display panels for controls and monitoring.

13 In addition, the software must be able to interface indirectly with external systems (e.g., cryogenics  
14 control system) and databases (e.g., beam database) to export data into slow controls process  
15 variables (or channels) for archiving and status displays. This allows us to integrate displays  
16 and warnings into one system for the experiment operators and provides integrated archiving for  
17 sampled data in the archived database. As one possibility, an input output controller running  
18 on a central DAQ server could provide soft channels for these data. Figure 1.29 shows a typical  
19 workflow of a slow controls system.

20 The key features of the software require highly evolved software designed to manage real-time data  
21 exchange, scalable to hundreds of thousands of channels sampled at intervals of hours to seconds as  
22 needed. The software must be well documented, supported, and reliable. The base software must  
23 also allow easy access to any channel by name. The archiver software must allow data storage in  
24 a database with adjustable rates and thresholds so data for any channel can be easily retrieved  
25 using channel name and time range. Among other key features, the alarm server software must  
26 remember the state, support an arbitrary number of clients, and provide logic for delayed alarms  
27 and acknowledging alarms. A standard naming convention for channels will be part of the software  
28 to help handle large numbers of channels and subsystems.

29 The ProtoDUNE detector control system software [5] provides a prototype for the FD slow controls  
30 software. In ProtoDUNE, the unified control system base is WinCC OA [14], a commercial toolkit  
31 used extensively at CERN, with device interfaces supported using several standardized interface  
32 protocols. A more detailed description is in Section 1.3.6 below. WinCC OA is our baseline for  
33 the FD slow control software. EPICS [15] is an alternative controls system which also meets the  
34 specifications; it is used in other neutrino experiments including MicroBooNE[16] and NOvA[17].

### 1.3.4 Slow Controls Quantities

The final set of quantities to monitor will ultimately be determined by the subsystems being monitored, documented in appropriate interface control documents (ICDs), and continually revised based on operational experience. The total number of quantities to monitor has been roughly estimated by taking the total number monitored in ProtoDUNE-SP [5], 7595 as of Nov. 19, 2018, and scaling by the detector length and the number of planes, giving approximately 150,000 per detector module. In the case of ProtoDUNE-DP, we do not have the exact total number monitored yet, but the expectation is that the DP numbers should not deviate substantially from SP and in fact maybe lower since the total number of channels are lower. We think the ProtoDUNE-SP-based estimate can be considered as an upper limit for DP. Quantities should update on average no more than once per minute. Transmitting a single update for each channel at that rate translates to a few thousand updates per second, or a few tens of thousands of bytes per second. While this is not a significant load on a network with an efficient slow controls protocol, it would correspond to approximately 1 TB per year per detector module if every timestamp and value were stored. The actual data volume will be less because values are stored only if they vary from previous values by more than an amount that is adjustable channel-by-channel. Database storage also allows data to be sparsified later. No slow controls data is planned to be written to the DAQ stream. With careful management of archiving thresholds for each quantity monitored and yearly reduction of stored sample time density, the retained data volume can be reduced to a few TB over the life of the experiment.

The subsystems to be monitored include the cryogenic instrumentation described in this chapter, the other detector systems, and relevant infrastructure and external devices. Table 1.6 lists the quantities expected from each system.

### 1.3.5 Local Integration

The local integration of slow controls consists entirely of software and network interfaces with systems outside the scope of the detector module. This includes the following:

- readings from the LBNF-managed external cryogenics systems, for status of pumps, flow rates, inlet, and return temperature and pressure, which are implemented via OPC-UA or a similar SCADA interface;
- beam status, such as protons-on-target, rate, target steering, and beam pulse timing, which are retrieved via IFbeam; and
- near detector status, which can be retrieved from a common slow controls database.

Integration occurs after both the slow controls and non-detector systems are in place. The LBNF-CISC interface is managed by the cryogenics systems working group in CISC (see Section 1.4), which includes members from both CISC and LBNF. The IFbeam DB interface for slow controls is an already well established method used in MicroBooNE, NOvA, and other Fermilab experiments. An internal near detector (ND)/FD working group can be established to coordinate detector status

Table 1.6: Slow controls quantities.

<b>System</b>	<b>Quantities</b>
<b>Detector cryogenic instrumentation</b>	
Purity monitors	anode and cathode charge, bias voltage and current, flash lamp status, calculated electron lifetime
Thermometers	temperature, position of dynamic thermometers
Liquid level	liquid level
Pressure meters	pressure readings
Gas analyzers	purity level readings
Cameras	camera voltage and current draw, temperature, heater current and voltage, lighting current and voltage
<b>Other detector systems</b>	
Cryogenic internal piping	feedthrough gas purge flow and temperature
HV systems	drift HV voltage and current, end-of-field cage current and bias voltage, electron diverter bias, ground plane currents
TPC electronics	voltage and current to electronics
PD	voltage and current for photodetectors and electronics
DAQ	warm electronics currents and voltages, run status, DAQ buffer sizes, trigger rates, data rates, GPS status, computer and disk health status, other health metrics as defined by DAQ group
CRP / APA	bias voltages and currents
<b>Infrastructure and external systems</b>	
Cryogenics (external)	status of pumps, flow rates, inlet and return temperature and pressure (via OPC-UA or similar SCADA interface)
Beam status	protons on target, rate, target steering, beam pulse timing (via IFbeam)
Near detector	near detector run status (through common slow controls database)
Rack power and status	power distribution unit current and voltage, air temperature, fan status if applicable, interlock status
<b>Detector calibration systems</b>	
Laser	laser power, temperature, operation modes, other system status as defined by calibration group
External neutron source	safety interlock status, power supply monitoring, other system status as defined by calibration group
External radioactive source	system status as defined by calibration group



1 exchange between the near and far sites.

### 2 **1.3.6 Validation in ProtoDUNE**

3 The ProtoDUNE slow control system has met all requirements for operation of ProtoDUNE-SP[5]  
4 and will be used for ProtoDUNE-DP. The requirements for ProtoDUNE are nearly identical to  
5 those for the DP module other than total channel count. Of particular note, the ProtoDUNE slow  
6 control system unified a heterogenous set of devices and data sources through several protocols  
7 into a single control system, as illustrated in Figure 1.31. In addition to what the figure shows,  
8 data were also acquired from external cryogenic and beam systems. The topology and data flow  
9 of the system matches the general shape shown in Figure 1.29.

10 In this control system, the unified control system base is WinCC-OA [14], a commercial SCADA  
11 system for visualizing and operating of processes, production flows, machines, and plants, used  
12 in many businesses. It was chosen at CERN as a basis for developing the control systems of  
13 the LHC experiments, the accelerators and the laboratory infrastructure for its flexibility and  
14 scalability, as well as for the openness of the architecture, allowing it to interface with many  
15 different types of hardware devices and communication protocols. Additional software developed  
16 at CERN is also used, including Joint COntrols Projects [18] and UNified Industrial COntrol  
17 System (UNICOS) [19]. WinCC-OA and the additional software developed on top of it in the  
18 past 20 years, have grown into a fairly complex ecosystem. While multiple collaboration members  
19 have experience using the ProtoDUNE-SP control system, customising and using WinCC-OA in  
20 an effective way for developing the control system of DUNE requires proper training and a non-  
21 negligible learning effort.

22 As noted in sections 1.3.3 and 1.3.4, the slow control archiver will gradually accumulate terabytes  
23 of data, requiring a sizable database to store the value history and allow efficient data retrieval.  
24 Individually adjustable rates and thresholds for each channel are key to keeping this database  
25 manageable. The ProtoDUNE-SP operations provided not only a test of these features as imple-  
26 mented in the ProtoDUNE slow control system, but also insight into reasonable values for these  
27 archiving parameters for each system.

## 28 **1.4 Organization and Management**

29 The organization of the CISC consortium is shown in Figure 1.32. The CISC consortium board  
30 currently comprises institutional representatives from 19 institutes as shown in Table 1.7. The  
31 consortium leader is the spokesperson for the consortium and responsible for the overall scien-  
32 tific program and managing the group. The technical leader of the consortium is responsible for  
33 managing the project for the group. Currently, the consortium has five working groups:

34 **Cryogenics Systems:** gas analyzers and differential pressure liquid level monitors; CFD simula-  
35 tions.

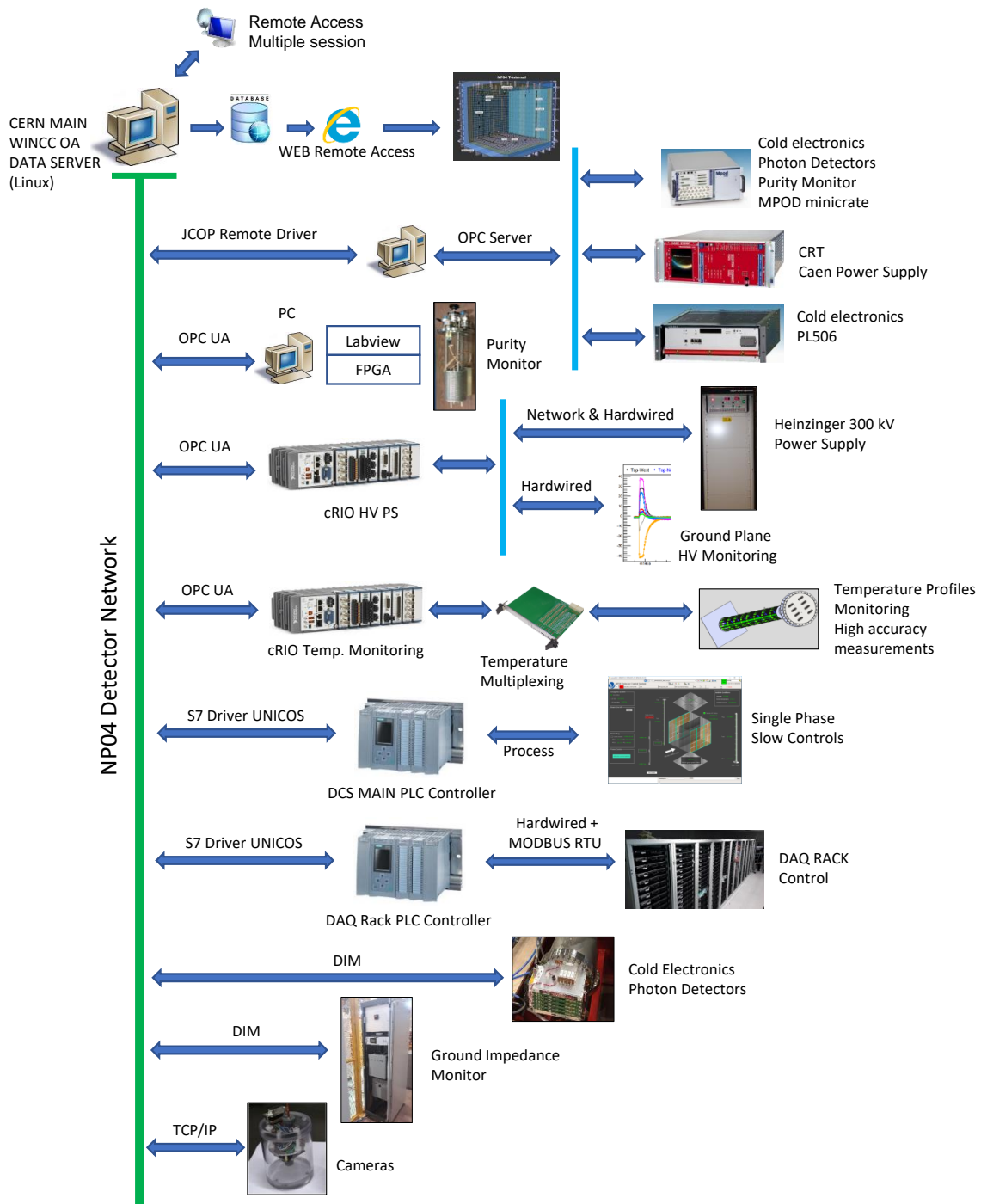


Figure 1.31: Diagram of the ProtoDUNE-SP control system topology, from [5].

- 1 **Argon Instrumentation:** purity monitors, thermometers (LAr and gaseous argon (GAr)), capac-
- 2 itive level meters, pressure meters (GAr), cameras and light emitting system, and CTF;
- 3 feedthroughs; E field simulations; instrumentation precision studies; ProtoDUNE data anal-
- 4 ysis coordination and validation.
- 5 **Slow Controls Base Software and Databases:** base I/O software, alarms and archiving databases,
- 6 and monitoring tools; variable naming conventions and slow controls quantities.
- 7 **Slow Controls Detector System Interfaces:** signal processing software and hardware interfaces
- 8 (e.g., power supplies); firmware; rack hardware; and infrastructure.
- 9 **Slow Controls External Interfaces:** interfaces with external detector systems (e.g., cryogenics
- 10 system, beam, facilities, DAQ, near detector status).

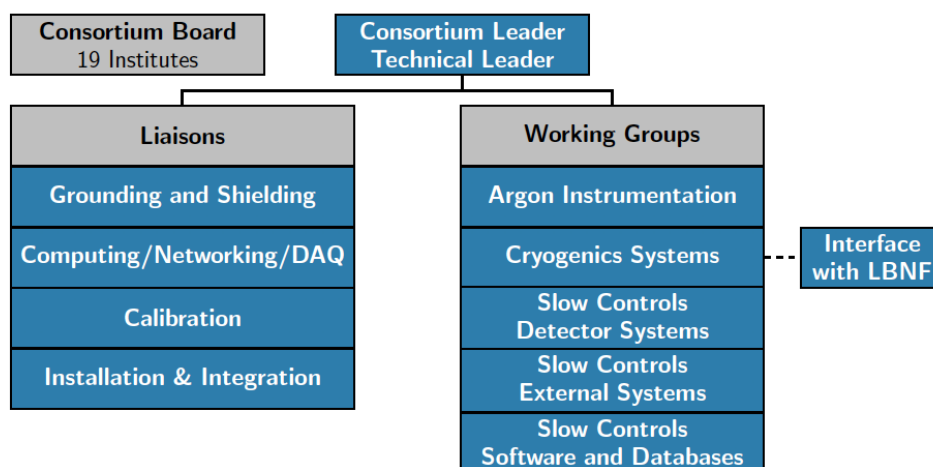


Figure 1.32: CISC Consortium organizational chart.

- 11 Moreover, because the CISC consortium broadly interacts with other groups, liaisons have been
- 12 named (see Figure 1.32). A short-term task force formed in 2017-2018 explored cryogenic modeling
- 13 for the consortium and corresponding simulation needs. A work plan for CFD simulations for both
- 14 ProtoDUNE and FD was developed based on input from the task force.

### 15 1.4.1 Institutional Responsibilities

- 16 The CISC will be a joint effort for SP and DP. A single slow controls system will be implemented
- 17 to serve both the SP module and the DP module.

- 18 Design and installation of cryogenic systems (e.g., gas analyzers, differential pressure liquid level
- 19 meters) will be coordinated with LBNF and the consortium providing resources and effort; exper-
- 20 tise is provided by LBNF. ProtoDUNE-SP and ProtoDUNE-DP designs for argon instrumentation
- 21 (e.g., purity monitors, pressure meters, thermometers, cameras) will be the basis for FD designs.

Table 1.7: Current CISC Consortium Board Members and their institutional affiliations.

<b>Member Institute</b>	<b>Country</b>
CIEMAT	Spain
Instituto de Fisica Corpuscular (IFIC)	Spain
University of Warwick	UK
University College London (UCL)	UK
Argonne National Lab (ANL)	USA
Brookhaven National Lab (BNL)	USA
University of California, Irvine (UCI)	USA
Drexel University	USA
Fermi National Accelerator Lab (Fermilab)	USA
University of Hawaii	USA
University of Houston	USA
Idaho State University (ISU)	USA
Kansas State University (KSU)	USA
University of Minnesota, Duluth (UMD)	USA
Notre Dame University	USA
South Dakota State University (SDSU)	USA
University of Tennessee at Knoxville (UTK)	USA
Virginia Tech (VT)	USA
Boston University (BU)	USA

- 1 Design validation, testing, calibration, and performance will be evaluated using ProtoDUNE-SP  
 2 and ProtoDUNE-DP data.
- 3 Following the conceptual funding model envisioned for the consortium, various responsibilities  
 4 have been distributed across institutions within the consortium pending final funding decisions.  
 5 Table 1.8 shows the current institutional responsibilities for primary CISC subsystems. Only lead  
 6 institutes are listed in the table for a given effort. For physics and simulations studies and for  
 7 validation using ProtoDUNE, a number of institutes are involved. A detailed list of tasks and  
 8 institutional responsibilities are presented in [20].

Table 1.8: Institutional responsibilities in the CISC consortium.

CISC Sub-system	Institutional Responsibility
Purity monitors	UCI, Houston, UCL
Static T-gradient monitors	IFIC, CIEMAT
Dynamic T-gradient monitors	Hawaii
Individual sensors	IFIC, CIEMAT
Vertical thermometer arrays (GAr)	TBA
Pressure meters (GAr)	TBA
Readout system for thermometers	IFIC, Hawaii, CIEMAT
Cold cameras	KSU, BNL
Warm cameras	KSU, BNL
Light-emitting system (for cameras)	Drexel
Gas analyzers	FNAL, LBNF
Differential pressure level meters	LBNF
Capacitive level meters	Notre Dame
cryogenic instrumentation test facility (CITF)	FNAL, ANL
CFD simulations	SDSU, ANL
Other simulation & validation studies	Number of Institutes
Slow controls hardware	UMD, UTK, Drexel
Slow controls infrastructure	UMD, UTK
Slow controls base software	KSU, UTK, BU, Drexel, Warwick, UCL, ANL, IFIC
Slow controls signal processing	A number of institutes
Slow controls external interfaces	VT, UTK, UMD

## 9 1.4.2 Schedule

- 10 Table 1.9 shows key construction milestones for the CISC consortium leading to commissioning of  
 11 the second FD module. CISC construction milestones align with the overall construction milestones  
 12 of the second FD module (highlighted in orange in the table). The technology design decisions  
 13 for CISC systems should be made by April 2021 followed by final design reviews in June 2021.

Table 1.9: Key CISC construction schedule milestones leading to commissioning of the second FD module.

Milestone	Date (Month YYYY)
Start of ProtoDUNE-SP-II installation	March 2021
Technology Decision Dates	April 2021
Final Design Review Dates	June 2021
Start of module 0 component production for ProtoDUNE-II	August 2021
End of module 0 component production for ProtoDUNE-II	January 2022
Start of ProtoDUNE-DP-II installation	March 2022
South Dakota Logistics Warehouse available	April 2022
Beneficial occupancy of cavern 1 and CUC	October 2022
CUC counting room accessible	April 2023
production readiness review (PRR) dates	September 2023
Start procurement of CISC hardware	December 2023
Top of detector module #1 cryostat accessible	January 2024
Start of production of CISC hardware	April 2024
Start of detector module #1 TPC installation	August 2024
Top of detector module #2 accessible	January 2025
End of CISC hardware production	April 2025
End of detector module #1 TPC installation	May 2025
Start integration of CISC hardware in the cavern	July 2025
Start of detector module #2 TPC installation	August 2025
Installation of gas analyzers and support structure for all instrumentation devices	September 2025
Installation of individual sensors, static T-gradient thermometers, and level meters	November 2025
All slow controls hardware, infrastructure, & networking installed	February 2026
Slow controls software for I/O, alarms, archiving, displays installed on production systems	May 2026
End of detector module #2 TPC installation	May 2026
Install dynamic T-gradient monitors, cameras, purity monitors, and pressure meters	June 2026
Install all feedthroughs for instrumentation devices	July 2026
Install slow control expert interfaces for all systems in time for testing	September 2026
Full slow controls systems commissioned and integrated into remote operations	July 2027

1 Design decisions will largely be based on how a given system performed (technically and physics-  
2 wise) in ProtoDUNE. This is currently actively ongoing with the ProtoDUNE-SP instrumentation  
3 data. As noted in section 1.2.8, since the designs aimed for the DP FD are not deployed in the  
4 current run of ProtoDUNE-DP, the plan is to test everything in the ProtoDUNE-2 DP except for  
5 pressure meters and long capacitive level meters as they are already deployed in the current run  
6 of ProtoDUNE-DP. The production of systems aimed for ProtoDUNE-2 DP should be finished by  
7 January 2022 followed by assembly and deployment in March 2022.

8 Designs may need review based on performance in ProtoDUNE-2 and any modifications will be  
9 incorporated into the final design before the start of production of CISC systems for the FD in  
10 April 2024. This will be followed by assembly of the systems underground in the detector cavern  
11 in July 2025. Installation of instrumentation devices will start in September 2025 following the  
12 beneficial occupancy of the interior of the cryostat. Installing gas analyzers, level meters, individual  
13 temperature sensors, static T-gradient thermometers, and support structure for all instrumentation  
14 devices will be finished before installing TPC, but installing dynamic T-gradient thermometers,  
15 purity monitors, pressure meters and cameras will occur afterward. CISC will work closely with  
16 LBNF to coordinate installation of the cryogenic systems and instrumentation devices. For slow  
17 controls, the goal is to have the full slow controls system commissioned and integrated into remote  
18 operations at least three months before the SP module is ready for operations.

### 19 **1.4.3 Risks**

20 Table 1.10 lists the possible risks identified by the CISC consortium along with corresponding  
21 mitigation strategies. A more detailed list of risks with additional descriptions can be found in  
22 [21]. The table shows 18 risks, all at medium or low level, mitigated with necessary steps and  
23 precautions. More discussion on all medium-level risks are provided in the text below.

- 24 • Risk 01: The risk associated with ProtoDUNE-based designs (mainly SP) being inadequate  
25 for FD, is important because this requires early validation from ProtoDUNE data so R&D  
26 of alternate designs can be timely. With ProtoDUNE-SP data now available, the consortium  
27 is focused on validating instrumentation designs.
- 28 • Risk 06: Temperature sensors in the dynamic T-gradient monitor are calibrated using two  
29 methods: lab calibration to 0.002 K (as in the static T-gradient monitor case) and in-situ  
30 cross-calibration moving the system vertically. Disagreement between the two methods can  
31 occur. In order to mitigate this we need to investigate and improve both methods.
- 32 • Risk 10: This risk involves not being able to build a working prototype for cold cameras  
33 during R&D phase that meets all the requirements & safety. For example, cold camera  
34 prototypes fail longevity tests or show low performance (e.g. bad resolution). This risk  
35 originates from past experience with cold cameras that became non-operational after a period  
36 of time in LAr or show low performance. In order to address this, we plan to pursue further  
37 R&D to improve thermal insulation and heaters, develop alternative camera models, etc.  
38 If problems persist one can use the cameras in the ullage (cold or inspection) with the  
39 appropriate field of view and lighting such that elements inside LAr can be inspected during  
40 filling.

- 1 • Risk 12: Cameras are delicate devices and some of them located near HV devices can be  
2 destroyed by HV discharges. This can be mitigated by ensuring that most important cold  
3 cameras have enough redundancy such that the loss of one camera does not compromise the  
4 overall performance. In the case of inspection cameras since they are replaceable, one can  
5 simply replace them.
- 6 • Risk 17: The gas analyzers and level meters may fail as these are commercial devices pur-  
7 chased at some point in their product cycle and cannot be required to last 20 years. Typical  
8 warranties are  $\sim 1$  year from date of purchase. The active electronics parts of both gas ana-  
9 lyzers and level meters are external to the cryostat so they can be replaced. To mitigate this,  
10 provisions will be made for future replacement in case of failure or loss of sensitivity. Also,  
11 the risk is not high since we have purity monitors in the filtration system that can cover the  
12 experiment during the time gas analyzers are being replaced or repaired.

13 Related to risks 12, 16 and 18, aging is an important aspect for several monitors, especially for those  
14 that are inaccessible. The ProtoDUNE tests demonstrate that the devices survive the commis-  
15 sioning phase and we continue to learn from ProtoDUNE experience. In addition to ProtoDUNE,  
16 other tests are planned. For example, in the case of purity monitors, photocathodes are expected  
17 to survive the first five years and if we prevent running them with high frequency at low purity  
18 (lifetime  $< 3$  ms), aging can be prevented for a longer time. To understand long-term aging, R&D  
19 is planned at CITF and at member institute sites for many of the devices. Other systems that are  
20 replaceable such as inline purity monitors, gas analyzers, and inspection cameras can be replaced  
21 when failures occur and maintained for the lifetime of the experiment.

Table 1.10: Risks for DP-FD-CISC (P=probability, C=cost, S=schedule) More information at risk probabilities. [ref tab:risks:DP-FD-CISC](#)

ID	Risk	Mitigation	P	C	S
RT-DP-CISC-001	Baseline design from ProtoDUNEs for an instrumentation device is not adequate for DUNE far detectors	Focus on early problem discovery in ProtoDUNE so any needed redesigns can start as soon as possible.	L	M	L
RT-DP-CISC-002	Swinging of long instrumentation devices (T-gradient monitors or PrM system)	Add additional intermediate constraints to prevent swinging.	L	L	L
RT-DP-CISC-003	High E-fields near instrumentation devices cause dielectric breakdowns in LAr	CISC systems shielded and placed as far from cathode and FC as possible.	L	L	L
RT-DP-CISC-004	Light pollution from purity monitors and camera light emitting system	Use PrM lamp and camera lights outside PDS trigger window; cover PrM cathode to reduce light leakage.	L	L	L
RT-DP-CISC-005	Temperature sensors can induce noise in cold electronics	Check for noise before filling and re-mediate, repeat after filling. Filter or ground noisy sensors.	L	L	L



RT-DP-CISC-006	Disagreement between lab and <i>in situ</i> calibrations for ProtoDUNE-SP dynamic T-gradient monitor	Investigate and improve both methods, particularly laboratory calibration.	M	L	L
RT-DP-CISC-007	Purity monitor electronics induce noise in TPC and PDS electronics.	Operate lamp outside TPC+PDS trigger window. Surround and ground light source with Faraday cage.	L	L	L
RT-DP-CISC-008	Discrepancies between measured temperature map and CFD simulations in ProtoDUNE-SP	Improve simulations with additional measurements inputs; use fraction of sensors to predict others	L	L	L
RT-DP-CISC-009	Difficulty correlating purity and temperature in ProtoDUNE-SP impairs understanding cryo system.	Identify causes of discrepancy, modify design. Calibrate PrM differences, correlate with RTDs.	L	L	L
RT-DP-CISC-010	Cold camera R&D fails to produce prototype meeting specifications & safety requirements	Improve insulation and heaters. Use cameras in ullage or inspection cameras instead.	M	M	L
RT-DP-CISC-011	HV discharge caused by inspection cameras	Study E-field in and on housing and anchoring system. Test in HV facility.	L	L	L
RT-DP-CISC-012	HV discharge destroying the cameras	Ensure sufficient redundancy of cold cameras. Warm cameras are replaceable.	L	M	L
RT-DP-CISC-013	Insufficient light for cameras to acquire useful images	Test cameras with illumination similar to actual detector.	L	L	L
RT-DP-CISC-014	Cameras may induce noise in cold electronics	Continued R&D work with grounding and shielding in realistic conditions.	L	L	L
RT-DP-CISC-015	Light attenuation in long optic fibers for purity monitors	Test the max. length of usable fiber, optimize the depth of bottom PrM, number of fibers.	L	L	L
RT-DP-CISC-016	Longevity of purity monitors	Optimize PrM operation to avoid long running in low purity. Technique to protect/recover cathode.	L	L	L
RT-DP-CISC-017	Longevity: Gas analyzers and level meters may fail.	Plan for future replacement in case of failure or loss of sensitivity.	M	M	L
RT-DP-CISC-018	Problems in interfacing hardware devices (e.g. power supplies) with slow controls	Involve slow control experts in choice of hardware needing control/monitoring.	L	L	L

## 1.4.4 Interfaces

CISC subsystems interface with all other detector subsystems and could affect the work of all detector consortia, as well as some working groups (physics, software/computing, beam instrumentation), and technical coordination, requiring interactions with all of these entities. We also interact heavily with LBNF beam and cryogenics groups. Detailed descriptions of CISC interfaces are maintained in DUNE DocDB. A brief summary is provided in this section. Table 1.11 lists the IDs of the different DocDB documents as well as their highlights. Descriptions of the interfaces and interactions that affect many systems follow.

Obviously, CISC interacts with the detector consortia because CISC will provide status monitoring of all important detector sub-systems along with controls for some components of the detector. CISC will also consult on selecting different power supplies to ensure monitoring and control can be established with preferred types of communication. Rack space distribution and interaction between slow controls and other modules from other consortia will be managed by technical coordination (TCN) in consultation with those consortia.

If heaters/RTDs are needed on flanges, CISC will specify the heaters/RTDs and will provide the readout/control, while the responsibility for the actual hardware will be discussed with the different groups.

Installing instrumentation devices will interfere with other devices and must be coordinated with the appropriate consortia. On the software side, CISC must define, in coordination with other consortia/groups, the quantities to be monitored/controlled by slow controls and the corresponding alarms, archiving, and GUIs.

## 1.4.5 Installation, Integration, and Commissioning

### 1.4.5.1 Purity Monitors

The purity monitor system will be built in modules, so it can be assembled outside the cryostat leaving few steps to complete inside the cryostat. The assembly itself comes into the cryostat with the individual purity monitors mounted to support tubes and with no HV cables or optical fibers yet installed. The support tube at the top and bottom of the assembly is then mounted to the brackets inside the cryostat and the brackets attached to the cables trays and/or the detector support structure. At much the same time, the FE electronics and light source can be installed on top of the cryostat, and the electronics and power supplies can be installed in the electronics rack.

Integration begins by running the HV cables and optical fibers to the purity monitors through the top of the cryostat. These cables are attached to the HV feedthroughs with sufficient length to reach each purity monitor inside the cryostat. The cables are run along cable trays through the port reserved for the purity monitor system. Each purity monitor will have three HV cables that connect it to the feedthrough and then further along to the FE electronics. The optical fibers are then run through the special optical fiber feedthrough into the cryostat and guided to the

Table 1.11: CISC system interface links.

<b>Interfacing System</b>	<b>Description</b>	<b>Linked Reference</b>
CRP	temperature sensors in the gas, cameras, and lights	DocDB 6760 [22]
PD system	PrMs, light emitting system for cameras	DocDB 6781 [23]
TPC Electronics	Noise, Power supply monitoring	DocDB 6784 [24]
HV Systems	shielding, bubble generation by inspection camera, cold camera locations, ground planes	DocDB 6787 [25]
DAQ	Description of CISC data storage, allowing bi-directional communications between DAQ and CISC.	DocDB 6790 [26]
Calibration	multifunctional CISC/CITF ports; space sharing around ports	DocDB 7072 [27]
Physics	Indirect interfaces through calibration, tools to extract data from the slow controls database	
Software & Computing	Slow Controls database design and maintenance	DocDB 7126 [28]
Cryogenics	must be designed and implemented. purity monitors, gas analyzers, interlock mechanisms to prevent contamination of LAr	-
Beam	beam status	-
TC Facility	Significant interfaces at multiple levels	DocDB 6991 [29]
TC Installation	Significant interfaces at multiple levels	DocDB 7018 [30]
TC Integration Facility	Significant interfaces at multiple levels	DocDB 7045 [31]

1 purity monitor system either using the cables trays or guide tubes, depending on which solution  
2 is adopted. This should protect fibers from breaking accidentally as the rest of the detector and  
3 instrumentation installation continues. The optical fibers are then run inside the purity monitor  
4 support tube and to the appropriate purity monitor, terminating the fibers at the photocathode  
5 of each monitor while protecting them from breaking near the purity monitor system itself.

6 Integration continues as the HV cables are connected through the feedthrough to the system  
7 FE electronics; then optical fibers are connected to the light source. The cables connecting the  
8 FE electronics and the light source to the electronics rack are also run and connected at this  
9 time. This allows the system to be turned on and the software to begin testing the various  
10 components and connections. Once all connections are confirmed successful, integration with the  
11 slow controls system begins, first by establishing communication between the two systems and then  
12 transferring data between them to ensure successful exchange of important system parameters and  
13 measurements.

14 Commissioning the purity monitor system begins once the cryostat is purged and a gaseous argon  
15 atmosphere is present. At this time, the HV for the purity monitors is ramped up without risk  
16 of discharge through the air, and the light source turned on. Although the drift electron lifetime  
17 in the gaseous argon would be very large and therefore not measurable with the purity monitors  
18 themselves, the signal strength at both the cathode and anode will give a good indication of  
19 how well the light source generates drift electrons from the photocathode. Comparing the signal  
20 strengths at the anode and cathode will indicate whether the electrons successfully drift to the  
21 anode. Although quality assurance (QA) and quality control (QC) should make it unlikely for a  
22 purity monitor to fail this final test, if that does happen then the electric and optical connections  
23 can be fixed before filling.

#### 24 1.4.5.2 Thermometers

25 **Static T-gradient monitors** will be installed after FCs along the long cryostat sides. The profiles  
26 are preassembled before they are delivered to SURF. Installation begins by anchoring the support  
27 holding the two vertical strings to bolts on the top corner of the cryostat. All cables can then be  
28 routed to the assigned cryostat ports. Second, the array is unrolled using a scissor lift, and once  
29 at the bottom, it is attached to bolts on the bottom corner of the cryostat. After checking string  
30 tension and verticality, cable and sensors supports are checked, and the individual Faraday cages  
31 are installed. A precision resistor is plugged into each IDC-4 connector, so noise studies can be  
32 performed. Sensors will be installed later.

33 **Individual temperature sensors** on pipes/PDs<sup>12</sup> and cryostat floor should be installed after PDs  
34 and the grounding grid. First, vertical strings for cable routing are installed following a procedure  
35 similar to the one described above for the static T-gradient monitors. Next, anchor all cable  
36 supports to pipes/PDs. Then each cable is routed individually starting from the sensor end (with  
37 IDC-4 female connector but without the sensor) to the corresponding cryostat port. Once all

---

<sup>12</sup>Actually on PD's support structure

1 cables going through the same port have been routed, the cables are cut to the same length, so  
2 they can be properly assembled into the corresponding connector(s). To avoid damaging them,  
3 sensors are installed later, once all operations at the bottom of the cryostat are complete.

4 **Dynamic T-gradient monitors** are installed after the TPC components are in place. Figure 1.8  
5 shows the design of the dynamic T-gradient monitor with its sensor carrier rod, enclosure above the  
6 cryostat, and stepper motor. Figure 1.9 shows detailed views of key components. Each monitor  
7 comes in several segments with sensors and cabling already in place. Additional slack will be  
8 provided at segment joints to make installation easier. Segments of the sensor carrier rod with  
9 preattached sensors are fed into the flange one at a time. Each segment, as it is fed into the  
10 cryostat, is held at the top with a pin that prevents the segment from sliding all the way in. The  
11 next segment is connected at that time to the previous segment. Then the pin is removed, the first  
12 segment is pushed down, and the next segment top is held with the pin at the flange. This process  
13 is repeated for each segment until the entire sensor carrier rod is in place. Next, the enclosure  
14 is installed on top of the flange, starting with the six-way cross at the bottom of the enclosure.  
15 (See Figure 1.9, right.) Again, extra cable slack at the top will be provided to ease connection  
16 to the D-sub flange and allow the entire system to move vertically. The wires are connected to  
17 a D-sub connector on the feedthrough on one side port of the cross. Finally, a crane positions  
18 the remainder of the enclosure over the top of the cross. This enclosure includes the mechanism  
19 used to move the sensor rod, which is preassembled, with the motor in place, on the side of the  
20 enclosure, and the pinion and gear is used to move the sensor inside the enclosure. The pinion is  
21 connected to the top of the rod. The enclosure is then connected to top part of the cross, which  
22 finishes the installation of the dynamic T-gradient monitor.

23 **Vertical arrays in gas phase:** The baseline design assumes twenty arrays, each of which is  
24 attached to a CRP frame. Thus, they should be installed on the corresponding CRP before being  
25 moved into the cryostat. Cables will be routed to the assigned cryostat port using the appropriate  
26 elements on the CRP frame.

27 Commissioning all thermometers will occur in several steps. In the first stage, only cables are  
28 installed, so the readout performance and the noise level inside the cryostat is checked again at  
29 room temperature. Spare cables, connectors and sensors are available for replacement at Sanford  
30 Underground Research Facility (SURF) if needed. The final commissioning phase takes place  
31 during and after cryostat filling.

### 32 1.4.5.3 Gas Analyzers

33 The gas analyzers are installed before the piston purge and gas recirculation phases of the cryostat  
34 commissioning. They are installed near the tubing switchyard to minimize tubing run length  
35 and for convenience when switching the sampling points and gas analyzers. Because each is a  
36 standalone module, a single rack with shelves is adequate to house the modules.

37 For integration, the gas analyzers typically have an analog output (4 mA to 20 mA or 0 V to 10 V),

1 which maps to the input range of the analyzers. They also usually have several relays to indicate  
2 the scale they are currently running. These outputs can be connected to the slow controls for  
3 readout. However, using a digital readout is preferable because this gives a direct analyzer reading  
4 at any scale. Currently, the digital output connections are RS-232, RS-485, USB, and Ethernet.  
5 The preferred option is chosen at the time of purchase.

6 The readout usually responds to a simple set of text query commands. Because of the natural  
7 time scales of the gas analyzers and lags in gas delivery times (which depend on the length of the  
8 tubing run), sampling every minute is adequate.

9 The analyzers must be brought online and calibrated before beginning the gas phase of the cryostat  
10 commissioning. Calibration varies by module because they differ, but calibration often requires  
11 using argon gas with zero contaminants, and argon gas with a known level of the contaminant  
12 to check the scale. Contaminants are usually removed with a local inline filter for the first gas  
13 sample. This gas phase usually begins with normal air, with the more sensitive analyzers valved off  
14 at the switchyard to prevent overloading their inputs (and potentially saturating their detectors).  
15 As the argon purge and gas recirculation progress, the various analyzers are valved back in when  
16 the contaminant levels reach the upper limits of the analyzer ranges.

#### 17 **1.4.5.4 Liquid Level Monitoring**

18 LBNF will install differential pressure level meters, but the capacitive level meters fall within scope  
19 of CISC. The exact number of capacitive level meters is not yet decided. We will need at least  
20 four, one for each of the four corners of the cryostat. They will be attached to the M10 bolts in  
21 the cryostat corners after the detector is installed. If additional capacitive level meters are needed  
22 in the central part of the cryostat, those will be installed after the nearby FC modules, attaching  
23 them to the bolts in the top cryostat corner<sup>13</sup>. In all cases, cables will be routed to the appropriate  
24 nearby port (not yet assigned).

#### 25 **1.4.5.5 Pressure Meters**

26 CISC will install the pressure meters. Six sensors will be mechanically installed in two dedicated  
27 flanges (three sensors each) at opposite sides of the cryostat after the detector is installed. Cables  
28 will be routed through the dedicated ports assigned for these devices. The pressure signals (absolute  
29 and relative) are read and converted to standard 4-20 mA current loop signals. A twisted pair  
30 shielded cable connects the sensors to the slow controls PLC controller using software to convert  
31 electrical signals to pressure values.

---

<sup>13</sup>These level meters must be shorter because no bolts run vertically as they do for the other level meters

#### 1.4.5.6 Cameras and light emitting system

Installing fixed cameras is, in principle, simple but involves several interfaces. The enclosure of each camera has exterior threaded holes for mounting the cameras on the cryostat wall, cryogenic internal piping, or DSS. Each enclosure is attached to a gas line to maintain appropriate under-pressure in the fill gas; therefore, an interface with cryogenic internal piping will be necessary. Each camera has a cable (coaxial or optical) for the video signal and a multiconductor cable for power and control. These are run through cable trays to flanges on assigned instrumentation feedthroughs.

The inspection camera is designed to be inserted and removed on any instrumentation feedthrough equipped with a gate valve at any time during operation. Installing the gate valves and purge system for instrumentation feedthroughs falls under cryogenic internal piping.

Fixed lighting sources separate from the cameras are mounted on cryostat wall, cryogenic internal piping, or DSS, and multiconductor cables for power are run through cable trays to flanges on assigned instrumentation feedthroughs.

#### 1.4.5.7 Slow Controls Hardware

Slow controls hardware installation includes several servers, network cables, any specialized cables needed for device communication, and possibly some custom-built hardware for monitoring racks. The installation sequence will be planned with the facilities group and other consortia. The network cables and rack monitoring hardware will be common across many racks and will be installed first as part of the basic rack installation as led by the facilities group. Specialized cables needed for slow controls and servers are installed after the common rack hardware. Selecting and installing these cables will be coordinated with other consortia, and server installation will be coordinated with the DAQ group.

#### 1.4.5.8 Transport, handling, and storage

Most instrumentation devices will be shipped in pieces to SURF via the South Dakota Warehouse Facility (SDWF) and mounted on site. Instrumentation devices are in general small, except for the support structures for purity monitors and dynamic T-gradient monitors that will cover the entire height of the cryostat. The load on those structures is relatively small ( $< 100$  kg), so they can be fabricated in sections smaller than 3 m, which can be easily transported to SURF, down the shaft, and through the tunnels. All instrumentation devices except the dynamic T-gradient monitors can be moved into the cryostat without the crane. The dynamic T-gradient monitors, which are introduced into the cryostat from above, require a crane for installing the external enclosure (with preassembled motor, pinion, and gear).

## 1.4.6 Quality Control

The manufacturer and the institution in charge of device assembly will conduct a series of tests to ensure the equipment can perform its intended function as part of QC. QC also includes post-fabrication tests and tests run after shipping and installation. For complex systems, the entire system will be tested before shipping. Additional QC procedures can be performed at the CITF and underground after installation.

The planned tests for each subsystem are described below.

### 1.4.6.1 Purity monitors

The purity monitor system will undergo a series of tests to ensure the system performs as intended. These tests include electronic tests with a pulse generator, mechanical and electrical connectivity tests at cryogenic temperatures in a cryostat, and vacuum tests for short and full assemblies in a dewar and in a long vacuum tube.

The QC tests for FD purity monitors begin with testing individual purity monitors in vacuum after each is fabricated and assembled. This test checks the amplitude of the signal generated by the drift electrons at the cathode and anode to ensure the photocathode can provide sufficient numbers of photoelectrons to measure the signal attenuation with the required precision and the field gradient resistors all work properly to maintain the drift field. A smaller version of the assembly with all purity monitors installed will be tested at the CITF to ensure the full system performs as expected in LAr and to study systematics that may influence the measured lifetime.

Next, the entire system is assembled on the full-length mounting tubes to check connections. Ensuring that all electric and optical connections are operating properly during this test reduces the risk of problems once the full system is assembled and ready for the final test in vacuum. The fully assembled system is placed in the shipping tube, which serves as a vacuum chamber, and tested at SURF before the system is inserted into the cryostat. During insertion, electrical connections are tested continuously with multimeters and electrometers.

### 1.4.6.2 Thermometers

**Static T-gradient thermometers:** Static T-gradient monitors undergo three type of tests at the production site before shipping to SURF: a mechanical rigidity test, a calibration of all sensors, and a test of all electrical cables and connectors. Mechanical rigidity is tested by installing the static T-gradient monitor between two dummy cryostat corners mounted 15 m apart. The tension of the strings is set to match the tension that would occur in a vertical deployment in LAr, and the deflection of the sensor and electrical cable strings is measured and compared to the expected value; this ensures any swinging or deflection of the deployed static T-gradient monitor will be  $< 5$  cm, mitigating any risk of touching the FCs and the cryostat membrane. The laboratory calibration of sensors will be performed as explained in Section 1.2.1. The main concern is reproducibility of



1 results because sensors could change resistance and hence their temperature scale when undergoing  
2 successive immersions in LAr. In this case, the calibration procedure itself provides QC because  
3 each set of sensors goes through five independent measurements. Sensors with RMS variation  
4 outside the requirement (2 mK for ProtoDUNE-SP) are discarded. This calibration also serves as  
5 QC for the readout system (similar to the final one) and of the PCB-sensor-connector assembly.  
6 Finally, the cable-connector assemblies are tested; sensors must measure the expected values with  
7 no additional noise introduced by either cable or connector.

8 An integrated system test at a LAr test facility on site, with sufficient linear dimension ( $>2$  m) to  
9 test a good portion of the system, would be desirable. This would ensure that the system operates  
10 in LAr at the required performance level.

11 The last phase of QC takes place after installation. The verticality of each array is checked, and  
12 the tensions in the stainless steel strings adjusted as necessary. Before closing the flange, the entire  
13 readout chain is tested. This allows a test of the sensor-connector assembly, the cable-connector  
14 assemblies at both ends, and the noise level inside the cryostat. If any sensor presents a problem,  
15 it is replaced. If the problem persists, the cable is checked and replaced as needed.

16 **Dynamic T-gradient thermometers:** The dynamic T-gradient monitor consists of an array of  
17 high-precision temperature sensors mounted on a vertical rod. The rod can move vertically to  
18 cross-calibrate the temperature sensors *in situ*. We will use the following tests to ensure that the  
19 dynamic T-gradient monitor delivers vertical temperature gradient measurements with a precision  
20 of a few mK.

- 21 • Before installation, temperature sensors are tested in LN to verify correct operation and to  
22 set the baseline calibration for each sensor to the absolutely calibrated reference sensor.
- 23 • Warm and cold temperature readings are taken with each sensor after it is mounted on the  
24 PCB board and the readout cables are soldered.
- 25 • The sensor readout is taken for all sensors after the cold cables are connected to electric  
26 feedthroughs on the flange and the warm cables outside of the cryostat are connected to the  
27 temperature readout system.
- 28 • The stepper motor is tested before and after connecting to the gear and pinion system.
- 29 • The fully assembled rod is connected to the pinion and gear and moved with the stepper motor  
30 on a high platform many times to verify repeatability, possible offsets, and any uncertainty in  
31 positioning. Finally, repeating this test many times will verify the sturdiness of the system.
- 32 • The full system is tested after it is installed in the cryostat; both motion and sensor operation  
33 are tested by checking sensor readout and vertical motion of the system.

34 **Individual sensors:** To address the quality of individual precision sensors, the same method is  
35 used as for the static T-gradient monitors. The QC of the sensors is part of the laboratory  
36 calibration. After mounting six sensors with their corresponding cables, a SUBD-25 connector  
37 is added, and the six sensors tested at room temperature. All sensors must give values within  
38 specifications. If any of the sensors present problems, they are replaced. If the problem persists,

1 the cable is checked and replaced as needed.

2 For standard RTDs to be installed on the cryostat walls, floor, and roof, calibration is not an issue.  
3 Any QC required for associated cables and connectors is performed following the same procedure  
4 as for precision sensors.

5 **Vertical arrays in gas phase:** These thermometers use standard RTDs that require no calibration.  
6 Any QC required for associated cables and connectors is performed following the same procedure  
7 as for precision sensors. The appropriate QC procedure for the PCB support structure will be  
8 elaborated once this is designed.

### 9 **1.4.6.3 Gas analyzers**

10 The gas analyzers will be guaranteed by the manufacturer. However, once received, the gas  
11 analyzer modules are checked for both *zero* and the *span* values using a gas-mixing instrument and  
12 two gas cylinders, one having a zero level of the gas analyzer contaminant species and the other  
13 cylinder with a known percentage of the contaminant gas. This verifies the proper operation of the  
14 gas analyzers. When they are installed at SURF, this process is repeated before commissioning  
15 the cryostat. Calibrations must be repeated using manufacturer recommendations over the gas  
16 analyzer lifetime.

### 17 **1.4.6.4 Liquid level monitoring**

18 The manufacturer will provide the QC for the differential pressure level meters; further QC during  
19 and after installation is the responsibility of LBNF.

20 The capacitive sensors will be tested with a modest sample of LAr in the laboratory before they  
21 are installed. After installation, they are tested *in situ* using a suitable dielectric in contact with  
22 the sensor.

### 23 **1.4.6.5 Pressure meters**

24 The manufacturer will provide the QC for the pressure meters; CISC will provide further QC  
25 during and after installation.

26 The pressure sensors will be tested with a modest sample of gaseous argon in the laboratory before  
27 they are installed. After installation, they are tested *in situ* at atmospheric pressure. The whole  
28 pressure readout chain, (including slow controls PLC and software protocol) will also be tested  
29 and cross-checked with LBNF pressure sensors.

#### 1 1.4.6.6 Cameras

2 Before transport to SURF, each cryogenic camera unit (comprising the enclosure, camera, and  
3 internal thermal control and monitoring) is checked for correct operation of all features, for recovery  
4 from 87 K non-operating mode, for leakage, and for physical defects. Lighting systems are similarly  
5 checked. Operations tests will verify correct current draw, image quality, and temperature readback  
6 and control. Each movable inspection camera apparatus is inspected for physical defects and  
7 checked for proper mechanical operation before shipping. A checklist is created for each unit, filed  
8 electronically in the DUNE logbook, and a hard copy is sent with each unit.

9 Before installation, each fixed cryogenic camera unit is inspected for physical damage or defects  
10 and checked at the CITF for correct operation of all features, for recovery from 87 K non-operating  
11 mode, and for contamination of the LAr. Lighting systems are similarly checked. Operations tests  
12 verify correct current draw, image quality, and temperature readback and control. After installing  
13 and connecting the wiring, fixed cameras and lighting are again checked for operation. The movable  
14 inspection camera apparatus is inspected for physical defects and, after integration with a camera  
15 unit, tested in the facility for proper mechanical and electronic operation and cleanliness before  
16 being installed or stored. A checklist will be completed for each QC check and filed electronically  
17 in the DUNE logbook.

#### 18 1.4.6.7 Light-emitting system

19 The entire light-emitting system is checked before installation to ensure functionality of light  
20 emission. Initial testing of the system (see Figure 1.28) begins with measuring the current when  
21 low voltage (1 V) is applied to check that the resistive LED failover path is correct. Next, the  
22 forward voltage is measured using nominal forward current to check that it is within 10% of the  
23 nominal forward voltage drop of the LED, that all of the LEDs are illuminated, and that each LED  
24 is visible over the nominal angular range. If the LEDs are infrared, a video camera with the IR filter  
25 removed is used for a visual check. This procedure is then duplicated with the current reversed for  
26 LEDs oriented in the opposite direction. Initial tests are performed at room temperature and then  
27 repeated in LN. Color shifts in the LEDs are expected and will be noted. A checklist is completed  
28 for each QC check and filed electronically in the DUNE logbook.

29 Room temperature tests are repeated during and immediately after installation to ensure that the  
30 system has not been damaged during transportation or installation. Functionality checks of the  
31 LEDs are repeated after the cameras are installed in the cryostat.

#### 32 1.4.6.8 Slow controls hardware

33 Networking and computing systems will be purchased commercially, requiring QA. The new servers  
34 are tested after delivery to confirm they suffered no damage during shipping. The new system is  
35 allowed to burn in overnight or for a few days, running a diagnostics suite on a loop to validate  
36 the manufacturer's QA process.

1 The system is shipped directly to SURF where an on site expert boots the systems and does basic  
2 configuration. Specific configuration information is pulled over the network, after which others  
3 may log in remotely to do the final set up, minimizing the number of people underground.

#### 4 **1.4.7 Safety**

5 Safety is critical during all phases of the CISC project, including R&D, laboratory calibration  
6 and testing, mounting tests, and installation. Safety experts review and approve the initial safety  
7 planning for all phases as part of the initial design review, as well as before implementation. All  
8 documentation of component cleaning, assembly, testing, and installation will include a section on  
9 relevant safety concerns and will be reviewed during appropriate pre-production reviews.

10 Several areas are of particular importance to CISC.

- 11 • Hazardous chemicals (e.g., epoxy compounds used to attach sensors to cryostat inner mem-  
12 brane) and cleaning compounds: All chemicals used will be documented at the consortium  
13 management level, with a material safety data sheet and approved handling and disposal  
14 plans in place.
- 15 • Liquid and gaseous cryogenics used in calibrating and testing: LN and LAr are used to calibrate  
16 and test instrumentation devices. Full hazard analysis plans will be in place at the consortium  
17 management level for full module or module component testing that involves cryogenics. These  
18 safety plans will be reviewed in appropriate pre-production and production reviews.
- 19 • High voltage safety: Purity monitors have a voltage of  $\sim 2$  kV. Fabrication and testing plans  
20 will show compliance with local HV safety requirements at any institution or laboratory that  
21 conducts testing or operation, and this compliance will be reviewed as part of the standard  
22 review process.
- 23 • Working at heights: Some fabrication, testing, and installation of CISC devices require  
24 working at heights. Both T-gradient monitors and purity monitors, which span the height of  
25 the detector, require working at heights exceeding 10 m. Temperature sensors installed near  
26 the top cryostat membrane and cable routing for all instrumentation devices also require  
27 working at heights. The appropriate safety procedures, including lift and harness training,  
28 will be designed and reviewed.
- 29 • Falling objects: all work involving heights has associated risks of falling objects. The cor-  
30 responding safety procedures, including proper helmet use and a well restricted safety area,  
31 will be included in the safety plan.

## 32 **1.5 Blank section for avoiding missing label errors**

# 1 Glossary

- 2 **35 ton prototype** A prototype cryostat and single-phase (SP) detector built at Fermilab before  
3 the ProtoDUNE detectors. 16, 29, 32, 38, 39
- 4 **anode plane assembly (APA)** A unit of the SP detector module containing the elements sensitive  
5 to ionization in the LAr. It contains two faces each of three planes of wires, and interfaces  
6 to the cold electronics and photon detection system. 11, 40, 49
- 7 **cold electronics (CE)** Analog and digital readout electronics that operate at cryogenic tempera-  
8 tures. 43
- 9 **European Organization for Nuclear Research (CERN)** The leading particle physics laboratory  
10 in Europe and home to the ProtoDUNEs. (In French, the Organisation Européenne pour la  
11 Recherche Nucléaire, derived from Conseil Européen pour la Recherche Nucléaire. 27, 35,  
12 44, 50, 73-75
- 13 **conventional facilities (CF)** Pertaining to construction and operation of buildings and conven-  
14 tional infrastructure, and for LBNF and DUNE project (LBNF/DUNE), CF includes the  
15 excavation caverns. 72
- 16 **computational fluid dynamics (CFD)** High performance computer-assisted modeling of fluid dy-  
17 namical systems. 4, 6, 8, 11-16, 23, 25-29, 35, 50, 52, 54
- 18 **cryogenic instrumentation and slow controls (CISC)** Includes equipment to monitor all detec-  
19 tor components and liquid argon (LAr) quality and behavior, and provides a control system  
20 for many of the detector components. 1, 3-6, 14, 33, 36, 43, 45-48, 52-56, 59, 60, 63, 67, 69
- 21 **cryogenic instrumentation test facility (CITF)** A facility at Fermilab with small ( $< 1$  ton) to  
22 intermediate ( $\sim 1$  ton) volumes of instrumented, purified TPC-grade LAr, used for testing  
23 devices intended for use in Deep Underground Neutrino Experiment (DUNE). 4, 7, 10, 34,  
24 41-43, 52, 54, 57, 60, 65, 68
- 25 **charge-parity symmetry violation (CPV)** Lack of symmetry in a system before and after charge  
26 and parity transformations are applied. 1

- 1 **charge-readout plane (CRP)** In the dual-phase (DP) technology, a collection of electrodes in a  
2 planar arrangement placed at a particular voltage relative to some applied E field such that  
3 drifting electrons may be collected and their number and time may be measured. 5, 16, 23,  
4 34, 39–41, 49, 60, 62
- 5 **central utility cavern (CUC)** The utility cavern at the 4850L of Sanford Underground Research  
6 Facility (SURF) located between the two detector caverns. It contains utilities such as central  
7 cryogenics and other systems, and the underground data center and control room. 45–47, 55
- 8 **data acquisition (DAQ)** The data acquisition system accepts data from the detector front-end  
9 (FE) electronics, buffers the data, performs a trigger decision, builds events from the selected  
10 data and delivers the result to the offline secondary DAQ buffer. 5, 32, 33, 46–49, 52, 60, 64,  
11 72
- 12 **DCS** Distributed Communications System. 28
- 13 **DUNE detector safety system (DDSS)** The system used to manage key aspects of detector  
14 safety. 5, 34
- 15 **detector module** The entire DUNE far detector is segmented into four modules, each with a  
16 nominal 10 kt fiducial mass. 3–5, 7, 8, 14–17, 23, 28, 29, 34, 39, 40, 42, 43, 48, 55, 71, 75
- 17 **dual-phase (DP)** Distinguishes one of the DUNE far detector technologies by the fact that it  
18 operates using argon in both gas and liquid phases. 1, 3, 4, 8, 11, 13, 16, 29, 35, 43, 44, 71,  
19 73–75
- 20 **DP module** dual-phase DUNE far detector (FD) module. 1, 4, 11, 13, 15, 20, 28, 30, 31, 33, 39,  
21 50, 52
- 22 **detector support system (DSS)** The system used to support a SP detector module within its  
23 cryostat. 21, 64
- 24 **Deep Underground Neutrino Experiment (DUNE)** A leading-edge, international experiment for  
25 neutrino science and proton decay studies. 3, 6, 9, 11, 13, 28, 34–36, 38–41, 43, 50, 59, 68,  
26 70, 72, 75
- 27 **field cage (FC)** The component of a liquid argon time-projection chamber (LArTPC) that con-  
28 tains and shapes the applied E field. 11, 16, 19, 40, 41, 61, 63, 65, 72
- 29 **far detector (FD)** The 40 kt fiducial mass DUNE detector, composed of four 10 kt modules, to  
30 be installed at the far site at SURF in Lead, SD, USA. 1, 3, 4, 11, 13, 29, 35, 41–44, 47, 48,  
31 52, 54, 56, 65, 71, 72, 75
- 32 **front-end (FE)** The front-end refers a point that is “upstream” of the data flow for a particular  
33 subsystem. For example the front-end electronics is where the cold electronics meet the sense

- 1 wires of the TPC and the front-end data acquisition (DAQ) is where the DAQ meets the  
2 output of the electronics. 32, 33, 46, 59, 61, 71
- 3 **Fermi National Accelerator Laboratory (Fermilab)** U.S. national laboratory in Batavia, IL. It  
4 is the laboratory that hosts DUNE and serves as its near site. 72–75
- 5 **far site conventional facilities (FSCF)** The conventional facilities (CF) at the DUNE far detec-  
6 tor site, SURF. 75
- 7 **gaseous argon (GAr)** argon in its gas phase. 52
- 8 **ground plane (GP)** An electrode held electrically neutral relative to Earth ground voltage; it is  
9 mounted on the field cage (FC) in a SP module to protect the cryostat wall. 39, 40
- 10 **GPIB** general purpose interface bus. 45
- 11 **high voltage (HV)** Generally describes a voltage applied to drive the motion of free electrons  
12 through some media, e.g., LAr. 3, 5, 6, 13, 27, 30–34, 38, 39, 41, 43, 44, 49, 57, 59–61, 69
- 13 **ICEBERG R&D cryostat and electronics (ICEBERG)** Integrated Cryostat and Electronics Built  
14 for Experimental Research Goals: a new double-walled cryostat built and installed at Fermi  
15 National Accelerator Laboratory (Fermilab) for liquid argon detector R&D and for testing  
16 of DUNE detector components. 43
- 17 **IFbeam** Database that stores beamline information indexed by timestamp. 48, 49
- 18 **IFIC** Instituto de Fisica Corpuscular (in Valencia, Spain). 21
- 19 **LabVIEW** Laboratory Virtual Instrument Engineering Workbench is a system-design platform and  
20 development environment for a visual programming language from National Instruments. 32,  
21 33
- 22 **Liquid Argon Puri./wty Demonstrator (LAPD)** Cryostat at Fermilab for long-term studies re-  
23 quiring a large volume of argon. 32
- 24 **liquid argon (LAr)** Argon in its liquid phase; it is a cryogenic liquid with a boiling point of  $-90^{\circ}\text{C}$   
25 ( $87\text{K}$ ) and density of  $1.4\text{g/ml}$ . 6, 8, 13–16, 23, 26–28, 34–36, 42, 43, 52, 56, 57, 66, 69, 70,  
26 73, 75
- 27 **liquid argon time-projection chamber (LARTPC)** A time projection chamber (TPC) filled with  
28 liquid argon; the basis for the DUNE FD modules. 29, 33, 71, 75
- 29 **Long-Baseline Neutrino Facility (LBNF)** The organizational entity responsible for developing  
30 the neutrino beam, the cryostats and cryogenics systems, and the conventional facilities for  
31 DUNE. 4, 34, 36, 48, 52, 54, 56, 59, 63, 67, 75

- 1 **LBNF and DUNE project (LBNF/DUNE)** The overall global project, including Long-Baseline  
2 Neutrino Facility (LBNF) and DUNE. 70
- 3 **LED** Light-emitting diode. 42, 43, 68
- 4 **large electron multiplier (LEM)** A micro-pattern detector suitable for use in ultra-pure argon  
5 vapor; LEMs consist of copper-clad PCB boards with sub-millimeter-size holes through which  
6 electrons undergo amplification. 6, 16, 35
- 7 **LHC** Large Hadron Collider. 27, 50
- 8 **LN** liquid nitrogen. 43, 66, 68, 69
- 9 **LV** low voltage. 33
- 10 **MicroBooNE** The LArTPC-based MicroBooNE neutrino oscillation experiment at Fermilab. 45,  
11 47
- 12 **near detector (ND)** Refers to the detector(s) installed close to the neutrino source at Fermilab.  
13 48
- 14 **NOvA** The NOvA off-axis neutrino oscillation experiment at Fermilab. 47
- 15 **OPC-UA** OPC Unified Architecture is a machine to machine communication protocol for indus-  
16 trial automation developed by the OPC Foundation. OPC stands for Object Linking and  
17 Embedding for Process Control. 28, 48, 49
- 18 **Proton Assembly Building (PAB)** Home of several LAr facilities at Fermilab. 43
- 19 **PCB** printed circuit board. 19, 21, 23, 66, 67
- 20 **PCI** Peripheral Component Interconnect. 32
- 21 **photon detector (PD)** The detector elements involved in measurement of the number and arrival  
22 times of optical photons produced in a detector module. 23, 43, 44, 49, 61
- 23 **photon detection system (PD system)** The detector subsystem sensitive to light produced in  
24 the LAr. 33, 42, 60
- 25 **PLC** programmable logic controller. 35, 63, 67
- 26 **parts per billion (ppb)** A concentration equal to one part in  $10^{-9}$ . 28
- 27 **parts per trillion (ppt)** A concentration equal to one part in  $10^{-12}$ . 28



- 28 **ProtoDUNE** Either of the two DUNE prototype detectors constructed at European Organization  
1 for Nuclear Research (CERN). One prototype implements SP technology and the other DP.  
2 13, 34, 35, 39, 41, 45, 47, 50, 52, 54, 56, 57, 70, 74
- 3 **ProtoDUNE-2** The second run of a ProtoDUNE detector. 56
- 4 **ProtoDUNE-DP** The DP ProtoDUNE detector at CERN. 3, 6, 11, 13–15, 23, 24, 29–31, 35, 39,  
5 41, 43, 44, 48, 50, 52, 54–56
- 6 **ProtoDUNE-SP** The SP ProtoDUNE detector at CERN. 3, 5, 6, 9, 11, 13–17, 20, 21, 23–25,  
7 27–31, 33, 35, 36, 39, 40, 42–44, 48, 50–52, 54–56, 66
- 8 **production readiness review (PRR)** A project management device by which the production readi-  
9 ness is reviewed. 55
- 10 **quality assurance (QA)** The set of actions taken to provide confidence that quality requirements  
11 are fulfilled, and to detect and correct poor results. 61, 68, 75
- 12 **quality control (QC)** An aggregate of activities (such as design analysis and inspection for de-  
13 fects) performed to ensure adequate quality in manufactured products. 61, 65–68
- 14 **risk probabilities** The risk probability, after taking into account the planned mitigation activities,  
15 is ranked as L (low < 10%), M (medium 10% to 25%), or H (high > 25%). The cost and  
16 schedule impacts are ranked as L (cost increase < 5%, schedule delay < 2 months), M (5%  
17 to 25% and 2–6 months, respectively) and H (> 20% and > 2 months, respectively). 57
- 18 **root mean square (RMS)** The square root of the arithmetic mean of the squares of a set of  
19 values, used as a measure of the typical magnitude of a set of numbers, regardless of their  
20 sign. 6, 20, 28
- 21 **Resistance temperature detector (RTD)** A temperature sensor consisting of a material with an  
22 accurate and reproducible resistance/temperature relationship. 16, 23, 34, 59, 67
- 23 **SBND** The Short-Baseline Near Detector experiment at Fermilab. 45
- 24 **SCADA** supervisory control and data acquisition. 48–50
- 25 **South Dakota Warehouse Facility (SDWF)** Warehousing operations in South Dakota responsi-  
26 ble for receiving LBNF and DUNE goods and coordinating shipping to the Ross Shaft at  
27 SURF. 64
- 28 **secondary DAQ buffer** A secondary DAQ buffer holds a small subset of the full rate as selected  
29 by a trigger command. This buffer also marks the interface with the DUNE Offline. 71
- 30 **supernova neutrino burst (SNB)** A prompt increase in the flux of low-energy neutrinos emitted

- 31 in the first few seconds of a core-collapse supernova. It can also refer to a trigger command  
1 type that may be due to this phenomenon, or detector conditions that mimic its interaction  
2 signature. 1
- 3 **single-phase (SP)** Distinguishes one of the DUNE far detector technologies by the fact that it  
4 operates using argon in its liquid phase only. 1, 11, 13, 35, 56, 70, 71, 73, 74
- 5 **SP module** single-phase DUNE FD module. 1, 11, 12, 34, 52, 56, 72
- 6 **Sanford Underground Research Facility (SURF)** The laboratory in South Dakota where the  
7 LBNF far site conventional facilities (FSCF) will be constructed and the DUNE FD will  
8 be installed and operated. 62, 71, 74
- 9 **TallBo** A cylindrical cryostat at Fermilab primarily used for developing scintillation light collection  
10 technologies for LArTPC detectors. 43
- 11 **technical coordination (TCN)** The DUNE organization responsible for overall integration of the  
12 detector elements and successful execution of the detector construction project; areas of  
13 responsibility include general project oversight, systems engineering, quality assurance (QA)  
14 and safety. 59
- 15 **technical design report (TDR)** A formal project document that describes the experiment at a  
16 technical level. 1, 34
- 17 **time projection chamber (TPC)** A type of particle detector that uses an E field together with  
18 a sensitive volume of gas or liquid, e.g., LAr, to perform a 3D reconstruction of a particle  
19 trajectory or interaction. The activity is recorded by digitizing the waveforms of current  
20 induced on the anode as the distribution of ionization charge passes by or is collected on the  
21 electrode. 1, 3, 6, 10, 13, 16, 28-30, 33, 39, 43, 44, 49, 55, 56, 60, 62, 72
- 22 **trigger candidate** Summary information derived from the full data stream and representing a  
23 contribution toward forming a trigger decision. 75
- 24 **trigger command** Information derived from one or more trigger candidates that directs elements  
25 of the detector module to read out a portion of the data stream. 74, 75
- 26 **trigger decision** The process by which trigger candidates are converted into trigger commands.  
1 71, 75
- 2 **WA105 DP demonstrator** The  $3 \times 1 \times 1 \text{ m}^3$  WA105 DP prototype detector at CERN. 39

## References

- [1] DOE Office of High Energy Physics, “Mission Need Statement for a Long-Baseline Neutrino Experiment (LBNE),” tech. rep., DOE, 2009. LBNE-doc-6259.
- [2] Strons, Ph., and Bailey, J. L., “Flow visualization methods for field test verification of CFD analysis of an open gloveport,” 2017.  
<https://www.osti.gov/pages/servlets/purl/1402050>.
- [3] G. J. Michna *et al.*, “CFD Analysis of Fluid, Heat, and Impurity Flows in DUNE FAR Detector to Address Additional Design Considerations,” DUNE doc 5915, South Dakota State University, 2017. <https://docs.dunescience.org/cgi-bin/private/ShowDocument?docid=5915&asof=2019-7-15>.
- [4] The Liquid Argon Technology @BNL, “Basic properties.”  
<https://lar.bnl.gov/properties/basic.html>. Accessed Jan. 15, 2019.
- [5] A. Kehrli, G. L. Miotto, X. Pons, S. Ravat, and M. J. Rodriguez, “The protoDUNE Single Phase Detector Control System, in Proceedings of CHEP 2018,” tech. rep., 2018.  
<https://docs.dunescience.org/cgi-bin/private/ShowDocument?docid=11098>.
- [6] W. Walkowiak, “Drift velocity of free electrons in liquid argon,” *Nucl. Instrum. Meth.* **A449** (2000) 288–294.
- [7] M. Adamowski *et al.*, “The Liquid Argon Purity Demonstrator,” *JINST* **9** (2014) P07005, [arXiv:1403.7236](https://arxiv.org/abs/1403.7236) [physics.ins-det].
- [8] **WA105** Collaboration, S. Murphy, “Status of the WA105-3x1x1 m<sup>3</sup> dual phase prototype,” tech. rep., 2017. <https://indico.fnal.gov/event/12345/session/1/contribution/5/material/slides/0.pdf>.
- [9] Delaquis, S. C. and Gornea, R. and Janos, S. and Lüthi, M. and Rudolf von Rohr, C. and Schenk, M. and Vuilleumier, J. -L., “Development of a camera casing suited for cryogenic and vacuum applications,” *JINST* **8** (2013) T12001, [arXiv:1310.6601](https://arxiv.org/abs/1310.6601) [physics.ins-det].
- [10] Auger, M. and Blatter, A. and Ereditato, A. and Goeldi, D. and Janos, S. and Kreslo, I. and Lüthi, M. and Rudolf von Rohr, C. and Strauss, T. and Weber, M. S., “On the Electric

- 3 Breakdown in Liquid Argon at Centimeter Scale,” *JINST* **11** no. 03, (2016) P03017,  
4 arXiv:1512.05968 [physics.ins-det].
- 5 [11] T. I. Banks *et al.*, “A compact ultra-clean system for deploying radioactive sources inside  
6 the KamLAND detector,” *Nucl. Instrum. Meth.* **A769** (2015) 88–96, arXiv:1407.0413  
7 [physics.ins-det].
- 8 [12] “LUXEON C Color Line (datasheet).”  
9 <https://www.lumileds.com/uploads/571/DS144-pdf>. Accessed: 2018-11-19.
- 10 [13] J. Carron, A. Philippon, L. S. How, A. Delbergue, S. Hassanzadeh, D. Cillierre, P. Danto,  
11 and M. Boutillier, “Cryogenic characterization of LEDs for space application,” *Proc. SPIE,*  
12 *Sixteenth International Conference on Solid State Lighting and LED-based Illumination*  
13 *Systems* **10378** (2017) 20.
- 14 [14] Siemens AG, “SIMATIC WinCC open architecture.”  
15 <http://www.siemens.com/wincc-open-architecture>. Accessed: 2018-11-27.
- 16 [15] “EPICS - Experimental Physics and Industrial Control System.”  
17 <https://epics-controls.org/>. Accessed: July 19, 2019.
- 18 [16] R. Acciarri *et al.*, “Design and construction of the microboone detector,” *Journal of*  
19 *Instrumentation* **12** no. 02, (2017) P02017.  
20 <http://stacks.iop.org/1748-0221/12/i=02/a=P02017>.
- 21 [17] G. Lukhanin, K. Biery, S. Foulkes, M. Frank, A. Hatzikoutelis, J. Kowalkowski, M. Paterno,  
22 and R. Rechenmacher, “Application of control system studio for the NOvA detector control  
23 system,” *J. Phys. Conf. Ser.* **396** (2012) 062012.
- 24 [18] “About JCOP.” <http://jcop.web.cern.ch/>. Accessed: July 19, 2019.
- 25 [19] “UNICOS,” 2015. <http://unicos.web.cern.ch/>.
- 26 [20] A. C. Villanueva and S. Gollapinni, “DUNE FD WBS: Slow Control,” DUNE doc 5609,  
27 2018. [https://docs.dunescience.org/cgi-bin/private/ShowDocument?docid=5609&](https://docs.dunescience.org/cgi-bin/private/ShowDocument?docid=5609&asof=2019-7-15)  
28 [asof=2019-7-15](https://docs.dunescience.org/cgi-bin/private/ShowDocument?docid=5609&asof=2019-7-15).
- 29 [21] S. Gollapinni *et al.*, “DUNE FD Risks: CISC,”. [https://docs.dunescience.org/cgi-bin/](https://docs.dunescience.org/cgi-bin/private/ShowDocument?docid=7192&asof=2019-7-15)  
30 [private/ShowDocument?docid=7192&asof=2019-7-15](https://docs.dunescience.org/cgi-bin/private/ShowDocument?docid=7192&asof=2019-7-15).
- 31 [22] A. C. Villanueva *et al.*, “DUNE FD Interface Document: DP CRP to Joint CISC,”. [https:](https://docs.dunescience.org/cgi-bin/private/ShowDocument?docid=6760&version=1)  
32 [//docs.dunescience.org/cgi-bin/private/ShowDocument?docid=6760&version=1](https://docs.dunescience.org/cgi-bin/private/ShowDocument?docid=6760&version=1).
- 33 [23] D. Duchesneau, I. Gil-Botella, , S. Gollapinni, and A. Villanueva, “DUNE FD Interface  
1 Document: DP Photon Detector to Joint CISC,”. [https:](https://docs.dunescience.org/cgi-bin/private/ShowDocument?docid=6781&version=1)  
2 [//docs.dunescience.org/cgi-bin/private/ShowDocument?docid=6781&version=1](https://docs.dunescience.org/cgi-bin/private/ShowDocument?docid=6781&version=1).

- 3 [24] D. Autiero *et al.*, “DUNE FD Interface Document: DP TPC Electronics to Joint CISC,”  
4 [https:](https://docs.dunescience.org/cgi-bin/private/ShowDocument?docid=6784&version=1)  
5 [//docs.dunescience.org/cgi-bin/private/ShowDocument?docid=6784&version=1](https://docs.dunescience.org/cgi-bin/private/ShowDocument?docid=6784&version=1).
- 6 [25] A. C. Villanueva *et al.*, “DUNE FD Interface Document: High Voltage to CISC,” [https:](https://docs.dunescience.org/cgi-bin/private/ShowDocument?docid=6787&version=1)  
7 [//docs.dunescience.org/cgi-bin/private/ShowDocument?docid=6787&version=1](https://docs.dunescience.org/cgi-bin/private/ShowDocument?docid=6787&version=1).
- 8 [26] A. C. Villanueva *et al.*, “DUNE FD Interface Document: DAQ to CISC,” [https:](https://docs.dunescience.org/cgi-bin/private/ShowDocument?docid=6790&version=1)  
9 [//docs.dunescience.org/cgi-bin/private/ShowDocument?docid=6790&version=1](https://docs.dunescience.org/cgi-bin/private/ShowDocument?docid=6790&version=1).
- 10 [27] S. Gollapinni *et al.*, “DUNE FD Interface Document: Calibration to Joint CISC,” [https:](https://docs.dunescience.org/cgi-bin/private/ShowDocument?docid=7072&version=1)  
11 [//docs.dunescience.org/cgi-bin/private/ShowDocument?docid=7072&version=1](https://docs.dunescience.org/cgi-bin/private/ShowDocument?docid=7072&version=1).
- 12 [28] S. Gollapinni *et al.*, “DUNE FD Interface Document: Software and Computing to Joint  
13 CISC,” [https:](https://docs.dunescience.org/cgi-bin/private/ShowDocument?docid=7126&version=1)  
14 [//docs.dunescience.org/cgi-bin/private/ShowDocument?docid=7126&version=1](https://docs.dunescience.org/cgi-bin/private/ShowDocument?docid=7126&version=1).
- 15 [29] F. Feyzi *et al.*, “DUNE FD Interface Document: Facility Interfaces to Joint CISC,”  
16 <https://docs.dunescience.org/cgi-bin/private/ShowDocument?docid=6991>.
- 17 [30] S. Gollapinni *et al.*, “DUNE FD Interface Document: Installation Interfaces to Joint CISC,”  
18 [https:](https://docs.dunescience.org/cgi-bin/private/ShowDocument?docid=7018&version=1)  
19 [//docs.dunescience.org/cgi-bin/private/ShowDocument?docid=7018&version=1](https://docs.dunescience.org/cgi-bin/private/ShowDocument?docid=7018&version=1).
- 20 [31] S. Gollapinni *et al.*, “DUNE FD Interface Document: Integration Facility to Joint CISC,”  
1906 [https:](https://docs.dunescience.org/cgi-bin/private/ShowDocument?docid=7045&version=1)  
1907 [//docs.dunescience.org/cgi-bin/private/ShowDocument?docid=7045&version=1](https://docs.dunescience.org/cgi-bin/private/ShowDocument?docid=7045&version=1).